

# **Cardiac gap junctions and action potential propagation**

## **Gap junctions in het hart en voortgeleiding van de actiepotentiaal**

(met een samenvatting in het Nederlands)

### **Proefschrift**

Ter verkrijging van de graad van doctor aan de Universiteit Utrecht  
op gezag van de Rector Magnificus, Prof.Dr. W.H. Gispen, ingevolge  
het besluit van het College voor Promoties in het openbaar te  
verdedigen op dinsdag 23 oktober 2001 des namiddags te 16.15  
uur.

door

**Antonius Adrianus Bartholomeus van Veen**

geboren 3 juni 1970 te Leiden

Promotor: **Prof. Dr. H.J. Jongsma**

Department of Medical Physiology  
University Medical Center Utrecht  
Utrecht, The Netherlands

The work presented in this thesis was performed at the Department of Medical Physiology, University Medical Center Utrecht and supported by a grant of the Netherlands Heart Foundation (NHS-97.184).

Financial support by the Netherlands Heart Foundation for the publication of this thesis is gratefully acknowledged.

# **Cardiac gap junctions and action potential propagation**

*in herinnering aan papa*

**ISBN:** 90-393-2820-X

**Drukwerk:** Febodruk BV, Enschede, Nederland

**Financial co-support:** Clean-Air Techniek BV  
J.E. Jurriaanse Stichting

## Contents

<b>Chapter 1:</b> Preface	7
<b>Chapter 2:</b> Cardiac gap junction channels: modulation of expression and channel properties	11
<b>Chapter 3:</b> Electrical conductance of mouse Connexin45 gap junction channels is modulated by phosphorylation.	33
<b>Chapter 4:</b> Electrophysiological and cellular characteristics of adrenergic stimulated neonatal cardiomyocytes cultured in a defined pattern.	53
<b>Chapter 5:</b> Differences in conductive properties of the rodent ventricular conduction system: correlation with expression of cardiac connexins and tissue morphology.	69
<b>Chapter 6:</b> Impaired conduction in the bundle branches of mouse hearts lacking the gap junction protein Connexin40.	87
<b>Chapter 7:</b> Remodeling of gap junctions in mouse hearts hypertrophied by forced retinoic acid signaling	101
<b>Chapter 8:</b> Summarizing Discussion	119
Nederlandse samenvatting	126
Dankwoord	129
Curriculum Vitae	130
List of Publications	131



# Chapter 1

---

## Preface

Toon A.B. van Veen

A beating heart is one of the most fascinating phenomena in mammalian physiology. Although subjectively stated due to the authors admiration, universal appreciation is reflected in the heart as a symbol for love and life. As it was already for centuries recognized that the heart played a decisive role between life and death, its physiology and performance have been studied extensively. However, in our nowadays highly developed world in which good health is one of the most cherished treasures, cardiac malfunctioning is still a mayor cause of human death. Medical care and scientific research are cooperatively able to tackle a lot of former lethal problems but the onset of various cardiac diseases remains barely understood. The basis for the up to now acquired knowledge is the fact that cardiac anatomy and physiology among mammals is highly comparable which allows for meaningful research. Where physiology, anatomy and pharmacology were the initial clarifying fields, introduction of molecular biology and genetics in cardiovascular research has been a major step forward in understanding the etiology of cardiac disease. This certainly holds for the field of cardiac electrophysiology.

Every heartbeat is the result of an orchestra of events which enable the heart to contract thereby fulfilling its task as the driving force of blood circulation. The success of the pump function depends on a highly coordinated sequence of events. Each contraction of the heart is triggered in the sinoatrial node by spontaneous depolarization of the cells in this small region in the right atrium. From here, the action potential is propagated along both atria causing them to contract. By contraction of the atria, deoxygenated blood from the venous part of the circulation collected in the right atrium, and blood re-oxygenated in the lungs collected in the left atrium, is pumped into the right and left ventricle respectively. After depolarization of the atria, propagation of the action potential is slowed in the atrio-ventricular node, the sole electrical connection between the atria and the ventricles, while the atria contract. Subsequently, the electric impulse is rapidly propagated through the ventricular conduction system (common bundle, bundle branches and Purkinje fibers) in order to depolarize the working ventricular myocardium from apex to base. By simultaneous contraction of the right and left ventricles, deoxygenated blood is pumped to the lungs (from the right ventricle) and oxygenated blood into the aorta (from the left ventricle).

Propagation of the electric impulse from cell to cell is mediated by clusters of intercellular channels called gap junctions which in the adult heart are primarily found at the longitudinal cell edges in structures known as intercalated disks. Each gap junction channel is constructed from two head to head aligned half channels (connexons) contributed by neighboring cells. A connexon is composed of 6 hexagonally arranged transmembrane proteins called connexins. Connexins (Cxs) form a large family of highly related proteins of which 3 members are expressed in gap junction channels between cardiomyocytes. Connexin43 (Cx43) is the most ubiquitously expressed isoform and is found in the working atrial and ventricular myocardium, connexin40 (Cx40) is found in the atrial working myocardium and large parts of the conduction system where also connexin45 (Cx45) is expressed.

The electrical coupling of cells is determined by the number of channels expressed, the open probability of these channels and the conductance of each single channel. Channels composed of different connexins possess different properties which are susceptible to regulation. The structural background for this are differences in amino acid sequence between the connexin molecules especially the intracellular domains of the protein. Here we find amino acid residues involved in pH- and

voltage sensitivity and consensus sequences for phosphorylation by different classes of protein kinases.

In many cardiac diseases an increased propensity for development of fatal arrhythmias occurs. During the onset of the disease, changes in expression of many genes and structural adaptations trigger a change in cardiac performance. These changes may be caused by alterations at the cellular level: specific up- and down regulation of the expression of several genes, reorganization of the contractile apparatus, adaptations in signal transduction pathways and cell homeostasis have been described, including changes in the expression level and subcellular distribution of gap junction proteins. *In vitro* experiments using isolated, cultured cardiomyocytes have demonstrated that several growth factors and signal transduction pathways known to be involved in cardiac disease are effective modulators of gap junction expression and distribution. Although it is generally accepted that gap junctions are essential for action potential conduction, it is virtually unknown how sensitive conduction velocity is for changes in gap junction density, distribution or conductance and thus how changes in these properties might contribute to the increased propensity to develop fatal arrhythmias under pathological conditions. This question brings us to the central question of this thesis:

*Do changes in expression, distribution and modulation of myocardial gap junctions influence conduction velocity of the action potential under normal and hypertrophic conditions?*

To answer this question, we structured our experiments in three levels of increasing complexity: 1) experiments on communication deficient cells transfected with a gene encoding one particular connexin isoform, 2) experiments on isolated, cultured cardiomyocytes expressing more than one connexin isoform, 3) *in vivo* and *in vitro* experiments on intact mouse and rat hearts. The foregoing, relatively brief introduction to the background of this thesis is extended in Chapter 2 where the present information is reviewed about gap junction composition, connexin structure, expression in heart and the modulatory mechanism affecting gap junction expression, distribution and properties. Compared to Cx40 and Cx43 gap junction channels, at the onset of the project relatively little was known about Cx45 channels. Chapter 3 describes the properties of mouse Cx45 channels transfected in HeLa cells and their modulation by phosphorylation. In Chapter 4, we investigated isolated cardiomyocytes which we cultured in a defined geometry. This allowed us to measure conduction velocity under control conditions and upon application of adrenergic stimuli in order to assess the participation of gap junction channels and ion channels.

In Chapter 5, 6 and 7 we used the intact heart as an experimental model. In Chapter 5 we compared the ventricular electrical activation of two commonly used animal models; mouse and rat heart. We describe a correlation between the electrical activation pattern, the morphology of the conduction system and the expression/distribution of gap junctions. In Chapter 6 we used a Cx40 knock-out mouse to study the effects of absence of Cx40 on impulse propagation through the ventricular conduction system. Finally, in Chapter 7 we describe a transgenic mouse model where forced retinoic acid signalling induces a dilated cardiomyopathy which is characterized by heterogenous Cx43 depletion and abnormal ventricular activation. In the summarizing discussion (Chapter 8), the results described in this thesis are put into perspective to investigate to what extent our results clarify the role gap junction channels play in cardiac activation.



# Chapter 2

---

## **Cardiac gap junction channels: modulation of expression and channel properties**

Toon A.B. van Veen, Harold V.M. van Rijen  
& Tobias OptHof

*Cardiovascular Research (2001) 51: 217-229*

## Abstract

In the heart, intercellular gap junction channels constructed from connexin molecules are crucial for conduction of the electric impulse. Cardiomyocytes can be interconnected by channels composed of 3 types of connexin proteins: Cx40, Cx43 or Cx45. In mammalian hearts, these three isoforms are regionally differently expressed and even between the species differences exist. Each of these channel-types possesses specific properties and are susceptible to modulation by various mechanisms. In this paper we compare the differences in properties of these channels as deduced from studies on transfected cells and isolated cardiomyocytes and discuss the factors involved in modulation of channel properties. Next, we evaluate the consequences of alterations in expression and modulation of channel properties for cardiac function. Therefore, we have compared reports on genetically engineered animals and discuss this information in relation with various pathophysiological disorders.

### Acronyms:

$\gamma_i$ , single channel conductance;  $g_j$ , gap junctional conductance;  $P_o$ , open probability;  $V_j$ , transjunctional voltage gradient;  $V_o$ , Voltage difference at half-maximal (in)activation; PKC, protein kinase C; PKA, protein kinase A; PKG, protein kinase G; MAPkinase, mitogen activated protein kinase; LY, lucifer yellow (Mw 443 dalton); 6CF, 6-carboxyfluorescein; DCF, 2',7'-dichlorofluorescein; mCx40, mCx43, mCx45, mouse connexin 40, -43, -45; rCx40, rCx43, rCx45, rat connexin 40, -43, -45; hCx40, hCx43, hCx45, human connexin 40, -43, -45; pS, pico Siemens; aa, amino acids.

## 1. Introduction

Normal growth, development and appropriate functioning of many tissues and organs depend on maintenance and regulation of intercellular communication. It can be mediated by extracellular neurohumoral factors, but most mammalian cells also directly connect by gap junctions. Gap junctions are agglomerates (plaques) of multiple intercellular channels which connect the cytoplasm of adjacent cells. Thereby they provide both electrical and metabolic coupling. Electrical coupling fulfills a key-role in excitable tissues (e.g. smooth and cardiac muscle) where propagation of the electric impulse is mediated by passage of ions through gap junction channels. Metabolic coupling, i.e. the transport of small metabolites, nucleotides and second messengers with a molecular weight up to 1.2 kD [13], might also play an important role in differentiated tissues (e.g. in electrical synapses of neurons) but certainly has a critical function in embryo- and organogenesis.

As depicted in figure 2.1A, each gap junction channel is composed of 12 connexin (Cx) molecules, assembled from two hexameric hemichannels (connexons), one of each delivered by both participating cells. The individual connexins form a multigene family of highly related but not identical transmembrane proteins (reviewed in [4]). In mammals, at least 15 members, named after their theoretical molecular mass (in kD), have been cloned up to now (for review see [5-7]). The overall gene- and protein structure is largely conserved among the various isoforms. Figure 2.1B shows that all connexin proteins consist of 4 transmembrane segments (M1-M4), 2 extracellular loops (E1, E2), 1 intracellular loop (CL) and a cytoplasmic amino- and carboxy terminus (for review see [4]). Strong conservation of the amino acid sequence is mainly found in both extracellular loops, the amino-terminus

and the 4 transmembrane segments. Three of these transmembrane segments (1, 2 and 4) consist predominantly of hydrophobic amino acids while the third segment has a more amphipathic character suggestive for a role in the inner lining of the aqueous pore [8]. The two extracellular loops (E1 and E2) each contain three conserved cysteines that likely participate in the process of docking of the two hemichannels [9-11]. Disulfide bonds in between the cysteines within E1 and E2 but also crossing the space between E1 and E2 create a  $\beta$ -sheet conformation required for interaction between the two opposing connexons (see [4]). After translation of the mRNA, connexins are inserted in the membranes of the endoplasmic reticulum [12], followed by oligomerization into connexons in the Golgi-complex [13]. Once in the sarcolemma, a functional channel is created by head-to-head docking of hemichannels at spots where both plasma membranes are in close apposition, thereby creating an aqueous pore between both cells. When both connexons are constructed from identical connexins (figure 2.1C), a *homotypic* channel is formed. The degree of conservation (among different connexin isoforms) of the second extracellular loop [10], provides the opportunity for connexons built from one particular type of connexin (*homomeric*), to dock with a connexon composed of another isoform thereby creating a *heterotypic*

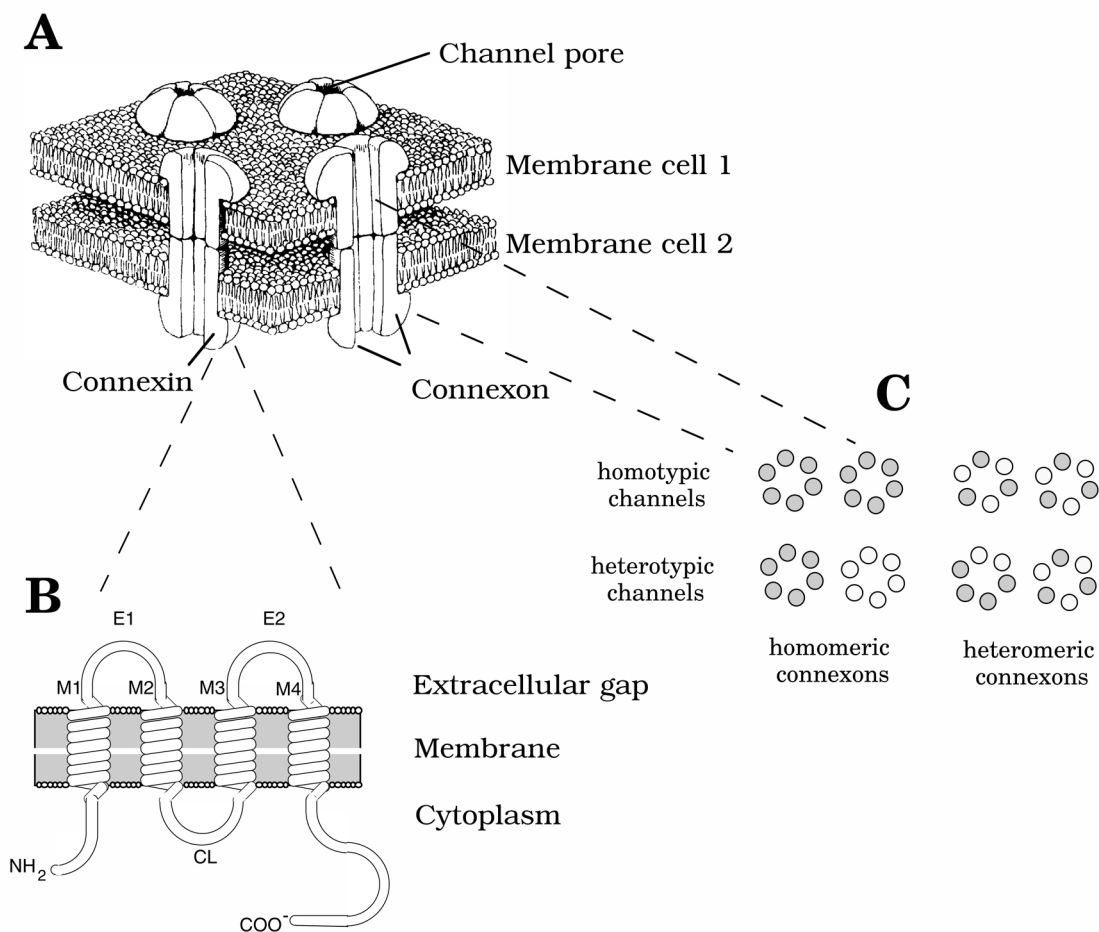


**Figure 2.1** Schematic illustration of gap junction structure. Panel A; Part of a gap junction plaque showing several channels interconnecting two cells and the composition of an individual channel from two half-channels (connexons) which are composed of connexin proteins. Panel B; Secondary structure of a single connexin protein. Panel C; Scheme explaining the composition of homotypic- and heterotypic channels from homomeric- and heteromeric connexons.

channel. Additionally, even within one hemichannel, different connexins can be integrated (*heteromeric* connexon) which can result in both homotypic- and heterotypic channel formation.

The biochemical- and electrical characteristics of gap junction channels depend on their constituent connexins. Moreover, the properties of gap junction channels can be modulated by various mechanisms like (de)phosphorylation of the individual connexin proteins, the transjunctional voltage gradient, intracellular hydrogen- and free calcium concentration, and extracellular fatty acid composition. Alterations in the amount of channels can be induced by changes in expression level of the connexin proteins, turn-over rate, and distribution (presumably affected by the phosphorylation state of the channels [14]). In this review we will focus on modulating factors affecting expression and characteristics of gap junctions in the mammalian heart.

## 2. Expression of gap junction proteins in the heart.

Propagation of the action potential from cell to cell is mediated by current flow through gap junction channels, primarily located in the intercalated disc (ID) at the end-to-end intercellular connections. Large and small ID's are found parallel to the long axis of the cell (interplicate) while only small ID's can be found in regions at right angles to the long axis (plicate) [15].

In mammalian hearts, cardiomyocytes most prominently express gap junctions built of connexin40 (Cx40), connexin43 (Cx43) and connexin45 (Cx45). Therefore, we will restrict this review to these three isoforms. Another three isoforms have been reported; in several species, connexin37 is expressed in the endothelial cells of the endocardium, aorta and coronary vessels [16-18], where it is co-expressed with Cx40 [19]. Connexin46 protein has in addition to other isoforms been demonstrated in the rabbit sino-atrial node [20]. Connexin50 protein has been detected in the atrio-ventricular valves of rat heart [21].

The expression patterns of Cx40, Cx43 and Cx45 are subject to remarkable spatio-temporal differences [17,22-24]. In adult hearts Cx43 is the major expressed

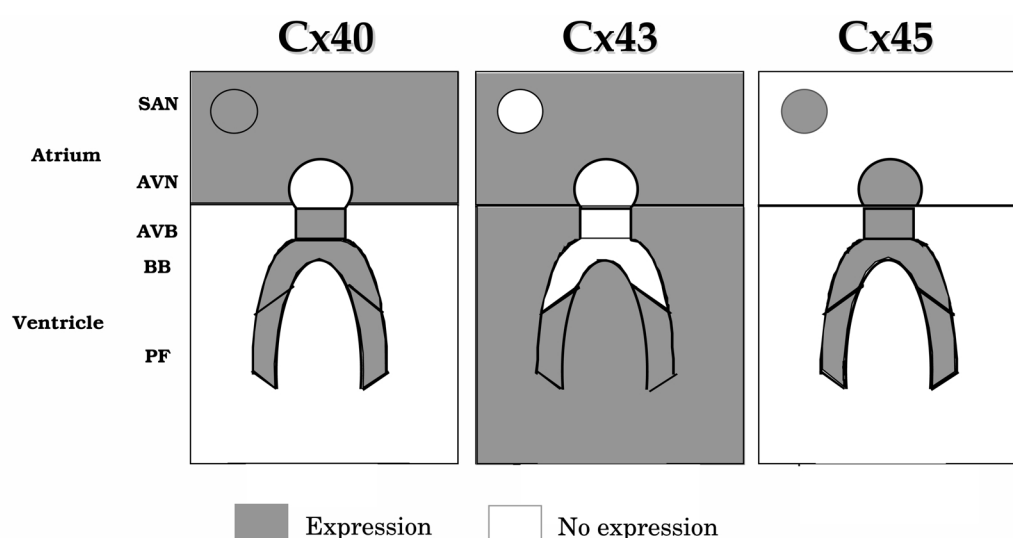


*Figure 2.2 Generalized expression pattern of Cx40, Cx43 and Cx45 in the different regions of the mammalian heart. SAN=sinoatrial node, AVN=atrioventricular node, AVB=atrioventricular bundle or His-bundle, BB=bundle branches, PF=Purkinje fibers.*

isoform. Figure 2.2 depicts the generalized adult expression patterns of Cx40, Cx43 and Cx45. In mammalian hearts, Cx43 is expressed in virtually all myocytes of the working atrial- and ventricular mammalian myocardium regardless the stage of development. No Cx43 is found in the nodal cells of the SA- and AV-node. In the ventricular conduction system of mouse and rat, Cx43 is absent in the common His-bundle and proximal parts of both bundle branches, but it is expressed in more distal parts of the bundle branches. In larger species as cow, dog, pig and human, Cx43 is expressed in all parts of the ventricular conduction system.

Cx45 is expressed in the rabbit SA node [25]. In rat and mouse hearts, Cx45 is found in the AV-node and complete ventricular conduction system but only at very low levels in the surrounding working myocardium of atria and ventricles [26,27].

The third connexin, Cx40, is strongly co-expressed with Cx43 in the working myocardium of the atria (except in rat). During fetal and neonatal development, Cx40 is still present in the ventricles where the intensity of expression gradually declines from endo- to epicard [28]. However, within days after birth, expression levels decrease and in adult stages Cx40 is absent in the ventricular working myocardium. Cx40 remains strongly expressed in the ventricular conduction system where it colocalizes with Cx45. Finally, low levels of Cx40 are present in the SA-node and AV-node of dog and cow [29], and the rabbit SA-node [20,25]. Differences in expression patterns between the hearts of different species have been described in detail by Gros and Jongsma [30], and quoted references.

### **3. Modulation of gap junction channels built of Cx40, Cx43 and Cx45 in a reduced cell-system.**

Cardiac gap junction channels have been intensively studied in cultured cardiac myocytes. Although ventricular cardiomyocytes probably exclusively express Cx43, other cardiomyocytes can express more than one type of connexin. The expression of more than one connexin isoform might give rise to heterotypic/heteromeric channel formation, thereby creating a plethora of different channel types with a high level of complexity. Appropriate assessment of the electrical properties of the individual gap junction isoforms requires a simplified cell system expressing only one isoform.

The genes encoding for the different cardiac connexins have been characterized, cloned and introduced in non-communicating tumor cells or *Xenopus* oocytes in order to create a reduced cell-system over-expressing (exogenous) gap junction channels built of one type of connexin only. Such a simplified system allows for evaluation of single channel properties and some of the modulating factors affecting these properties. We will focus our attention on the genes cloned from human, mouse and rat.

The isoform- but also species specific characteristics are particularly determined by variations in the amino acid sequence of the cytoplasmic loop (between transmembrane segment 2 and 3) and the C-terminus where multiple amino acid-motifs are found to be susceptible to phosphorylation by different intracellular protein kinases [6,31-33]. Phosphorylation occurs predominantly on serine residues, but also on threonine and tyrosine residues. Interestingly, cyclic nucleotides which activate protein kinases, are also able (in nanomolar concentrations) to modulate channel properties directly [34]. Together with more conserved domains of the protein, the cytoplasmic loop and carboxy-terminus might be involved in different modes of regulation. The C-terminus, N-terminus,

first transmembrane segment, first extracellular loop and a conserved proline residue in the second transmembrane segment, are reported to participate in the voltage gating properties of the channels [35,36], possibly similar to pH gating, according to a “ball-and-chain” model [37]. In addition, voltage gating might be influenced by the interaction of a connexon with its opposing connexon [38]. Protonation of three conserved histidine residues in the cytoplasmic loop might be required in the process of pH gating [39-41]. In Cx43 channels, these histidines may serve as a receptor for yet unidentified parts of the carboxy-terminus in order to facilitate pH gating according to the mentioned “ball-and-chain” model [42,43]. A similar model was postulated for Cx40 but not for Cx45 [44]. A cooperative interaction has been described for Cx40 and Cx43 which increases the pH sensitivity of those channels [45]. Within the physiologically relevant range of intracellular  $\text{Ca}^{2+}$  and  $\text{H}^{+}$  concentrations, it's unlikely that  $\text{Ca}^{2+}$  or  $\text{H}^{+}$  independently strongly affect the conductive properties of Cx43 channels [41,46]. Yet, there might be a (not completely understood) synergistic mechanism between  $\text{Ca}^{2+}$  and  $\text{H}^{+}$  that potentiates their effect on Cx43 channels and could be of importance under conditions of cardiac ischemia when intracellular  $\text{Ca}^{2+}$  and  $\text{H}^{+}$  are elevated [47,48].

Intercellular coupling concerns macroscopic (electrical) conductance ( $g_j$ ) and metabolic coupling. Both are determined by the number of expressed channels ( $N$ ), the single channel conductance ( $\gamma_j$ ) or permeability and the open probability of a single channel ( $P_o$ ). Single channel properties can be affected by modulation of  $\gamma_j$  but also by changes in  $P_o$  of the channels. Electrical coupling of cells can be studied using the double-voltage-clamp technique [49,50]. Metabolic coupling is evaluated by the passage of small fluorescent (dye) metabolites [1]. Most commonly used tracers are Lucifer Yellow (LY, 443 Da), 2',7'-dichlorofluorescein (DCF, 401 Da) and 6-carboxyfluorescein (6CF, 376 Da). The next sections summarize the characteristics of homotypic channels built of Cx40, Cx43 and Cx45 as deduced from studies on transfected cells (see also table I).

### 3.1 Cx40 channel properties.

The Cx40 gene has been characterized and cloned from several species (see [6]). The coding region exists of 358 aminoacids in humanCx40 (hCx40) and mouseCx40 (mCx40) and of 356 in ratCx40 (rCx40). On Western blot, the protein can be separated in two bands of 40- and 42 kD [51,52]. To study the single channel characteristics, the gene has been introduced in several communication deficient cell-lines.

Cx40 channels are mildly sensitive to the transjunctional voltage gradient ( $V_j$ ) with a half-maximal inactivation at  $\pm 50$  mV [53,54]. Depending on the composition of the pipette solution [55], single channel recordings in transfected cell-lines show a variety of large conductance states of 120-200 pS and less frequently, a much smaller substate of  $\sim 30$ -40 pS [51,52,54,56]. Although rCx40 transfected in N2A cells appears cation selective, this was not found for mCx40 [54,57]. Both hCx40 and mCx40 are permeant to LY [9,52], while rCx40 is permeant to DCF and 6CF [54]. Sequence analysis of the cytoplasmic loop and the carboxy-terminus has revealed multiple consensus motifs for phosphorylation by several intracellular protein kinases [31,32]. Western analysis showed that Cx40 indeed exists in a phosphorylated and non-phosphorylated configuration [51,52]. The sequences for hCx40, rCx40 and mCx40 differ significantly. The hCx40 protein contains 7 putative sites for modulation by protein kinase C (PKC), but rCx40 and mCx40 contain 12 and 15 sites

respectively. The number of putative sites for modulation by PKA and PKG are 2 and 1 in human but 1 and 3 in rat and mouse. Consensus sites were not found for modulation by MAP-kinase in the 3 species.

In Hela cells transfected with mCx40, direct activation of both PKC and PKA increased phosphorylation of Cx40 (measured by incorporation of  $^{32}\text{P}$ ), but did not alter electrophoretic mobility of the 40 kD native protein on Western blot [51]. In contrast, in hCx40 transfected cells, a shift from 40 kD to 42 kD was found after stimulation of PKA [52]. In addition  $g_j$ ,  $\gamma_j$  and dye permeability increased significantly [52]. Up till now, no modulatory role for activated PKG has been reported.

### 3.2 Cx43 channel properties.

Characteristics of Cx43 channels, the main cardiac connexin, have been studied extensively (see [6]). The coding region exists of 382 amino acids in human, mouse and rat.

Like Cx40 channels, Cx43 channels are not very sensitive to  $V_j$ . Conductance starts to decrease when  $\Delta V_j$  exceeds  $\pm 40$  mV and half-maximal inactivation occurs at  $\pm 60$  mV [58]. Cx43 channels are not ion selective [57]. rCx43 and hCx43 channels exhibit three  $\gamma_j$ 's; a major state at 40-60 pS, and two states of minor occurrence of 20-30 pS and 70-100 pS. In mCx43 only the two largest are detected [51,59,60]. Dye permeability has been shown for LY [9,51,61,62].

hCx43 contains 10 putative phosphorylation sites [31,32] for PKC, 4 for PKA, 3 for PKG and 2 for MAPkinase. In rCx43 and mCx43, 14 sites for PKC, 3 for PKA, 4 for PKG and 3 for MAPkinase can be identified (see table 2.I). In most studies, the protein presents on Western blot as three bands with molecular weights ranging from 41 kD to 46 kD. They represent the non-phosphorylated state (NP), a phosphorylated state (P1) and a highly phosphorylated state (P2) of gradually larger molecular size [60,63-65]. Phosphorylation of Cx43 has been described mainly on serine but also on tyrosine residues and seems to be involved in trafficking and insertion into the membrane [14]. Direct stimulation of PKC with TPA (a phorbol ester) rapidly (hyper)-phosphorylates Cx43 on Ser368 [66]. After prolonged stimulation, down-regulation of Cx43 and trafficking failure are observed (see [4]). Additionally, phosphorylation of rCx43 on Ser255 accelerates internalization and degradation [67].

Serine phosphorylation, mediated by PKA, PKC, PKG and MAP-kinase, merely stimulates the prevalence of the smallest  $\gamma_j$ . In contrast, treatment of cells with agents promoting dephosphorylation, shifts  $\gamma_j$  to the largest state [60]. Permeation to dye molecules seems closely related to the size of  $\gamma_j$ . However, changes in  $\gamma_j$  appear not exclusively related to changes in  $g_j$  because phosphorylation might also affect  $P_o$ . Stimulation of PKG (in rCx43 transfected cells) and PKC (in rCx43 and hCx43 transfected cells), reduces both dye permeability and  $\gamma_j$  [59,65,68]. Surprisingly, PKG stimulation causes a reduction in  $g_j$ , whereas stimulation of PKC increases  $g_j$  although both decrease  $\gamma_j$ . This can only be explained by a different effect on  $P_o$  assuming that time limits a substantial change in the number of channels (the effect of phosphorylation occurs within minutes while half-life of Cx43 is about 1.5 hours [69]). As mentioned, hCx43 channels are insensitive to modulation by PKG [65]. The substitution of Ala at position 257 in hCx43 instead of Ser in rCx43 explains why rCx43 is susceptible to phosphorylation by PKG and hCx43 is not. PKA activation using cAMP and forskolin reduces  $\gamma_j$  in hCx43 channels [68], but has no effect on rCx43 channels [59].

Finally, tyrosine phosphorylation reduces  $g_j$  which can be induced by inhibition

of tyrosine-phosphatase, or by activation of viral tyrosine kinases as p130<sup>gag-fps</sup> and v-Src [70,71]. This is illustrated by an reduction of  $g_j$  when Cx43 is phosphorylated by v-Src on tyr265 [72]. Besides the tyrosine kinase activity of v-Src, downstream activation of MAP-kinase induces phosphorylation on serine residues [73]. In rat liver epithelial cells, activation of MAP kinase by epidermal growth factor and of PKC and MAP-kinase by platelet-derived growth factor, rapidly decreases  $g_j$  by phosphorylation of Cx43 on Ser255, 279 and 282 [74-76].

### 3.3 Cx45 channel properties.

Cx45 is the least extensively studied of the three connexins expressed in cardiomyocytes. The gene has been cloned from mouse and human (see [6]), and also from rat (personal communication, Dr. MFA Bierhuizen). The coding region of the gene consists of 396 aminoacids in human and rat, and 395 in mouse. Most investigations concern hCx45 endogenously expressed in SkHep1 cells [41,77,78] or mCx45 transfected in Hela cells [9,79]. Cx45 channels are selective for cations [80]. They are steeply voltage dependent compared to Cx40 and Cx43, with half maximal activation at  $\pm 20$  mV [56,78]. Cx45 channels are more sensitive to changes in intracellular pH than Cx43 channels, with a complete block of junctional communication at pH 6.3 [41]. Unitary conductances are small with values of about 20 pS and 40 pS [59,79,80]. mCx45 but not hCx45 channels appear moderately permeable for LY [9,59,62]. Veenstra *et al.* showed that hCx45 channels are permeant to DCF but not to 6CF which depends on the charge of the molecules [80].

There are 15 putative phosphorylation sites [31,32] for PKC in hCx45 and 17 in rCx45 and mCx45. In all three species 1 site is found for modulation by PKA but no consensus sites were found for modulation by PKG or MAP-kinase. As with Cx40 and Cx43, Cx45 is phosphorylated mainly on serine-, but also on tyrosine residues [77,79,81,82]. Phosphorylation of serine residues in the carboxy-tail of mCx45 stabilizes the protein [83]. There is debate on the electrophoretic mobility of the protein. Some groups have separated Cx45 as a single band of 45 kD [26,83], or of 48 kD [24,78], while others claim to have detected two bands of 46 kD and 48 kD of which the 46 kD band was proposed to be either a proteolytic product [77], or the unphosphorylated state of the native protein [79]. Kwak *et al.* have reported that  $\gamma_j$  of hCx45 channels increases upon stimulation of PKC, but not of PKA and PKG. Phosphorylation by PKC elicits a third conductance state of 16 pS [59].  $\gamma_j$  of mCx45 channels is not affected by stimulation of PKC, PKA, PKG nor by tyrosine phosphatase inhibition mediated by pervanadate. However,  $g_j$  decreases upon stimulation of PKA and inhibition of tyrosine-phosphatase, but increases upon stimulation of PKC. Changes in  $g_j$  upon stimulation of PKA and phosphatase inhibition were accompanied by an increase in phosphorylation as shown on Western blot [79].

### 3.4 From transfected cells back to the heart.

Even in a simplified cell-system there is complexity in regulation, because of differences in properties of homotypic channels of Cx40, Cx43 and Cx45 with their differential modulation by protein kinases. Additionally, at least in transfected cells, heterotypic channels exist for Cx40/Cx45 and Cx43/Cx45 [9,84]. Recently, two studies suggested the formation of both heterotypic and heteromeric Cx40/Cx43 channels [85,86] which is in contrast with previous data [11,53,87].

Table 2.1		Cx40			Cx43			Cx45		
species		human	rat	mouse	human	rat	mouse	human	rat	mouse
Coding region (aa)		358	356	358	382	382	382	396	396	395
Motifs for PKC		7	12	15	10	14	14	15	17	17
PKA		2	1	1	4	3	3	1	1	1
PKG		1	3	3	3	4	4	0	0	0
MAPkinase		0	0	0	2	3	3	0	0	0
Dye permeability		+LY <sup>(52)</sup>	+DCF, +6CF <sup>(54)</sup>	+LY <sup>(9)</sup>	+LY <sup>(61)</sup>	+LY <sup>(59)</sup>	+LY <sup>(9)</sup>	-DCF,-LY <sup>(59)</sup> -6CF,+DCF <sup>(80)</sup>	N.D.	+LY <sup>(9)</sup>
Single channel conductance (pS)		30,80,120 <sup>(52)</sup>	158,180 <sup>(54)</sup>	121,153 <sup>(51)</sup> 36,198 <sup>(56)</sup>	30,60,90 <sup>(60)</sup> 20,40,70 <sup>(65)</sup>	30,60,90 <sup>(59)</sup> 20,40,70 <sup>(65)</sup>	40,60 <sup>(51)</sup>	22,36 <sup>(59)</sup> 28 <sup>(80)</sup>	N.D.	22,39 <sup>(51)</sup>
V <sub>0</sub>		N.D.	+/- 50 mV <sup>(54)</sup>	N.D.	+/- 60 mV <sup>(60)</sup>	N.D.	N.D.	+/- 20 mV <sup>(78)</sup>	N.D.	N.D.

Table 2.1: general properties of Cx40, Cx43 and Cx45 from human, mouse and rat.

Heterotypic- and heteromeric channel properties differ from those of the two participating connexins when expressed as a homotypic channel [85,86,88]. In transfected cells the connexins are under control of an artificial promoter. Therefore, modulation of properties is restricted to short term processes. In cardiomyocytes prolonged stimulation of protein kinases and exposure to signalling molecules may provoke additional effects on expression and distribution of the channels. In the next paragraph, we will discuss the regulation of channel properties in cardiomyocytes.

#### **4. Modulatory mechanisms of gap junction channels in cardiac myocytes.**

In cardiomyocytes, most studies regarding short term regulation of gap junction channels (affecting single channel properties) are performed using cultured neonatal myocytes or pairs/clusters of freshly isolated adult myocytes derived from incomplete dissociation of cardiac tissue. Studies on changes in expression/distribution of connexins induced by prolonged stimulation of protein kinases or by application of growth factors, are generally performed using cultured neonatal (1-2 days old) rat ventricular myocytes. These cells are relatively easy to isolate in large amounts and can be cultured in monolayers for more than a week meanwhile retaining their electrical activity. In contrast, adult myocytes lose their expression of connexins very rapidly upon isolation. Also, they do not attach in confluent monolayers.

Cultured neonatal ventricular myocytes express Cx40 and Cx43 and a small amount of Cx45 [28,89]. In culture, similar to the intact neonatal ventricle, the heterogenic expression of Cx40 declines in time and is susceptible to culture conditions [28]. It is unknown whether the heterogeneity of Cx40 expression (including regulation) in culture is a reflection of the original expression in the heart.

In neonatal cardiomyocytes, gap junctional coupling is characterized by channels with a main  $\gamma_j$  of 40-45 pS, but also a substate of 20 pS (using K-gluconate as charge carrier) [90-92]. Dephosphorylation of Cx43 channels increases  $\gamma_j$  to 70 pS [91]. Dye permeability seems related to the size of  $\gamma_j$ . Although channels of other connexins might be present, the measured  $\gamma_j$ 's closely resemble those described for Cx43 channels in transfected cells.

In adult myocytes,  $\gamma_j$ 's have been measured both in ventricular and atrial cells. Both guinea-pig and rabbit ventricular cells express channels insensitive to  $V_j$  with a main  $\gamma_j$  of ~100 pS (using CsCl as charge carrier), presumably reflecting Cx43 channels [18,93]. In rabbit atrial cells, next to the 100 pS conductance a larger conductance of 185 pS was measured which likely represents the gating of Cx40 channels [18].

Several studies on modulation of channel properties show that especially under conditions of ischemia,  $g_j$  might be synergistically modulated by  $H^+$ ,  $Ca^{2+}$  and amphiphatic lipid metabolites [47,48,94-96]. The effect of phosphorylation of connexin molecules on modulation of channel properties can be studied using membrane permeant drugs which directly activate the protein kinases. In addition, application of several extracellular factors has been used to study receptor mediated activation of kinases (see figure 2.3).

Acute stimulation of PKG, as described for rCx43 channels in transfected cells, reduces  $g_j$ ,  $\gamma_j$  and dye permeability [90,97]. In many (but not all [90]) reports an increase of  $g_j$  is found upon application of cAMP [97-99], isoproterenol [99,100], forskolin [99], norepinephrin [101], or by dialyzing the catalytic subunit of PKA into the cells [102]. The modulating role of PKC is debated. Stimulation of PKC

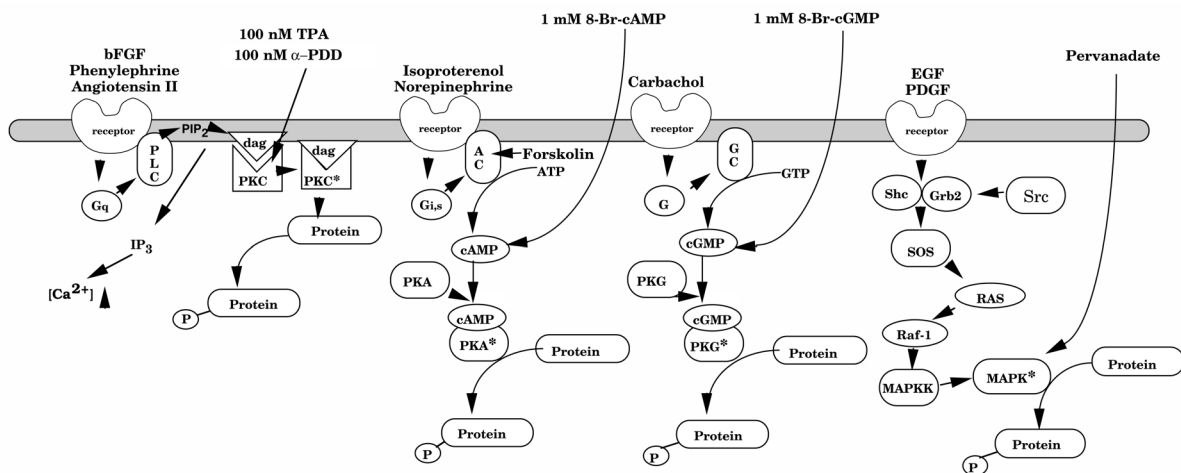


Figure 2.3 Simplified scheme showing signal transduction pathways initiated by receptor-binding of extracellular neuro-humoral factors (or synthetic analogues) or application of membrane-permeant drugs, finally resulting in the intracellular activation of protein kinases. Abbreviations: PLC=phospholipase C, IP<sub>3</sub>=inositol-tri-phosphate, DAG=di-acyl-glycerol, AC=adenylate cyclase, GC=guanylate cyclase. For more abbreviations see the acronyms and regarding MAP kinase signalling in review [159].

increased phosphorylation of Cx43 on seryl residues [103]. Reports describing modulation mediated by PKC show a decrease of  $\gamma_j$  and dye coupling but an overall increase in  $g_j$  [90], or a decrease in  $g_j$  without changes in  $\gamma_j$  [104].

Cardiomyocytes possess a local renin-angiotensin system in which Angiotensin-I (AngI) is converted by Angiotensin-Converting-Enzyme (ACE) to Angiotensin-II (AngII). AngII, the effective metabolite of the system, exerts its action through binding at AT-1- and AT-2 receptors, thereby activating PKC and MAP-kinases Erk1 and Erk2, respectively. De Mello *et al.* have shown that administration of renin, Ang-I or Ang-II to adult rat myocytes rapidly reduces  $g_j$  due to activation of PKC [105-108]. In contrast, inhibition of ACE increases  $g_j$  [107]. Phenylephrine binding to  $\alpha_1$ -adrenergic receptors also activates PKC and similarly to Ang-II decreases  $g_j$  [109]. Additionally, basic FGF (bFGF) reduced metabolic coupling as assessed by dye-transfer while phosphorylation of Cx43 was strongly increased mainly on serine residues but also on tyrosine residues [110].

These short term effects (within 5-10 minutes) on gap junctional conductance are probably caused by connexin phosphorylation because within this limited period no changes in expression or translocation are expected. When the stimulation period is prolonged to 6-24 hours, additional changes have been reported in expression level of the connexin proteins in rat neonatal cardiomyocytes.

Myotrophin, strongly increased the amount of Cx43 mRNA [111] while cAMP significantly increased conduction velocity in strands of cultured myocytes [82]. This effect was accompanied by an increased expression (gap junctions increased in number and size) of Cx43 and Cx45 which resulted from an increase in Cx43 mRNA and an enhanced translation of Cx45 mRNA. A similar increase in Cx43 expression, functionally shown by more and larger gap junctions, was observed in an AT-1 receptor mediated response after stimulating cells with Ang-II [112]. Wnt-1 stimulation of neonatal rat cardiomyocytes increased Cx43 mRNA and protein which resulted in an enhanced dye permeability and propagation of calcium [113]. In non-myocyte cardiac cells like fibroblasts, bFGF increased both Cx43 mRNA and protein thereby increasing dye transfer [114]. Additionally, potentially

interesting factors as epidermal growth factor (EGF), platelet derived growth factor (PDGF), transforming growth factor  $\beta$  (TGF $\beta$ ), tumor necrosis factor  $\alpha$  (TNF $\alpha$ ) and interleukin 1 $\beta$  (IL-1 $\beta$ ), affect Cx43 channel properties in non-cardiac cells [75,76,115-117]. Finally, mechanical stretch which activates multiple signaling pathways has been reported to strongly increase expression of Cx43 but not of Cx40 in rat neonatal cardiomyocytes [118,119]. Increased expression of Cx43 resulted both from an increase in mRNA and an decrease in turn-over of the protein [119].

## **5. Implications of gap junction modulation for cardiac function.**

Results from studies on transfected cells and cardiomyocytes are reasonably comparable. The question remains to what extent modulation of intercellular coupling affects cardiac performance. In only one study on patients suffering from complex congenital heart defects, a Ser364Pro mutation was detected which in transfected cells appeared to induce abnormal behavior of Cx43 channels [120] but this was not confirmed by others [121]. The spatial differences in expression of Cx40, Cx43 and Cx45 channels (section 2) combined with differences in connexin properties and modulation (section 3 and 4), appear to be reflected into specific conductive properties in different regions of the heart. The most direct approach to unravel the specific role of a given connexin is targeted deletion of the gene involved. Using this strategy, Cx40, Cx43 and Cx45 knock-out (KO) mice have been generated.

Another approach is to study the function of gap junction channels in multiple forms of cardiac disease where changes in expression, distribution and phosphorylation during the progression of the underlying pathophysiology have been reported.

### **5.1 Connexin knock-out mice.**

Cx43 KO mice die perinatally due to an obstruction of the right outflow tract caused by cardiac malformations [122,123]. Isolated and perfused neonatal Cx43 KO hearts were completely unexcitable [124]. In contrast, heterozygous mice are viable and reproductive. The heterozygous hearts have a normal morphology and show a 50% reduction in expression of Cx43 mRNA and -protein [125]. The consequences of this severe reduction in Cx43 protein for ventricular conduction are debated. Initial reports mention a 30-40% reduced ventricular conduction velocity and a prolongation of the QRS complex. [125,126] However, detailed optical mapping did not reveal differences [127]. During ischemia an increased susceptibility to ventricular arrhythmias was found [128]. A similar 50% reduction in Cx43 expression was found in the atria but this did not affect conduction velocity [126]. Transgenic mice overexpressing a dominant-negative form of Cx43 (leading to non-functional channels) are phenotypically similar to Cx43 KO mice [129].

Electrophysiological characteristics of mice heterozygous for Cx40 deletion are comparable to wild-type mice [130], but Cx40 KO mice show multiple aberrations: prolongation of PQ interval [130,131], reduced atrial conduction velocity with a prolonged P-wave, prolonged sinus-node-recovery time, prolonged Wenckebach period, atrial tachyarrhythmias following burst pacing, and reduced A-V conduction; [132,133], impaired left and right bundle branch conduction[134,160], or right bundle branch block [134]. No differences were found between WT and KO mice

regarding ventricular conductive properties which is explained by the absence of Cx40 in the ventricle. A prolongation of QRS duration was described [130,133], but not when the ventricle was paced from the apex [133] which indicates that the prolongation is due to impairment of the conduction system [134].

Two groups have reported the generation of a Cx45 KO mouse [135,136]. Heterozygous mice are comparable with WT animals as with heterozygous Cx40 KO mice. However, Cx45 KO mice die *in utero* on day 10.5 pc. Embryonic hearts were dilated due to defective vascular development [136]. Interestingly, within 24 hours after the first contractions of these developing hearts *in utero*, severe impairment of atrial contraction develops and atrio-ventricular conduction block appears [135].

Obviously, gap junctions play an important role in growth and development. Thus, deletion of connexin genes not only affects their specific cardiac function but may also induce developmental alterations. To date, inducible KO mice are constructed in which the connexin gene is surrounded by loxP sites. With this approach, an inducible system activates a recombinase protein (Cre) which connects both loxP sites by deletion of the DNA (connexin gene) in between [137]. In this way, deletion of the genes can be induced at any stage of development which may result in a more clear distinction between the role of gap junctions in development and cardiac function.

## 5.2 Ischemic heart disease and cardiac hypertrophy.

Most myocardial diseases are marked by alterations at the expression level of the connexins and/or the anisotropic distribution of gap junction plaques [138-140]. A decrease in expression level of ventricular Cx43 is often detected by Western (protein)- or Northern (mRNA) analysis [141,142]. Obviously, changes in cell- and tissue homeostasis and alterations in (circulating) levels of second messengers and growth factors (see section 4) have an impact on the alteration in expression pattern. In hearts of hypertensive rats (spontaneous or renin transgenic) where the renin-angiotensin signaling is forced, a 3 fold increase in Cx40 expression and a 3 fold decrease in Cx43 expression was reported [143]. Regardless the nature of cardiac disease, one of the most commonly found alterations is a shift in distribution of gap junction plaques from the end-to-end ID's to lateral cell borders (see [144]). In healthy myocardium, the anisotropic distribution of gap junctions contributes to differences between conduction velocity in longitudinal and transverse directions. A redistribution of Cx43 gap junctions has been reported in the borderzone of infarcts [142] where it was associated with the localization of reentrant circuits [145], but also in hibernating myocardium [146], in hypertrophied hearts [139], in ischemic hearts [141] and in hypertrophic cardiomyopathy [138]. Often, the redistribution is accompanied by a decrease in size of the gap junction plaques [146] or in the total amount of plaques per ID [139]. In the study of Uzzaman, this change was associated with a 30% reduction in longitudinal conduction velocity [139].

Despite the fact that in most cardiomyopathies an increased propensity to arrhythmias has been reported, the functional contribution of both type of alterations, i.e. change in density and distribution, are not completely understood. The significance of redistribution to lateral cell-borders is debatable because lateral gap junctions may prove non-functional if located in intracellular invaginations of the sarcolemma [147]. However, both redistribution and a 20%-40% reduction in gap junctions per se will decrease the anisotropy in the tissue which is often considered as anti-arrhythmic [148], but by some as pro-arrhythmic because it

decreases the “wavelength” of the myocardium [149]. Despite these significant alterations, Jongsma and Wilders computed only small to moderate changes in conduction velocity and anisotropy ratio [150]. Both Spach and Jongsma showed that the contribution of changes in cytoplasmic resistivity (cellular geometry) might be equally important especially for longitudinal conduction [150,151]. Additionally, Fast *et al.* showed that discontinuity in anisotropy, which results in non-linear conduction, increases the propensity for arrhythmias far more than uniform changes in anisotropy ratio in a continuous system. This implies that conduction block in a discontinuous system can be induced by minor alterations in intercellular coupling compared to the extensive uncoupling required in a continuous system [152].

Modulation by phosphorylation of the connexin proteins has been introduced as an important factor for remodeling of gap junctions in diseased hearts. In normal hearts, Cx43 exists in a phosphorylated state. Beardslee *et al.* suggested that unphosphorylated Cx43 is principally degraded by the proteosomal pathway and phosphorylated Cx43 by the lysosomal pathway [69]. Recently, the same group showed in a model of acute ischemia that uncoupling of cardiac tissue is associated with dephosphorylation of Cx43 and accumulation of unphosphorylated Cx43 in the gap junction plaques [153]. In hereditary cardiomyopathic hamsters, endstage congestive heart failure correlates with a c-Src mediated increase in phosphorylation of Cx43 on tyrosine residues. As a consequence,  $g_j$  between pairs of myocytes decreased [154]. These studies suggest that in the intact heart phosphorylation serves as an important modulator of cardiac conduction.

Studies on remodeling of gap junctions in atrium are scarce. In dog atrium, atrial fibrillation induced by pacing increased the expression of Cx43. In chronic atrial fibrillation in the goat, Cx40 expression is reduced. Moreover, this reduction is heterogenous. In contrast to the dog, in the goat atrium no changes in the amount of Cx43 mRNA and protein have been detected, but the prevalence of unphosphorylated Cx43 seems increased [140,155,156].

## 6. Concluding remarks.

A vast amount of information regarding the specific properties of different gap junction channels, their expression in the heart and the mechanisms to modulate their properties, has been acquired during the past decade. Extrapolation of this knowledge obtained from experiments with transfected cells or isolated and cultured cardiomyocytes to the intact heart is a challenge for the near future. Deletion of connexin genes affects cardiac conduction only to a moderate extent. This is illustrated by heterozygous Cx40- and Cx43 KO mice in which conduction properties are comparable to WT hearts. These observations were supported by a theoretical study [150]. In cardiomyopathic hearts, alterations in gap junctions expression/distribution may be involved in the increased propensity to arrhythmogenesis, but changes in cellular dimensions following the pathophysiological process, may be relevant as well [151]. Inducible KO mice will be an adequate tool in the near future. Generation of mice with (inducible) forced expression- or targeted deletion of potentially involved genes, allows to focus the attention on specific factors in the variety of involved signalling processes. For example, Nguyen-Tran *et al.* showed that mice deficient for HF-1b, a transcription factor preferentially expressed in the cardiac conduction system, display sudden cardiac death. This was associated with a reduced expression, and redistribution of Cx40 in the cardiac conduction system [157]. Furthermore, in another mouse model, a constitutive active retinoic acid receptor provokes cardiac hypertrophy

accompanied with a heterogeneous reduction of Cx43 expression in the ventricles [158]. These are examples of new models that in the near future may advance our knowledge on the relevance of gap junctions in cardiovascular disease.

## Acknowledgements

A.A.B.v.V. and H.V.M.v.R. were financially supported by grant no. 97.184 from the Netherlands Heart Foundation.

## References

- [1] Simpson, I, Rose, B, Loewenstein, WR. Size limit of molecules permeating the junctional membrane channels. *Science* 1977;195:294-296.
- [2] Bevens, CG, Kordel, M, Rhee, SK, Harris, AL. Isoform composition of connexin channels determines selectivity among second messengers and uncharged molecules. *J Biol Chem* 1998;273:2808-16.
- [3] Goldberg, GS, Lampe, PD, Nicholson, BJ. Selective transfer of endogenous metabolites through gap junctions composed of different connexins. *Nat Cell Biol* 1999;1:457-459.
- [4] Goodenough, DA, Goliger, JA, Paul, DL. Connexins, connexons, and intercellular communication. *Annu Rev Biochem* 1996;65:475-502.
- [5] Kumar, R, Wilders, R, Joyner, RW, *et al.* An experimental model for an ectopic focus coupled to ventricular cells. *Circulation* 1996;94:833-841.
- [6] Bruzzone, R, White, TW, Paul, DL. Connections with connexins: The molecular basis of direct intercellular signaling. *Eur.J.Biochem.* 1996;238:127.
- [7] White, TW, Paul, DL. Genetic diseases and gene knockouts reveal diverse connexin functions. *Annu Rev Physiol* 1999;61:283-310.
- [8] Zhou, XW, Pfahnl, A, Werner, R, *et al.* Identification of a pore lining segment in gap junction hemichannels. *Biophys J* 1997;72:1946-53.
- [9] Elfgang, C, Eckert, R, Lichtenberg-Fraté, H, *et al.* Specific permeability and selective formation of gap junction channels in connexin-transfected HeLa cells. *J Cell Biol.* 1995;129:805-817.
- [10] White, TW, Bruzzone, R, Wolfram, S, Paul, DL, Goodenough, DA. Selective interactions among the multiple connexin proteins expressed in the vertebrate lens: the second extracellular domain is a determinant of compatibility between connexins. *J Cell Biol* 1994;125:879-92.
- [11] White, TW, Paul, DL, Goodenough, DA, Bruzzone, R. Functional analysis of selective interactions among rodent connexins. *Mol Biol Cell* 1995;6:459-70.
- [12] Falk, MM, Kumar, NM, Gilula, NB. Membrane insertion of gap junction connexins: Polytopic channel forming membrane proteins. *J Cell Biol.* 1994;127:343-355.
- [13] Musil, LS, Goodenough, DA. Multisubunit assembly of an integral plasma membrane channel protein, gap junction connexin43, occurs after exit from the ER. *Cell* 1993;74:1065-77.
- [14] Musil, LS, Goodenough, DA. Biochemical analysis of connexin43 intracellular transport, phosphorylation, and assembly into gap junctional plaques. *J Cell Biol* 1991;115:1357-74.
- [15] Severs, NJ. The cardiac gap junction and intercalated disc. *Int J Cardiol* 1990;26:137-73.
- [16] Reed, KE, Westphale, EM, Larson, DM, *et al.* Molecular cloning and functional expression of human connexin37, an endothelial cell gap junction protein. *J Clin Invest* 1993;91:997-1004.
- [17] Delorme, B, Dahl, E, Jarry-Guichard, T, *et al.* Developmental regulation of Connexin40 gene expression in mouse heart correlates with the differentiation of the conduction system. *Dev Dyn* 1995;204:358-371.
- [18] Verheule, S, Van Kempen, MJA, Te Welscher, PHJA, Kwak, BR, Jongsma, HJ. Characterization of gap junction channels in adult rabbit atrial and ventricular myocardium. *Circ Res* 1997;80:673-681.
- [19] Van Kempen, MJA, Ten Velde, I, Wessels, A, *et al.* Differential connexin expression accommodates

cardiac function in different species. *Microsc Res Tech* 1995;31:420-436.

[20] Verheule, S, Van Kempen, MJA, Postma, S, Rook, MB, Jongsma, HJ. Gap junctions in the rabbit sinoatrial node. *Am J Physiol* 2001;in press.

[21] Gourdie, RG, Green, CR, Severs, NJ, Thompson, RP. Immunolabelling patterns of gap junction connexins in the developing and mature rat heart. *Anat Embryol* 1992;185:363-78.

[22] Van Kempen, MJA, Vermeulen, JLM, Moorman, AFM, *et al.* Developmental changes of connexin40 and connexin43 mRNA distribution patterns in the rat heart. *Cardiovasc Res* 1996;32:886-900.

[23] Delorme, B, Dahl, E, Jarry-Guichard, T, *et al.* Expression pattern of connexin gene products at the early developmental stages of the mouse cardiovascular system. *Circ Res* 1997;81:423-37.

[24] Alcoléa, S, Théveniau-Ruissy, M, Jarry-Guichard, T, *et al.* Downregulation of Connexin45 gene products during mouse heart development. *Circ Res* 1999;84:1365-1379.

[25] Coppen, SR, Kodama, I, Boyett, MR, *et al.* Connexin45, a major connexin of the rabbit sinoatrial node, is co-expressed with connexin43 in a restricted zone at the nodal-crista terminalis border. *J Histochem Cytochem* 1999;47:907-18.

[26] Coppen, SR, Dupont, E, Rothery, S, Severs, NJ. Connexin45 expression is preferentially associated with the ventricular conduction system in mouse and rat heart. *Circ Res* 1998;82:232-243.

[27] Coppen, SR, Severs, NJ, Gourdie, RG. Connexin45 ( $\alpha 6$ ) expression delineates an extended conduction system in the embryonic and mature rodent heart. *Dev Genet* 1999;24:82-90.

[28] Kwak, BR, van Kempen, MJA, Théveniau-Ruissy, M, Gros, DB, Jongsma, HJ. Connexin expression in cultured neonatal rat cardiomyocytes reflects the pattern of the intact ventricle. *Cardiovasc Res* 1999;44:370-380.

[29] Kwong, KF, Schuessler, RB, Green, KG, *et al.* Differential expression of gap junction proteins in the canine sinus node. *Circ Res* 1998;82:604-12.

[30] Gros, D, Jongsma, HJ. Connexins in mammalian heart function. *BioEssays* 1996;18:719-730.

[31] Kemp, BE, Pearson, RB. Protein kinase recognition sequence motifs. *Trends Biochem.Sci.* 1990;15:342-346.

[32] Kennely, PJ, Krebs, EG. Consensus sequences as substrate specificity determinants for protein kinases and protein phosphatases. *J Biol Chem.* 1991;266:15555-15558.

[33] Pinna, LA, Ruzzene, M. How do protein kinases recognize their substrates? *Biochim Biophys Acta* 1996;1314:191-225.

[34] Bevans, CG, Harris, AL. Direct high affinity modulation of connexin channel activity by cyclic nucleotides. *J Biol Chem* 1999;274:3720-5.

[35] Suchyna, TM, Xu, LX, Gao, F, Fourtner, CR, Nicholson, BJ. Identification of a proline residue as a transduction element involved in voltage gating of gap junctions. *Nature* 1993;365:847-849.

[36] Verselis, VK, Ginter, CS, Bargiello, TA. Opposite voltage gating polarities of two closely related connexins. *Nature* 1994;368:348-351.

[37] Revilla, A, Castro, C, Barrio, LC. Molecular dissection of transjunctional voltage dependence in the connexin-32 and connexin-43 junctions. *Biophys J* 1999;77:1374-83.

[38] White, TW, Bruzzone, R, Goodenough, DA, Paul, DL. Voltage gating of connexins [letter]. *Nature* 1994;371:208-9.

[39] Spray, DC, Burt, JM. Structure-activity relations of the cardiac gap junction channel. *Am J Physiol.* 1990;258:C195-C205.

[40] Ek, JF, Delmar, M, Perzova, R, Taffet, SM. Role of histidine 95 on pH gating of the cardiac gap junction protein connexin43. *Circ Res* 1994;74:1058-64.

[41] Hermans, MMP, Kortekaas, P, Jongsma, HJ, Rook, MB. pH sensitivity of the cardiac gap junction proteins, connexin45 and 43. *Pflgers Archiv* 1995;431:138-140.

[42] Morley, GE, Taffet, SM, Delmar, M. Intramolecular interactions mediate pH regulation of connexin43 channels. *Biophys J* 1996;70:1294-302.

[43] Morley, GE, Ek-Vitorin, JF, Taffet, SM, Delmar, M. Structure of connexin43 and its regulation by pH. *J Cardiovasc Electrophysiol* 1997;8:939-51.

- [44] Stergiopoulos, K, Alvarado, JL, Mastroianni, M, *et al.* Hetero-domain interactions as a mechanism for the regulation of connexin channels. *Circ Res* 1999;84:1144-55.
- [45] Gu, H, Ek-Vitorin, JF, Taffet, SM, Delmar, M. Coexpression of connexins 40 and 43 enhances the pH sensitivity of gap junctions: a model for synergistic interactions among connexins. *Circ Res* 2000;86:E98-E103.
- [46] Firek, L, Weingart, R. Modification of gap junction conductance by divalent cations and protons in neonatal rat heart cells. *J Mol Cell Cardiol* 1995;27:1633-1643.
- [47] Burt, JM. Block of intracellular communication: interaction of intercellular H<sup>+</sup> and Ca<sup>2+</sup>. *Am J Physiol*. 1987;253:C607-C612.
- [48] White, RL, Doeller, JE, Verselis, VK, Wittenberg, BA. Gap junctional conductance between pairs of ventricular myocytes is modulated synergistically by H<sup>+</sup> and Ca<sup>++</sup>. *J Gen Physiol* 1990;95:1061-75.
- [49] Neyton, J, Trautmann, A. Single-channel currents of an intercellular junction. *Nature* 1985;317:331-335.
- [50] White, RL, Spray, DC, Campos de Carvalho, AC, Wittenberg, BA, Bennett, MVL. Some electrical and pharmacological properties of gap junctions between adult ventricular myocytes. *Am J Physiol*. 1985;249:C447-C455.
- [51] Traub, O, Eckert, R, Lichtenberg-Fraté, H, *et al.* Immunochemical and electrophysiological characterization of murine connexin40 and -43 in mouse tissues and transfected human cells. *Eur J Cell Biol*. 1994;64:1011-12.
- [52] Van Rijen, HVM, van Veen, AAB, Hermans, MMP, Jongsma, HJ. Human connexin40 gap junction channels are modulated by cAMP. *Cardiovasc Res* 2000;45:941-951.
- [53] Bruzzzone, R, Haefliger, JA, Gimlich, RL, Paul, DL. Connexin40, a component of gap junctions in vascular endothelium, is restricted in its ability to interact with other connexins. *Mol Biol Cell* 1993;4:7-20.
- [54] Beblo, DA, Wang, HZ, Beyer, EC, Westphale, EM, Veenstra, RD. Unique conductance, gating, and selective permeability properties of gap junction channels formed by connexin40. *Circ Res* 1995;77:813-22.
- [55] Valiunas, V, Bukauskas, FF, Weingart, R. Conductances and selective permeability of connexin43 gap junction channels examined in neonatal rat heart cells. *Circ Res* 1997;80:708-719.
- [56] Bukauskas, FF, Elfgang, C, Willecke, K, Weingart, R. Biophysical properties of gap junction channels formed by mouse Connexin40 in induced pairs of transfected human HeLa cells. *Biophys J* 1995;68:2289-2298.
- [57] Veenstra, RD, Wang, HZ, Beblo, DA, *et al.* Selectivity of connexin-specific gap junctions does not correlate with channel conductance. *Circ Res* 1995;77:1156-1165.
- [58] Moreno, AP, Rook, MB, Fishman, GI, Spray, DC. Gap junction channels, distinct voltage-sensitive and -insensitive conductance states. *Biophys J* 1994;67:113-119.
- [59] Kwak, BR, Hermans, MMP, De Jonge, HR, *et al.* Differential regulation of distinct types of gap junction channels by similar phosphorylating conditions. *Mol Biol Cell* 1995;6:1707-1719.
- [60] Moreno, AP, Sáez, JC, Fishman, GI, Spray, DC. Human connexin43 gap junction channels. *Circ Res* 1994;74:1050-1057.
- [61] Fishman, GI, Spray, DC, Leinwand, LA. Molecular characterization and functional expression of the human cardiac gap junction channel. *J Cell Biol* 1990;111:589-598.
- [62] Steinberg, TH, Civitelli, R, Geist, ST, *et al.* Connexin43 and Connexin45 form gap junctions with different molecular permeabilities in osteoblastic cells. *EMBO J* 1994;13:744-750.
- [63] Musil, LS, Cunningham, BA, Edelman, GM, Goodenough, DA. Differential phosphorylation of the gap junction protein connexin43 in junctional communication-competent and -deficient cell lines. *J Cell Biol* 1990;111:2077-88.
- [64] Laird, DW, Puranam, KL, Revel, JP. Turnover and phosphorylation dynamics of connexin43 gap junction protein in cultured cardiac myocytes. *Biophys J* 1991;273:67-72.
- [65] Kwak, BR, Sáez, JC, Wilders, R, *et al.* Effects of cGMP-dependent phosphorylation on rat and human Connexin43 gap junction channels. *Pflügers Archiv* 1995;430:770-778.

- [66] Lampe, PD, TenBroek, EM, Burt, JM, *et al.* Phosphorylation of connexin43 on serine368 by protein kinase C regulates gap junctional communication. *J Cell Biol* 2000;149:1503-12.
- [67] Lampe, PD, Kurata, WE, Warn-Cramer, BJ, Lau, AF. Formation of a distinct connexin43 phosphoisoform in mitotic cells is dependent upon p34cdc2 kinase. *J Cell Sci* 1998;111:833-41.
- [68] Moreno, AP, Fishman, GI, Spray, DC. Phosphorylation shifts unitary conductance and modifies voltage dependent kinetics of human connexin43 gap junction channels. *Biophys J* 1992;62:51-53.
- [69] Beardslee, MA, Laing, JG, Beyer, EC, Saffitz, JE. Rapid turnover of Connexin43 in the adult rat heart. *Circ.Res.* 1998;83:629-635.
- [70] Kurata, WE, Lau, AF. p130gag-fps disrupts gap junctional communication and induces phosphorylation of connexin43 in a manner similar to that of pp60v-src. *Oncogene* 1994;9:329-35.
- [71] Warn-Cramer, BJ, Cottrell, GT, Burt, JM, Lau, AF. Regulation of Connexin43 gap junctional intercellular communication by mitogenactivated protein kinase. *J Biol Chem* 1998;273:9188-9196.
- [72] Swenson, KI, Piwnica-Worms, H, McNamee, H, Paul, DL. Tyrosine phosphorylation of the gap junction protein connexin43 is required for the pp60v-src-induced inhibition of communication. *Cell Regul* 1990;1:989-1002.
- [73] Zhou, L, Kasperek, EM, Nicholson, BJ. Dissection of the molecular basis of pp60(v-src) induced gating of connexin 43 gap junction channels. *J Cell Biol* 1999;144:1033-45.
- [74] Lau, AF, Kanemitsu, MY, Kurata, WE, Danesh, S, Boynton, AL. Epidermal growth factor disrupts gap-junctional communication and induces phosphorylation of connexin43 on serine. *Mol Biol Cell* 1992;3:865-874.
- [75] Warn-Cramer, BJ, Lampe, PD, Kurata, WE, *et al.* Characterization of the MAPK phosphorylation sites in the Cx43 gap junction protein. *J Biol Chem* 1996;271:3779-3786.
- [76] Hossain, MZ, Ao, P, Boynton, AL. Platelet-derived growth factor-induced disruption of gap junctional communication and phosphorylation of connexin43 involves protein kinase C and mitogen-activated protein kinase. *J Cell Physiol* 1998;176:332-41.
- [77] Laing, JG, Westphale, EM, Engelmann, GL, Beyer, EC. Characterization of the gap junction protein, Connexin45. *J Membrane Biol* 1994;139:31-40.
- [78] Moreno, AP, Laing, JG, Beyer, EC, Spray, DC. Properties of gap junction channels formed of connexin45 endogenously expressed in human hepatoma (SKHep1) cells. *Am J Physiol.* 1995;268:C356-C365.
- [79] van Veen, TA, van Rijen, HV, Jongsma, HJ. Electrical conductance of mouse connexin45 gap junction channels is modulated by phosphorylation. *Cardiovasc Res* 2000;46:496-510.
- [80] Veenstra, RD, Wang, HZ, Beyer, EC, Brink, PR. Selective dye and ionic permeability of gap junction channels formed by Connexin45. *Circ Res* 1994;75:483-490.
- [81] Butterweck, A, Gergs, U, Willecke, K, Traub, O. Immunochemical characterization of the gap junction protein Connexin45 in mouse kidney and transfected human HeLa cells. *J Membrane Biol.* 1994;141:247-256.
- [82] Darrow, BJ, Fast, VG, Kléber, AG, Beyer, EC, Saffitz, JE. Functional and structural assessment of intercellular communication: Increased conduction velocity and enhanced connexin expression in dibutyryl cAMP-treated cultured cardiac myocytes. *Circ Res* 1996;79:174-183.
- [83] Hertlein, B, Butterweck, A, Haubrich, S, Willecke, K, Traub, O. Phosphorylated carboxy terminal serine residues stabilize the mouse gap junction protein Connexin45 against degradation. *J Membrane Biol* 1998;162:247-257.
- [84] Moreno, AP, Fishman, GI, Beyer, EC, Spray, DC. Voltage dependent gating and single channel analysis of heterotypic gap junctions formed of Cx45 and Cx43. *Progress in Cell Res* 1995;4:405-408.
- [85] He, DS, Jiang, JX, Taffet, SM, Burt, JM. Formation of heteromeric gap junction channels by connexins 40 and 43 in vascular smooth muscle cells. *Proc Natl Acad Sci USA* 1999;96:6495-500.
- [86] Valiunas, V, Weingart, R, Brink, PR. Formation of heterotypic gap junction channels by

connexins 40 and 43. *Circ Res* 2000;86:E42-9.

[87] Haubrich, S, Schwarz, HJ, Bukauskas, F, *et al.* Incompatibility of connexin 40 and 43 Hemichannels in gap junctions between mammalian cells is determined by intracellular domains. *Mol Biol Cell* 1996;7:1995-2006.

[88] Koval, M, Geist, ST, Westphale, EM, *et al.* Transfected Connexin45 alters gap junction permeability in cells expressing endogenous Connexin43. *J Cell Biol* 1995;130:987-995.

[89] Darrow, BJ, Laing, JG, Lampe, PD, Saffitz, JE, Beyer, EC. Expression of multiple connexins in cultured neonatal rat ventricular myocytes. *Circ Res* 1995;76:381-387.

[90] Kwak, BR, Jongsma, HJ. Regulation of cardiac gap junction channel permeability and conductance by several phosphorylating conditions. *Mol Cell Biochem* 1996;157:93-99.

[91] Kwak, BR, Van Veen, TAB, Analbers, LJS, Jongsma, HJ. TPA increases conductance but decreases permeability in neonatal rat cardiomyocyte gap junction channels. *Exp Cell Res* 1995;220:456-463.

[92] Rook, MB, Van Ginneken, ACG, De Jonge, B, *et al.* Differences in gap junction channels between cardiac myocytes, fibroblasts, and heterologous pairs. *Am J Physiol* 1992;263:C959-C977.

[93] Rüdüsili, A, Weingart, R. Electrical properties of gap junction channels in guinea-pig ventricular cell pairs revealed by exposure to heptanol. *Pflügers Archiv* 1989;415:12-21.

[94] Massey, KD, Minnich, BN, Burt, JM. Arachidonic acid and lipoxygenase metabolites uncouple neonatal rat cardiac myocyte pairs. *Am J Physiol* 1992;263:C494-C501.

[95] Wu, J, McHowat, J, Saffitz, JE, Yamada, KA, Corr, PB. Inhibition of gap junctional conductance by long chain acylcarnitines and their preferential accumulation in junctional sarcolemma during hypoxia. *Circ Res* 1993;72:879-889.

[96] Dekker, LR, Fiolet, JW, VanBavel, E, *et al.* Intracellular Ca<sup>2+</sup>, intercellular electrical coupling, and mechanical activity in ischemic rabbit papillary muscle. Effects of preconditioning and metabolic blockade. *Circ Res* 1996;79:237-46.

[97] Burt, JM, Spray, DC. Intropic agents modulate gap junctional conductance between cardiac myocytes. *Am J Physiol* 1988;254:H1206-H1210.

[98] De Mello, WC, van Loon, P. Influence of cyclic nucleotides on junctional permeability in atrial muscle. *J Mol Cell Cardiol* 1987;19:83-94.

[99] De Mello, WC. Impaired regulation of cell communication by betaadrenergic receptor activation in the failing heart. *Hypertension* 1996;27:265-8.

[100] De Mello, WC. Increase in junctional conductance caused by isoproterenol in heart cell pairs is suppressed by cAMP-dependent protein kinase inhibitor. *Biochem Biophys Res Commun* 1988;154:509-14.

[101] De Mello, WC. Influence of alpha-adrenergic-receptor activation on junctional conductance in heart cells: interaction with beta-adrenergic adrenergic agonists. *J Cardiovasc Pharmacol* 1997;29:273-7.

[102] De Mello, WC. Further studies on the influence of cAMP-dependent protein kinase on junctional conductance in isolated heart cell pairs. *J Mol Cell Cardiol* 1991;23:371-9.

[103] Saez, JC, Nairn, AC, Czernik, AJ, *et al.* Phosphorylation of connexin43 and the regulation of neonatal rat cardiac myocyte gap junctions. *J Mol Cell Cardiol* 1997;29:2131-45.

[104] Münster, PN, Weingart, R. Effects of phorbol esters on gap junctions of neonatal rat heart cells. *Pflügers Archiv* 1993;423:181-188.

[105] De Mello, WC. Influence of intracellular renin on heart cell communication. *Hypertension* 1995;25:1172-7.

[106] De Mello, WC. Is an intracellular renin-angiotensin system involved in control of cell communication in heart? *J Cardiovasc Pharmacol* 1994;23:640-6.

[107] De Mello, W, Altieri, P. The role of the renin-angiotensin system in the control of cell communication in the heart: effects of enalapril and angiotensin II. *J Cardiovasc Pharmacol* 1992;20:643-51.

[108] De Mello, WC. Renin-angiotensin system and cell communication in the failing heart. *Hypertension* 1996;27:1267-72.

- [109] De Mello, WC, Cherry, RC, Manivannan, S. Electrophysiologic and morphologic abnormalities in the failing heart: effect of enalapril on the electrical properties. *J Card Fail* 1997;3:53-61.
- [110] Doble, KS, Chen, Y, Bose, DG, Litchfield, DW, Kardami, E. FGF-2 decreases metabolic coupling and stimulates phosphorylation as well as masking of Cx43 epitopes in cardiac myocytes. *Circ Res* 1996;79:647-658.
- [111] Mukherjee, DP, McTiernan, CF, Sen, S. Myotrophin induces early response genes and enhances cardiac gene expression. *Hypertension* 1993;21:142-148.
- [112] Dodge, SM, Beardslee, MA, Darrow, BJ, *et al.* Effects of angiotensin II on expression of the gap junction channel protein connexin43 in neonatal rat ventricular myocytes. *J Am Coll Cardiol* 1998;32:800-7.
- [113] Ai, Z, Fischer, A, Spray, DC, Brown, AM, Fishman, GI. Wnt-1 regulation of connexin43 in cardiac myocytes. *J Clin Invest* 2000;105:16171.
- [114] Doble, BW, Kardami, E. bFGF stimulates Cx43 expression and intercellular communication of cardiac fibroblasts. *Mol Cell Biochem.* 1995;143:81-87.
- [115] Maldonado, PE, Rose, B, Loewenstein, WR. Growth factors modulate junctional cell-to-cell communication. *J Membr Biol* 1988;106:203-10.
- [116] Van Rijen, HVM, Van Kempen, MJA, Postma, S, Jongsma, HJ. Tumour necrosis factor  $\alpha$  alters the expression of Connexin43, Connexin40, and Connexin37 in human umbilical vein endothelial cells. *Cytokine* 1998;10:258-264.
- [117] Tonon, R, D'Andrea, P. Interleukin-1 $\beta$  increases the functional expression of connexin 43 in articular chondrocytes: evidence for a Ca<sup>2+</sup>-dependent mechanism. *J Bone Miner Res* 2000;15:1669-77.
- [118] Zhuang, J, Yamada, KA, Saffitz, JE, Kleber, AG. Pulsatile stretch remodels cell-to-cell communication in cultured myocytes. *Circ Res* 2000;87:316-22.
- [119] Wang, TL, Tseng, YZ, Chang, H. Regulation of connexin 43 gene expression by cyclical mechanical stretch in neonatal rat cardiomyocytes. *Biochem Biophys Res Commun* 2000;267:551-7.
- [120] Britz-Cunningham, SH, Shah, MM, Zuppan, CW, Fletcher, WH. Mutations in the Connexin43 Gap-Junction gene in patients with heart malformations and defects of laterality. *N Engl J Med* 1995;332:1323-1329.
- [121] Gebbia, M, Towbin, JA, Casey, B. Failure to detect connexin43 mutations in 38 cases of sporadic and familial heterotaxy. *Circulation* 1996;94:1909-12.
- [122] Reaume, AG, de Sousa, PA, Kulkarni, S, *et al.* Cardiac malformation in neonatal mice lacking connexin43. *Science* 1995;267:1831-4.
- [123] Ya, J, Erdtsieck-Ernste, EBHW, de Boer, PAJ, *et al.* Heart defects in Connexin43-deficient mice. *Circ Res* 1998;82:360-366.
- [124] Johnson, CM, Green, KG, Kanter, EM, *et al.* Voltage-gated Na<sup>+</sup> channel activity and connexin expression in Cx43- deficient cardiac myocytes. *J Cardiovasc Electrophysiol* 1999;10:1390-401.
- [125] Guerrero, PA, Schuessler, RB, Davis, LM, *et al.* Slow ventricular conduction in mice heterozygous for a connexin43 null mutation. *J Clin Invest* 1997;99:1991-1998.
- [126] Thomas, SA, Schuessler, RB, Berul, CI, *et al.* Disparate effects of deficient expression of connexin43 on atrial and ventricular conduction: evidence for chamber-specific molecular determinants of conduction. *Circulation* 1998;97:686-91.
- [127] Morley, GE, Vaidya, D, Samie, FH, *et al.* Characterization of conduction in the ventricles of normal and heterozygous Cx43 knockout mice using optical mapping. *J Cardiovasc Electrophysiol* 1999;10:1361-75.
- [128] Lerner, DL, Yamada, KA, Schuessler, RB, Saffitz, JE. Accelerated onset and increased incidence of ventricular arrhythmias induced by ischemia in Cx43-deficient mice. *Circulation* 2000;101:547-52.
- [129] Sullivan, R, Huang, GY, Meyer, RA, *et al.* Heart malformations in transgenic mice exhibiting dominant negative inhibition of gap junctional communication in neural crest cells. *Dev Biol* 1998;204:224-34.
- [130] Kirchhoff, S, Nelles, E, Hagendorff, A, *et al.* Reduced cardiac conduction velocity and

- predisposition to arrhythmias in connexin40deficient mice. *Curr Biol* 1998;8:299-302.
- [131] Simon, AM, Goodenough, DA, Paul, DL. Mice lacking connexin40 have cardiac conduction abnormalities characteristic of atrioventricular block and bundle branch block. *Curr Biol* 1998;8:295-8.
- [132] Hagendorff, A, Schumacher, B, Kirchhoff, S, Lüderitz, B, Willecke, K. Conduction disturbances and increased atrial vulnerability in Connexin40 deficient mice analyzed by transesophageal stimulation. *Circulation* 1999;99:1508-1515.
- [133] Verheule, S, van Batenburg, CA, Coenjaerts, FE, *et al.* Cardiac conduction abnormalities in mice lacking the gap junction protein connexin40. *J Cardiovasc Electrophysiol* 1999;10:1380-9.
- [134] Van Rijen, HVM, Van Veen, AAB, Van Kempen, MJA, Wilms-Schopman, FJ, Potse, M, Kruger, O, Willecke, K, Opthof, T, Jongsma, HJ, De Bakker, JMT. Impaired conduction in the bundle branches of mouse hearts lacking the gap junction protein connexin40. *Circulation* 2001;103:1591-1598.
- [135] Kumai, M, Nishii, K, Nakamura, K, *et al.* Loss of connexin45 causes a cushion defect in early cardiogenesis. *Development* 2000;127:3501-12.
- [136] Kruger, O, Plum, A, Kim, J, *et al.* Defective vascular development in connexin 45-deficient mice. *Development* 2000;127:4179-4193.
- [137] Kistner, A, Gossen, M, Zimmermann, F, *et al.* Doxycycline-mediated quantitative and tissue-specific control of gene expression in transgenic mice. *Proc Natl Acad Sci USA* 1996;93:10933-8.
- [138] Sepp, R, Severs, NJ, Gourdie, RG. Altered patterns of intercellular junction distribution in human patients with hypertrophic cardiomyopathy. *Heart* 1996;76:412-417.
- [139] Uzzaman, M, Honjo, H, Takagishi, Y, *et al.* Remodeling of gap junctional coupling in hypertrophied right ventricles of rats with monocrotaline-induced pulmonary hypertension. *Circ Res* 2000;86:871-8.
- [140] Van der Velden, HMW, Van Kempen, MJA, Wijffels, MCEF, *et al.* Altered pattern of Connexin40 distribution in persistent atrial fibrillation in the goat. *J Cardiovasc Electrophysiol.* 1998;9:596-607.
- [141] Peters, NS, Green, CR, Poole-Wilson, PA, Severs, NJ. Reduced content of connexin43 gap junctions in ventricular myocardium from hypertrophied and ischemic human hearts. *Circulation* 1993;88:864-875.
- [142] Smith, JH, Green, CR, Peters, NS, Rothery, S, Severs, NJ. Altered patterns of gap junction distribution in ischemic heart disease. *Am J Pathol* 1991;139:801-821.
- [143] Bastide, B, Neyses, L, Ganten, D, *et al.* Gap junction protein connexin40 is preferentially expressed in vascular endothelium and conductive bundles of rat myocardium and is increased under hypertensive conditions. *Circ Res* 1993;73:1138-1149.
- [144] Severs, NJ. The cardiac muscle cell. *Bioessays* 2000;22:188-99.
- [145] Peters, NS, Coromilas, J, Severs, NJ, Wit, AL. Disturbed connexin43 gap junction distribution correlates with the location of reentrant circuits in the epicardial border zone of healing canine infarcts that cause ventricular tachycardia. *Circulation* 1997;95:988-96.
- [146] Kaprielian, RR, Gunning, M, Dupont, E, *et al.* Downregulation of immunodetectable connexin43 and decreased gap junction size in the pathogenesis of chronic hibernation in the human left ventricle. *Circulation* 1998;97:651-60.
- [147] Matsushita, T, Oyamada, M, Fujimoto, K, *et al.* Remodeling of cell-cell and cell-extracellular matrix interactions at the border zone of rat myocardial infarcts. *Circ Res* 1999;85:1046-55.
- [148] Spach, MS. Changes in the topology of gap junctions as an adaptive structural response of the myocardium. *Circulation* 1994;90:1103-1106.
- [149] Rensma, PL, Allesie, MA, Lammers, WJ, Bonke, FI, Schalij, MJ. Length of excitation wave and susceptibility to reentrant atrial arrhythmias in normal conscious dogs. *Circ Res* 1988;62:395-410.
- [150] Jongsma, HJ, Wilders, R. Gap junctions in cardiovascular disease. *Circ Res* 2000;86:1193-1197.
- [151] Spach, MS, Heidlage, JF, Dolber, PC, Barr, RC. Electrophysiological effects of remodeling cardiac gap junctions and cell size. Experimental and model studies of normal cardiac growth.

Circ Res 2000;86:302-311.

[152] Fast, VG, Darrow, BJ, Saffitz, JE, Kleber, AG. Anisotropic activation spread in heart cell monolayers assessed by high- resolution optical mapping. Role of tissue discontinuities. Circ Res 1996;79:115-27.

[153] Beardslee, MA, Lerner, DL, Tadros, PN, *et al.* Dephosphorylation and Intracellular Redistribution of Ventricular Connexin43 During Electrical Uncoupling Induced by Ischemia. Circ Res 2000;87:656-662.

[154] Toyofuku, T, Yabuki, M, Otsu, K, *et al.* Functional role of c-Src in gap junctions of the cardiomyopathic heart. Circ Res 1999;85:672-81.

[155] van der Velden, HM, Ausma, J, Rook, MB, *et al.* Gap junctional remodeling in relation to stabilization of atrial fibrillation in the goat. Cardiovasc Res 2000;46:476-86.

[156] Elvan, A, Huang, XD, Pressler, ML, Zipes, DP. Radiofrequency catheter ablation of the atria eliminates pacing-induced sustained atrial fibrillation and reduces connexin 43 in dogs. Circulation 1997;96:1675-85.

[157] Nguyen-Tran, VT, Kubalak, SW, Minamisawa, S, *et al.* A novel genetic pathway for sudden cardiac death via defects in the transition between ventricular and conduction system cell lineages. Cell 2000;102:671-82.

[158] Hall, DG, Morley, GE, Vaidya, D, *et al.* Early onset heart failure in transgenic mice with dilated cardiomyopathy. Pediatr Res 2000;48:36-42.

[159] Seger, R, Krebs, EG. The MAPK signaling cascade. FASEB J 1995;9:726-735.

[160] Tamaddon, HS, Vaidya, D, Simon, AM, Paul, DL, Jalife, J, Morley, GE. High-resolution optical mapping of the right bundle branch in connexin40 knockout mice reveals slow conduction in the specialized conduction system. Circ Res 2000;87:929-936.

# Chapter 3

---

## **Electrical conductance of mouse Connexin45 gap junction channels is modulated by phosphorylation**

Toon A.B. van Veen, Harold V.M. van Rijen  
& Habo J. Jongsma.

*Cardiovascular Research (2000) 46: 496-510*

## **Abstract**

In this study we report about the modulation of Cx45 gap junction channel properties by phosphorylation of the connexin molecules through different protein kinases. Phosphorylation of Cx45 was studied in HeLa cells transfected with mouse Cx45 (mCx45). Using Western blotting (WB) and immunocytochemistry, these cells were found exclusively positive for Cx45 and the protein was separated as a doublet of bands with a calculated mass of 46- and 48 kD. After dephosphorylation using Calf Intestine Phosphatase (CIP), the 48 kD band disappeared almost completely leaving a single band at 46 kD. This effect can be prevented by including phosphatase inhibitors during CIP treatment. These results indicate that the 48 kD signal represents a phosphorylated form of Cx45.

To investigate the effects of (de)phosphorylation of Cx45 on the conductive properties of gap junction channels built of this connexin, cell pairs were subjected to dual voltage clamp experiments and coupling was determined before and after addition of PMA, 4 $\alpha$ -PDD, cAMP, cGMP, and pervanadate to the superfusate. 100 nM of the PKC activating phorbol ester PMA increased normalized junctional conductance by 50.9 $\pm$ 28 %. 100 nM of the inactive phorbol ester 4 $\alpha$ -PDD had no significant effect. Activation of PKA with 1mM 8-Br-cAMP decreased coupling by 20.9 $\pm$ 5.7 % while 1 mM 8-Br-cGMP (PKG-activation) was ineffective. 100  $\mu$ M pervanadate, a tyrosine phosphatase inhibitor, reduced coupling by 43.7 $\pm$ 11.1%. Single channel measurements, under identical phosphorylating conditions, were not significantly different from each other and all frequency histograms exhibited two conductance peaks at approximately 20 and 40 pS.

WB analysis revealed, as compared to control conditions, a relative increase of the 48 kD signal upon stimulation with pervanadate (142 $\pm$ 42%) and 8-Br-cAMP (50 $\pm$ 23%) whereas neither stimulation with PMA nor 8-Br-cGMP had a significant effect.

These experiments show that electrical intercellular conductance via Cx45 gap junction channels is differentially regulated by phosphorylation. However, regulation does not act by changing single channel conductance, but most likely by modulation of the open probability of Cx45 gap junction channels.

## **Introduction**

Electrical activation of the heart is initiated in the sinoatrial node. From this locus, the action potential is conducted along the atria, through the AV-node, His-bundle, bundle branches, and the purkinje system, finally resulting in a synchronous activation of the ventricles. The action potential is propagated from cell to cell by current flow through specialized membrane structures called gap junctions. Gap junctions are agglomerates of intercellular channels that directly connect the cytoplasm of adjacent cells. Individual gap junction channels are composed of twelve gap junction molecules (connexins, Cx), assembled from two hexameric hemichannels in adjacent cells, head to head aligned. Connexins belong to a family of highly related, but not identical proteins, of which up to now, in mammals, 15 members have been cloned, identified, and named after their theoretical molecular mass (for a review see [1]).

In the heart, at least four connexin types are reported to be present, i.e., Cx37, Cx40, Cx43, and Cx45. Cx37 was detected in the endocardial layer of rabbit hearts [2]. In myocardium, Cx40 is preferentially expressed in the atria and the conduction system [3-9], Cx43 is mainly found in the working myocardium and parts of the conduction system [5,6,9].

Initially, Cx45 was reported to be ubiquitously expressed throughout the myocardium [7,8,10,11]. However, recently Coppen *et al.*[12], showed that this apparent generic expression of Cx45 was mainly caused by a non specific cross reaction of the antibody with Cx43, which suggested that Cx45, like Cx43 is expressed throughout the heart. Coppen *et al.*[12] used a new, non cross-reacting antibody to localize Cx45 in rat and mouse heart. They reported Cx45 expression to be regional and associated with the atrioventricular node, His bundle and peripheral ventricular conduction system where it is located at the borderzone between the purkinje-fibers and the working ventricular myocardium [12,13]. In this position, Cx45 may play an significant role in the propagation of the action potential from the conduction system to the working myocardium. However, little is known about the regulation of Cx45 gap junction channels. Earlier studies have shown that Cx45 is a highly voltage sensitive connexin, that forms cation selective channels with low conductance [14-17]. It also appeared that the Cx45 molecule, like Cx40 and Cx43, contains multiple potential phosphorylation sites which allows for modulation of channel properties through (de)phosphorylation by protein kinases/phosphatases. Several studies have shown that Cx45 can indeed exist in a phosphorylated configuration [18-21]. Kwak *et al.*[14], reported that the single channel conductance of Cx45 gap junction channels is changed by activation of protein kinase C (PKC) with PMA, but not by activation of protein kinase A (PKA) with 8-Br-cAMP or protein kinase G (PKG) with 8-Br-cGMP. Intercellular conduction of the cardiac action potential is maintained by many channels, and the electrical conductance of gap junctions is not only regulated by their single channel conductance, but also by the number of channels and their open probability. Until now, no studies have been published on the modulation of the total macroscopic conductance of gap junctions composed of Cx45. In this study we report that the macroscopic conductance of gap junctions formed of mCx45 is increased by stimulation with PMA, decreased by stimulation with 8-Br-cAMP and pervanadate (a tyrosine phosphatase inhibitor and activator of MAPkinase), but is not affected by stimulation with 8-Br-cGMP. In addition, WB analysis of isolated Cx45 protein reveals a doublet of bands with a calculated mass of 46- and 48 kD in which the 48 kD band represents a phosphorylated form. The relative intensity of the 48 kD band is increased upon stimulation with 8-Br-cAMP and pervanadate but not significantly changed upon stimulation with PMA and 8-Br-cGMP.

## **Materials and Methods**

### *Cells and culture conditions*

Human cervix carcinoma HeLa cells, nontransfected (wild type) or stably transfected with mouse Cx45 (mCx45) cDNA, were kindly provided by Dr. K. Willecke. Cell culture conditions were as previously described [22].

### *Antibodies*

For both immunocytochemistry (IC) and Western blotting (WB), the following antibodies and dilutions were used; a rabbit polyclonal antibody raised against a peptide, representing aminoacids 285-298 of mCx45 (Alpha Diagnostics), 5 µg/ml (IC) and 2 µg/ml (WB), a rabbit polyclonal antibody (crude serum) raised against aminoacids 259-396 of mCx45, kindly provided by Dr. T.H. Steinberg, Washington University, St.Louis, 1:4000 (IC) and 1:2000 (WB), a rabbit polyclonal antibody raised against 19 aminoacids in the carboxyterminus of mCx40 (Alpha Diagnostics), 0.5 µg/ml (IC) and 4 µg/ml (WB), a mouse monoclonal antibody

raised against aminoacids 236-382 of rat Cx43 (Transduction Laboratories), 1  $\mu\text{g/ml}$  (IC) and 0.5  $\mu\text{g/ml}$  (WB) and a rabbit polyclonal antibody raised against aminoacids 4-17 of human PKG-1 $\beta$  (Stress Gen), 2  $\mu\text{g/ml}$  (IC) and 0.5  $\mu\text{g/ml}$  (WB).

Secondary antibodies were purchased from Jackson Laboratories; Texas Red conjugated goat-anti-mouse IgG (IH, 13  $\mu\text{g/ml}$ ), Fluorescein Isothiocyanate (FITC)-conjugated goat-anti-rabbit IgG (IH, 3  $\mu\text{g/ml}$ ), or from Biorad-Life Science; Horse Radish Peroxidase (HRP) conjugated antibodies, raised in goat against rabbit (WB, 62.5 ng/ml), and mouse (WB, 112.5 ng/ml).

#### *Electrophysiological measurements*

For electrophysiology, cells were seeded in 35 mm petri dishes (Falcon 3001) at  $1.5 \cdot 10^3$  cells/cm<sup>2</sup>. Prior to each measurement, culture medium was replaced by modified Tyrode's solution [23], containing (in mM) NaCl 140, KCl 5.4, MgCl<sub>2</sub>·6H<sub>2</sub>O 1, CaCl<sub>2</sub>·2H<sub>2</sub>O 1.8, HEPES 5, Glucose 5, pH 7.4. Patch electrodes were backfilled with 0.22  $\mu\text{m}$  filtered solution containing (in mM): CsCl 135, MgCl<sub>2</sub> 1, CaCl<sub>2</sub> 0.5, ethylene glycol-bis( $\beta$ -aminoethyl ether)-N,N,N',N'-tetraacetic acid (EGTA) 10, Na<sub>2</sub>ATP 5, HEPES 10, pH 7.2 (adjusted with CsOH).

Measurements of gap junctional conductance and single gap junction channel currents were performed as described before [24].

#### *Phosphorylating conditions*

For each experiment, fresh Tyrode's solution containing 1 mM 8-bromo-cAMP (Sigma) or 1mM 8-bromo-cGMP (Sigma) was prepared. Phorbol 12-myristate 13-acetate (PMA, Sigma) and 4 $\alpha$ -phorbol 12,13-didecanoate (4 $\alpha$ -PDD, Sigma), were first dissolved in dimethyl sulfoxide (DMSO, Sigma) at a concentration of 100  $\mu\text{M}$  and diluted in Tyrode to a final concentration of 100 nM. Pervanadate was prepared freshly before each experiment as a 500x stock solution by mixing equal volumes of 0.1M H<sub>2</sub>O<sub>2</sub> and 0.1M Na<sub>3</sub>VO<sub>4</sub>. In whole cell experiments, cells were exposed to a phosphorylating treatment by switching the superfusion (6 ml/min.) from control tyrode to one containing a phosphorylating substance after steady state conductance was reached.

For single channel experiments, cells were pre-incubated for 10 minutes with normal tyrode or tyrode containing phosphorylating drugs. Dephosphorylation was achieved by addition of 1 I.U. / ml Calf Intestine Phosphatase (CIP), an alkaline phosphatase, to the internal pipette solution.

#### *Immunocytochemistry*

Passaged cells were plated on 16-mm-diameter sterile glass coverslips and grown within 2 days to sub-confluency. Next, coverslips were rinsed in PBS, fixed in methanol (-20°C, 2 minutes) and washed 3 times with PBS. Fixed cells were permeabilized with 0.2% Triton X-100/PBS for 1 hour, and prior to the first and second antibody incubation, non-specific binding was blocked with 2% bovine serum albumin (BSA) for 30 min. Incubation with primary antibodies raised against Cx40, Cx43, Cx45 or PKG-1 $\beta$  was performed overnight in PBS/10% normal goat serum (NGS), in a total volume of 50  $\mu\text{l}$ /coverslip. Immunolabeling was performed using Texas Red- or fluorescein isothiocyanate (FITC)-conjugated secondary antibodies against either mouse- or rabbit IgG. All incubation steps were performed at room temperature (20-23°C), and in between all incubation steps, cells were washed 3 times with PBS (except after blocking with BSA). Sections were mounted in Vectashield (Vector Laboratories) and examined with a Nikon Optiphot-2 light microscope equipped for epifluorescence.

To test the specificity of the observed labeling patterns, coverslips were incubated

with 1) a mixture of primary antibody and a 500-fold excess of the synthetic peptide to which the antibodies were raised, 2) 10% NGS and 3) the second antibody alone.

#### *Protein isolation*

Cells destined for protein isolation were grown to subconfluency in 10 cm diameter Costar tissue culture disks. Prior to treatment with the various phosphorylating agents, cells were washed extensively with PBS and normal culture medium was replaced for 2 hours by serum-free medium. In order to activate the various kinases, 1 mM 8-Br-cAMP, 1 mM 8-Br-cGMP, 100 nM PMA and 0.1 mM pervanadate were added to the cultures. 100 nM 4- $\alpha$ PDD, a non activating analogue of PMA, was used as a negative control for PKC induced phosphorylation. Pre-incubation of the cells, (prior to stimulation with pervanadate), with 50  $\mu$ M PD90859, a specific inhibitor of MAPkinase, was used to study the effect of pervanadate. After 10 minutes, cells were washed with PBS, collected in lysisbuffer (400  $\mu$ l/10 cm dish; 50 mM Tris-HCl pH 7.4, 150 mM NaCl, 0.5% Nonidet-P40, 0.5% Sodium deoxycholate, 0.1% Sodium dodecyl sulfate (SDS), 2 mM Phenylmethylsulfonyl Fluoride (PMSF), protease-inhibitor-cocktail) and sonicated on ice (3x10 seconds, 60W, Branson Sonic Power). Cellular debris was concentrated by centrifugation (5 min, 14000 rpm) and total cellular protein in the supernatant was determined using the Lowry protein assay [25].

#### *Dephosphorylation of mCx45*

250  $\mu$ g of total cellular protein, isolated as described, was incubated for 3 hours at 37°C in presence of 2 I.U. calf intestine phosphatase (CIP, Boehringer). Incubation was stopped by addition of 4x Laemmli buffer (200 mM Tris-HCl pH 6.8, 8% SDS, 40% glycerin, 20%  $\beta$ -mercaptoethanol, 0.1% broomphenolblue) and boiling the samples for 5 minutes [26]. Control incubations were performed in presence of phosphatase inhibitors (10 mM EDTA, 11 mM Na<sub>3</sub>VO<sub>4</sub> and 50 mM NaF).

#### *SDS-PAGE and Western Blotting (WB)*

Aliquots were diluted with 4x Laemmli buffer and boiled for 5 minutes. Equal amounts (50  $\mu$ g/lane) of each sample were separated overnight (80 V) on 10% SDS-polyacrylamide gels [26], (18x24 cm) and electrophoretically transferred (4°C, 3 hrs, 350 mA) to nitrocellulose membrane (0.45  $\mu$ m, Biorad). Protein transfer was assessed by Ponceau S staining. Prior to primary antibody incubation with antibodies raised against Cx40, Cx43, Cx45 or PKG-1 $\beta$  (overnight, 4°C, in 0.1% BSA/0.1% Tween20/PBS), the nitrocellulose membrane was blocked with 5% dried milk powder (1 hr, RT, in 0.1% Tween20/PBS). Next morning, the membrane was washed (3x5 minutes, 0.1% Tween20/PBS), incubated with Horse-Radish-Peroxidase conjugated secondary antibody (1 hr, 4°C, 0.1% BSA/0.1% Tween20/PBS), and washed again (6x5 minutes, 0.1% Tween20/PBS). Signals were visualized by 1 minute development in Enhanced Chemo Luminiscence reagent (ECL, Amersham) and exposure to XB-1 film (Kodak) .

#### *Statistical analysis and quantification of Cx45 Western Blotting*

Macroscopic gap junctional conductance was measured and corrected for both series and membrane resistance as previously described [27]. Initial conductances and steady state values after exposure to the phosphorylating drug were determined and subjected to a paired Students *t*-test.

Steps in single channel current were measured by hand from digitized I<sub>j</sub> traces and converted into step amplitude histograms with a 4 pS bin width, using custom

software (MacDAQ, kindly provided by A.C.G. van Ginneken. Department of Physiology, University of Amsterdam), running on a Macintosh microcomputer (Apple Inc.).

Mean single channel conductances ( $\gamma_j$ ) of each individual experiment were determined by fitting a sum of two Gaussian distributions to step amplitude histograms, using KaleidaGraph data analysis and graphics presentation software (version 3.0.8, Adelbeck Software). All experiments contained at least 50 events. For each treatment, the number of events in each bin were averaged and plotted with the standard error for each bin.

WB signals were transferred to Adobe Photoshop software through high resolution scanning (Microtek ScanMaker 630) of the XB-1 films and digitized with Image Quant software. From 3 independent experiments, for all different samples, the ratio between the 48 KD and the 46 kD band was calculated. Within each separate experiment, ratio's of the samples were compared to the ratio obtained from control cells which was set at 100%. Statistics were performed using SchoolStat 2.0.6 software. Significance between the different groups was tested with a one-way ANOVA and an two-sided independent T-test. Significance was accepted when  $P \leq 0.05$ .

## **Results**

### ***Immunocytochemistry***

To ensure that HeLa/mCx45 transfected cells express Cx45 channels exclusively, cell cultures grown to subconfluency (Fig.3.1A), were immunocytochemically stained using antibodies raised against Cx40, Cx43, and Cx45. Cx45 transfected cells stained positive for Cx45 exclusively using two different antibodies raised against different epitopes (aminoacids 285-298 and 259-396) in the carboxyterminus of mCx45. Staining was found as strong punctate intercellular labeling (Fig.3.1B, 3.1C). Almost all of the fluorescent labeling was concentrated at the contact sides between cells while only little was localized in the cytoplasm of the cells. In particular, the Cx45 antibody provided by Dr.Steinberg revealed, as shown previously, some fine speckled non-specific labeling in the cytoplasm but this signal was clearly distinguishable from specific intercellular gap junction labeling[16]. Preincubation of the Cx45 antibody (raised against aminoacids 285-298) with an 500 fold excess of the peptide to which it was raised prevented the punctate intercellular labeling (Fig.3.1D).

Recently, it has been shown that the most commonly used Cx45 antibody raised against aminoacid residues 285-298, does not only recognize Cx45 but also Cx43 [12]. We have confirmed this non-specific cross-reactivity using HeLa cells transfected with mouse Cx43 and SKHep1 cells transfected with rat Cx43 (data not shown). In contrast, the Cx45 antibody raised against aminoacid residues 259-396 failed to stain these Cx43 transfected cells. Furthermore, mCx45 transfected HeLa cells were found to be completely negative both for Cx40 and Cx43 as identified in a double-labeling experiment using well characterized antibodies raised against mouse Cx40 and rat Cx43 (Fig.3.1E). All together, these experiments justify the use of both Cx45 antibodies in our experiments since both recognize Cx45 equally well and our cells prove to express no Cx43. Finally, the untransfected HeLa cells were negative for Cx45 antibody staining (Fig.3.1F) which implies that our cells solely express the transfected mCx45.

### ***Modulation of macroscopic conductance***

In general, HeLa/mCx45 cell pairs were well coupled (coupling after correction

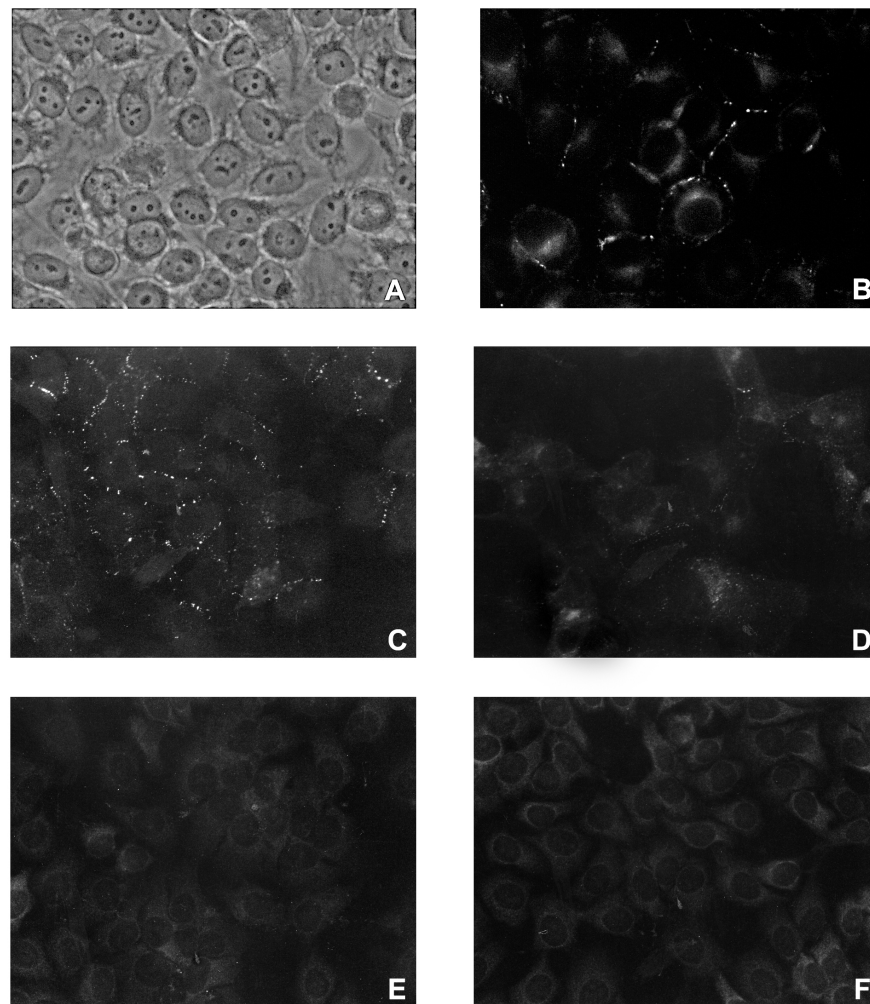


*Figure 3.1 Immunocytochemical staining of connexin expression in HeLa cells transfected with mCx45. Panel A: Phase-contrast view of transfected cells cultured to subconfluency. Cx45 expression is shown as clear punctate intercellular labeling in panel B and -C after labeling with two different antibodies raised against mouse Cx45. Preincubation of the Cx45 antibodies (Alpha Diagnostics) with the peptide to which they were raised prevented intercellular labelling almost completely as depicted in panel D. Double labeling with antibodies raised against Cx40 and Cx43 did not result in any positive staining as shown in panel E. Finally, panel F shows that untransfected (wild type) HeLa cells are negative for labeling with Cx45 antibodies.*

for series and membrane resistance varied between 2 and 100 nS). Fig.3.2 shows typical examples of modulation of macroscopic conductance by phosphorylation. When 100 nM of the phorbol ester PMA was added, a strong increase in electrical conductance, in this case from 2 to 4.9 nS, was measured (Fig.3.2A). Addition of 100 nM 4 $\alpha$ -PDD, the inactive phorbol ester had no noticeable effect (Fig.3.2B). When 1 mM 8Br-cAMP was present in the bathing solution, coupling decreased from 27.3 to 18.6 nS (Fig.3.2C). Administration of 1 mM 8Br-cGMP had no effect (Fig.3.2D), while stimulation with pervanadate reduced coupling from 10.5 nS to 4.5 nS (Fig.3.2E). In most cases, the time from the onset of the effect to a new steady state level was about 1.5-2 minutes.

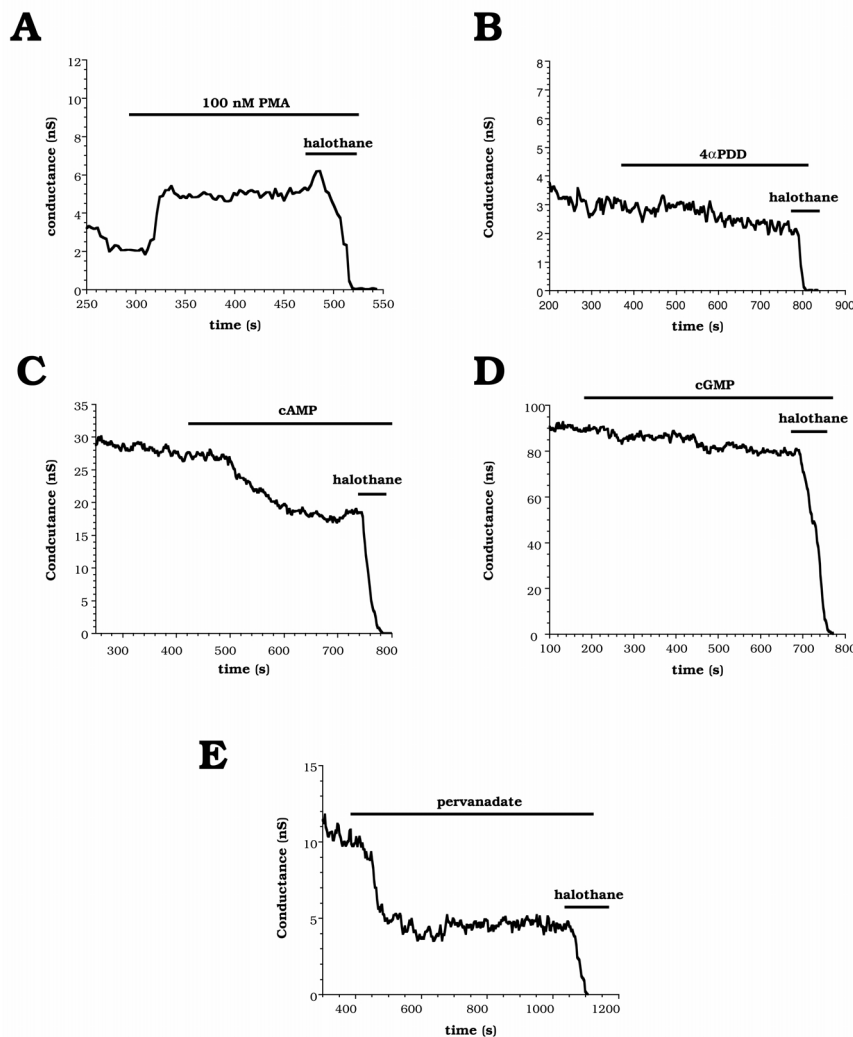


**Figure 3.2** Typical examples of the effect of phosphorylating treatment on macroscopic conductance between HeLa/mCx45 cell pairs. A. Exposure to 100 nM PMA increases conductance from 2.0 to 4.9 nS (145% increase). B. 100 nM 4  $\alpha$ -PDD had no effect on the macroscopic conductance. C. 1 mM cAMP reduced conductance from 27.3 to 18.6 nS (32% decrease). D. 1 mM cGMP did not alter macroscopic conductance. E. 0.1 mM pervanadate strongly reduces gap junctional conductance from 10.5 to 4.5 nS (57% reduction).

The statistical result from 8 experiments for each treatment is shown in Fig.3.3. PMA significantly increased junctional conductance by  $50.9 \pm 28\%$  (mean  $\pm$  S.E.M.,  $P \leq 0.033$ ), while the inactive phorbol ester 4 $\alpha$ -PDD had no significant effect ( $-5.9 \pm 8.1\%$ ,  $P \leq 0.26$ ). On the average, 8-Br-cAMP decreased coupling significantly by  $20.9 \pm 5.7\%$ ,  $P \leq 0.005$ , while 8-Br-cGMP had no effect ( $-0.3 \pm 7.0\%$ ,  $P \leq 0.29$ ). Pervanadate, however, significantly reduced coupling by  $43.7 \pm 11.1\%$ ,  $P \leq 0.0006$ . Although the initial macroscopic conductance within the treatment groups was rather variable, no significant differences in average baseline conductance between the treatments were detected, nor was there any correlation between the initial conductance and the observed effect (data not shown).

### **Modulation of microscopic conductance**

Macroscopic gap junctional conductance is determined by the number of channels, the conductance of a single channel and the open probability. To assess whether

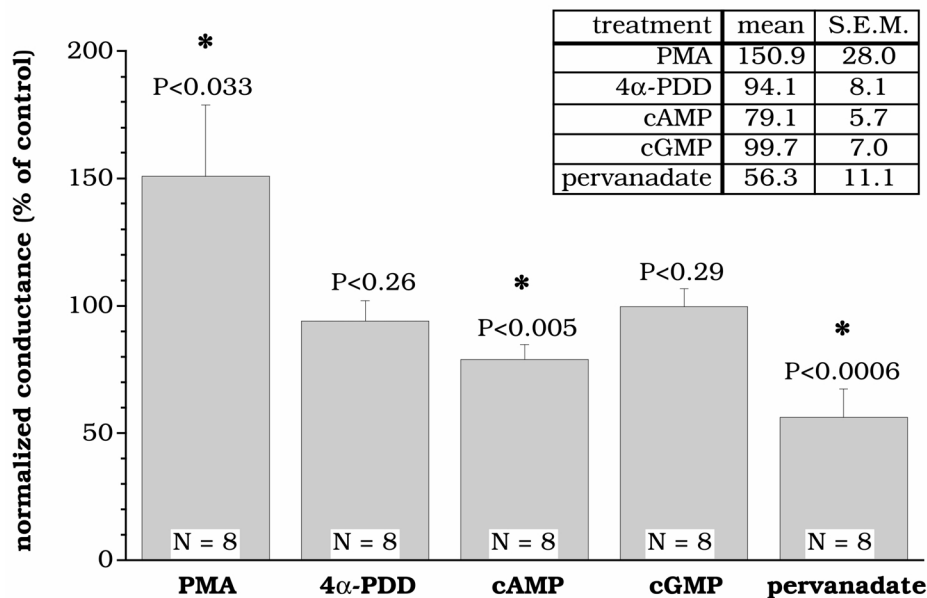
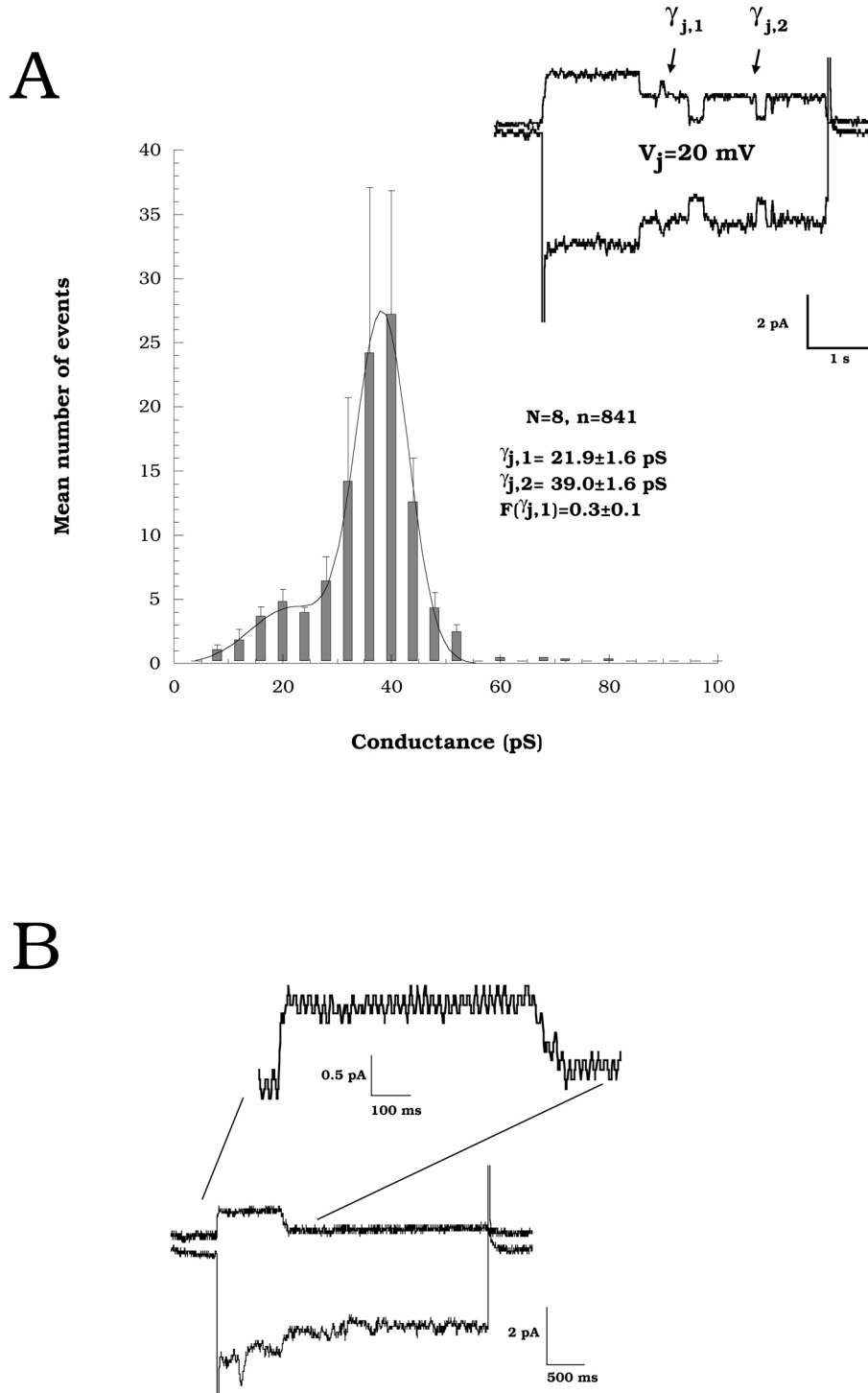


Figure 3.3 Means of the modulatory effect of the phosphorylating treatments of 8 individual experiments. The effect of the treatment is given as percentage of the control conductance (100%). The control conductances of the different treatments were not significantly different ( $P=0.09$ , not shown).

single channel conductance ( $\gamma_j$ ) is influenced by the phosphorylating treatments mentioned, we measured  $\gamma_j$ . We used 2 mM halothane to reduce junctional current flow to a level where single channel currents could be measured.

Under control conditions, two sizes of current transitions were detected (Fig.3.4A, inset). One transition corresponding to an average conductance of 21.9 pS ( $\gamma_{j,1}$ ), and a second transition corresponding to an average conductance of 39.0 pS ( $\gamma_{j,2}$ ). Occasionally, independent of treatment and transjunctional voltage, slow closures of the Cx45 gap junction channel large conductance state ( $\gamma_{j,2}$ ) were observed (Fig.3.4B).

Figure 3.5 shows the single channel histograms after preincubation with the different phosphorylating agents. In these experiments we have also added CIP (1U/ml) to the pipette solution to dephosphorylate gap junctions (Fig.3.5F). All histograms show slightly different, but similar single channel conductances. The ratio between the amplitudes of the two conductances is however somewhat variable. To verify whether these variations are statistically significant, the fraction of events under the gaussian of  $\gamma_{j,1}$  was divided by the area under both gaussians for each experiment [ $F(\gamma_{j,1})$ ]. The values for  $\gamma_{j,1}$ ,  $\gamma_{j,2}$ , and  $F(\gamma_{j,1})$  were subjected to analysis of variance (ANOVA) to check if the variance between the treatments was significantly different from the variance within the treatments. The results are presented in figure 3.6. No differences were detected for  $\gamma_{j,1}$  (Fig.3.6A,  $P \leq 0.17$ ),  $\gamma_{j,2}$  (Fig.3.6B,  $P \leq 0.77$ ), or for the values of  $F(\gamma_{j,1})$  (Fig.3.6C,  $P \leq 0.063$ ).



**Figure 3.4** Single channel characteristics under normal conditions using halothane to resolve single channels. **A**, inset. Current trace of non-stepped and stepped cell of a HeLa / mCx45 cell pair (upper and lower trace respectively) at a transjunctional voltage of 20 mV. This trace shows a small current transition ( $\gamma_{j,1}$ ) and a large current transition ( $\gamma_{j,2}$ ). The histogram is an average of 8 experiments (bars represent 4 pS bin averages  $\pm$  S.E.M.). Gaussian curve fitting revealed two mean channel conductances of  $21.9 \pm 1.6$  and  $39.0 \pm 1.6$  pS (mean  $\pm$  S.E.M.). The fraction of events belonging to  $\gamma_{j,1}$ ,  $F(\gamma_{j,1})$ , was 0.3 (mean  $\pm$  S.E.M.). **B**: Current trace of non-stepped and stepped cell (upper and lower trace, respectively) of cell pair under control conditions, showing slow closure of the Cx45 channel.

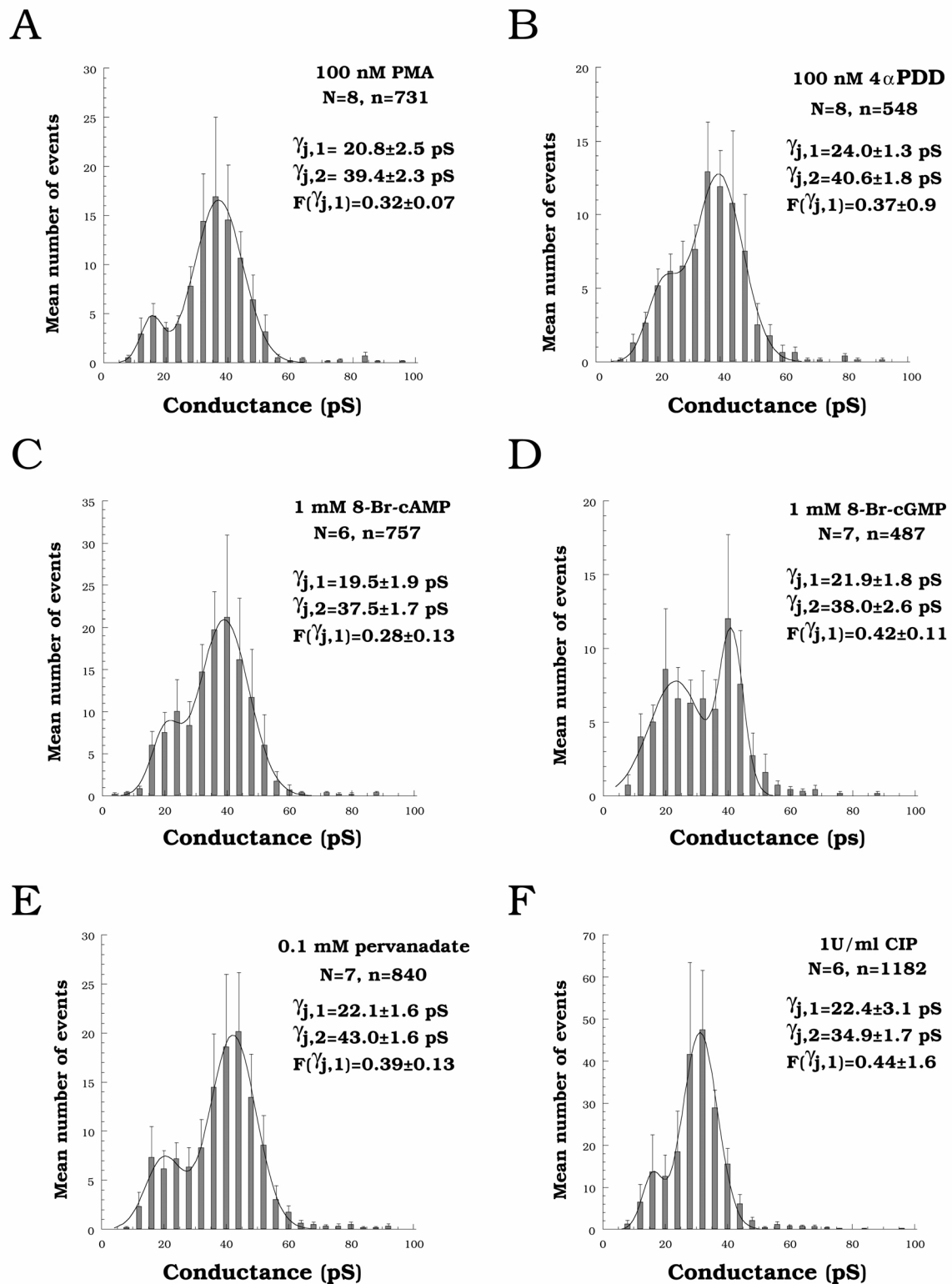


Figure 3.5 Averaged single channel histograms of HeLa/mCx45 cell pairs after pretreatment with 100 nM PMA (A), 100 nM 4  $\alpha$ -PDD (B), 1 mM 8-Br-cAMP (C), 1 mM 8-Br-cGMP (D), 0.1 mM pervanadate (E), 1U/ml CIP (F).

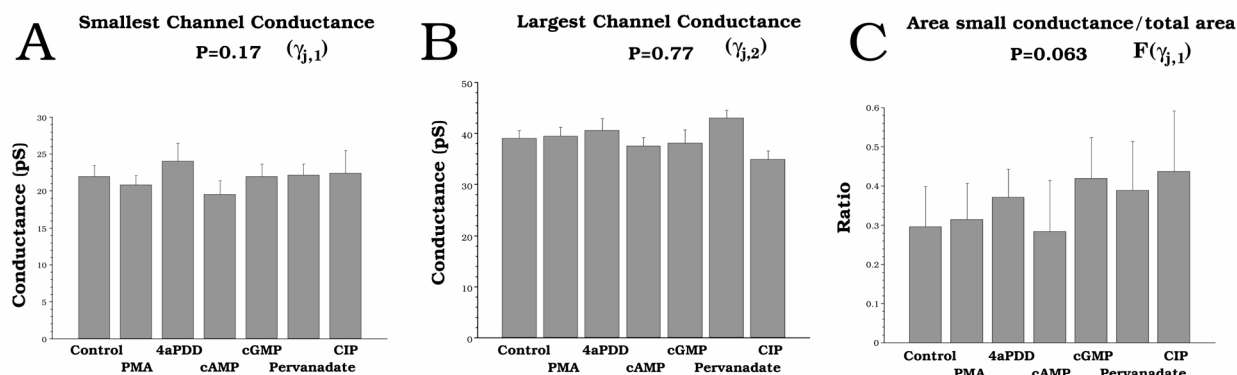


Figure 3.6 Bar plots of smallest channel conductance (mean $\pm$ S.E.M., A), largest channel conductance (Mean $\pm$ S.E.M., B), and the fraction of events belonging to  $\gamma_{j,1}$ , [ $F(\gamma_{j,1})$ ] (mean $\pm$ S.E.M., C). To verify whether exposure to (de)phosphorylating agents altered the size or distribution of single channel conductances, these parameters were subjected to Analysis of Variance (ANOVA). No statistical differences between the treatments were detected.  $P=0.17$ ,  $P=0.77$ , and  $P=0.063$  for  $\gamma_{j,1}$ ,  $\gamma_{j,2}$ , and  $F(\gamma_{j,1})$ , respectively.

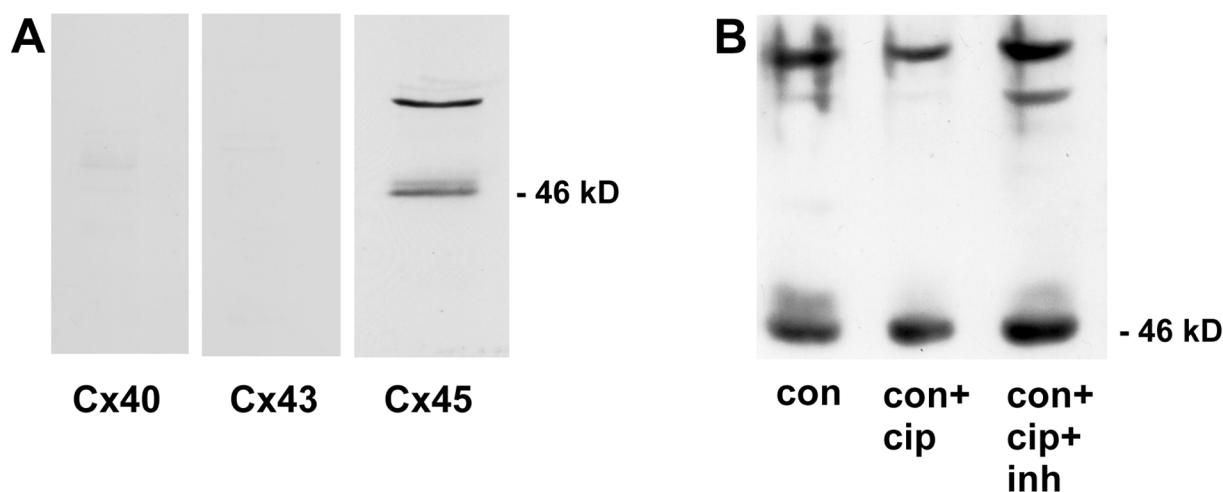


Figure 3.7 A; WB showing expression of Cx40, Cx43 and Cx45 in HeLa cells transfected with mCx45. No specific positive staining can be detected upon incubations with antibodies raised against Cx40 and Cx43. Incubation with antibodies raised against Cx45 results in staining of two bands with a calculated molecular mass of 46- and 48 kD. B; Cx45 antibodies recognize two specific bands of 46- and 48 kD in untreated control (con) cells. Upon treatment with calf intestine phosphatase (CIP), the 48 kD band disappears almost completely which can be avoided by simultaneously inclusion of phosphatase inhibitors (inh). All Cx45 stained samples additionally show aspecific signals of 55-60 kD.

### Western blotting of phosphorylated Cx45

WB analysis of samples prepared from untransfected HeLa cells confirmed the results obtained with immunocytochemistry: wild type HeLa cells do not express

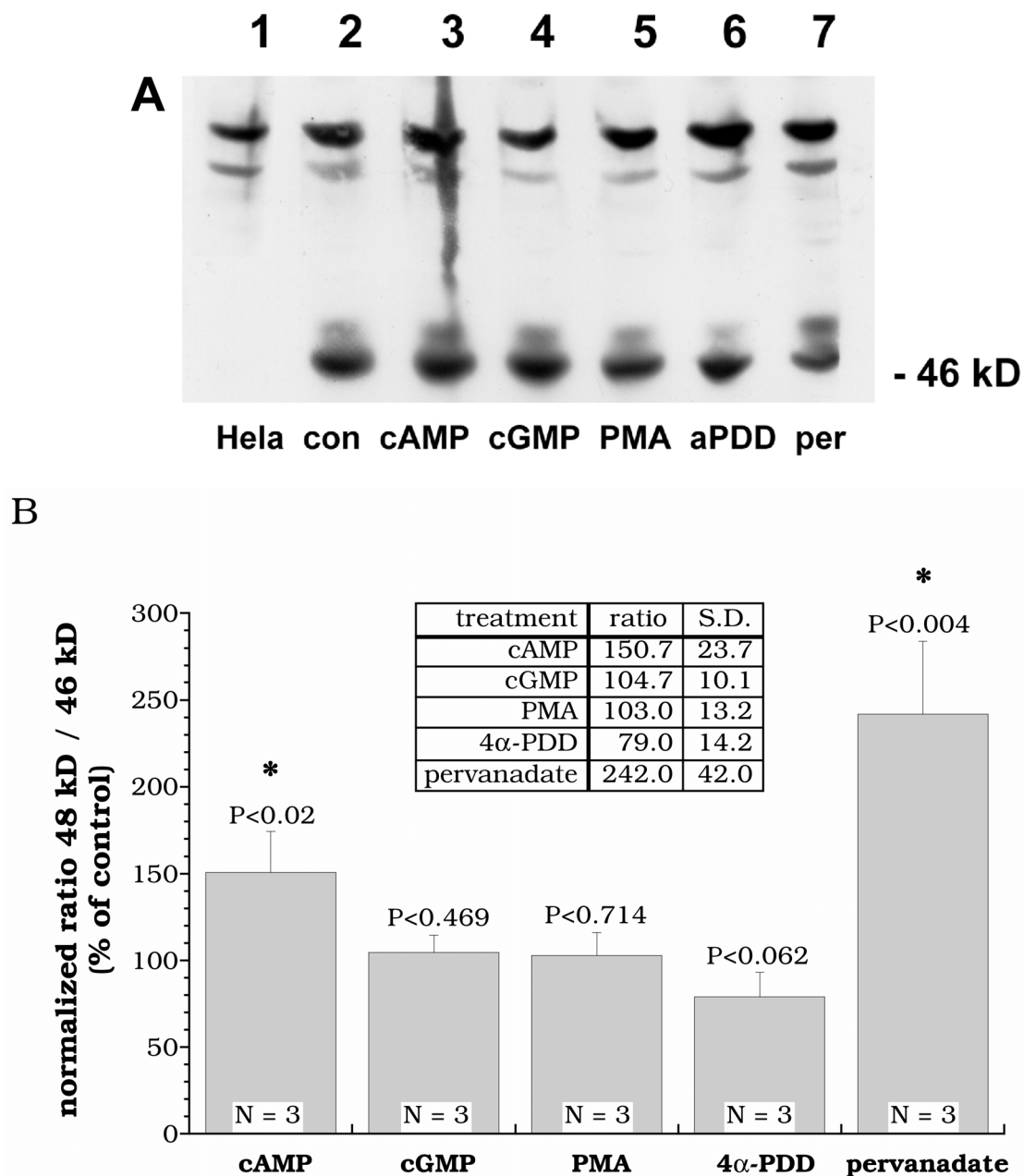


Figure 3.8 A; Representative WB showing the effects evoked by activation of various protein kinases on phosphorylation of Cx45. Untransfected HeLa cells serve as a negative control for Cx45 expression (HeLa). HeLa cells transfected with mCx45 were stimulated with cAMP, cGMP, PMA, 4 α-PDD and pervanadate (per). Phosphorylation of Cx45 in treated cells was compared with phosphorylation of untreated control cells (con). B. Relative changes in phosphorylation measured by the ratio 48 kD / 46 kD and compared to the control conditions (100%) as calculated from 3 independent experiments. Pre-incubation of the cells with 50 μM PD90859 did not alter the ratio compared to that of pervanadate treated cells (not shown).

detectable levels of Cx40, Cx43 (not shown), or Cx45 protein (Fig.3.8A-lane1). However, total protein isolated from HeLa cells transfected with mCx45, was found positive for Cx45 (Fig.3.7A-lane 3), but as expected negative for Cx40 or Cx43 (Fig.3.7A, lane 1 and 2 respectively). The Cx45 antibody (raised against aminoacids

259-396) revealed two bands with a calculated molecular mass of 46- and 48 kD of which the 46 kD band was most prominent. To clarify whether these bands represented phosphorylated forms of the Cx45 protein, an aliquot of isolated protein was treated with calf intestine phosphatase (CIP). After treatment with CIP, the 48 kD band, but not the 46 kD band, disappeared which could be prevented by including phosphatase inhibitors during CIP treatment (Fig.3.7B). These results suggest that the 48 kD band is a phosphorylated form of Cx45 and that under normal culture conditions, a fraction of expressed Cx45 protein exists in this phosphorylated form. In our hands, the commercially available Cx45 antibody (raised against aminoacid residues 285-298 of mCx45) proved to be inadequate for use on WB since background signals were unacceptably high. In order to test whether short term activation of various intracellular protein kinases induced differences in the degree of phosphorylation of Cx45, cells were stimulated for 10 minutes in serum-free medium with the previously mentioned activators. Figure 3.8A depicts a representative WB stained for Cx45. As shown in lane 1, untransfected HeLa cells do not show positive labeling for Cx45. All protein samples isolated from differentially stimulated HeLa cells transfected with mCx45, show bands of 46- and 48 kD (Fig.3.8A, lane 2-7). Additionally to the specific labeling of Cx45 protein, all separated samples, both from wild type- and transfected HeLa cells, show two non-specific bands of unknown nature with a calculated molecular mass of 55-60 kD. In all samples the unphosphorylated 46 kD band appeared to be most prominent whereas the intensity of the 48 kD band varied between the different treatments. Figure 3.8B shows the relative differences of the ratio between the density of the 48 kD band and that of the 46 kD band as calculated for the different treatments (mean  $\pm$  SD,  $n=3$ ,  $P\leq 0.05$ ). Ratio of untreated (control) cells was set to 100%. As compared to control cells (lane 2), stimulation with 8-Br-cAMP (lane 3) and pervanadate (lane 7) significantly increased the relative intensity of the phosphorylated 48 kD band with  $50\pm 23\%$  and  $142\pm 42\%$ , respectively. Pre-incubation of the cells (prior to stimulation with pervanadate) with  $50\text{ }\mu\text{M}$  PD90859, a specific inhibitor of MAPkinase, did not alter the 48 kD/46 kD ratio compared to the ratio of pervanadate treated cells (not shown). In contrast, stimulation with 8-Br-cGMP (lane 4) and PMA (lane 5) appeared to be ineffective in altering phosphorylation of Cx45 as the signal could not be discriminated from that of untreated cells. Although stimulation of the cells with  $4\alpha$ -PDD (lane 6), the non phosphorylating analogue of PMA, decreased the intensity of the 48 kD signal with  $21\pm 14\%$ , this was not found to be significant either when compared to control cells or to PMA stimulated cells.

## **Discussion**

### ***Expression and phosphorylation of Cx45***

Until now, little was known about the effects of phosphorylation on channels built of Cx45. This study was performed to provide data concerning the phosphorylation of Cx45 protein in relation to the conductance of Cx45 gap junction channels.

Previous studies have shown that untransfected HeLa cells are sometimes weakly coupled by endogenous gap junction channels although they proved to be negative for several connexin mRNA transcripts, including Cx45 mRNA [22,28]. The biophysical properties of these channels, however, are rather similar to those of Cx45. Similar to other studies [18], we were not able to demonstrate Cx45 protein in our wild type cultures neither with immunocytochemical staining nor on WB. Using both techniques, we showed unambiguously that our HeLa cells transfected with mCx45 were positive exclusively for Cx45. Staining of the cells with two

different Cx45 antibodies resulted in clear punctate intercellular labeling. Total protein samples prepared from HeLa/mCx45 cells were positive for Cx45 which was shown on WB as a doublet of bands with a calculated mass of 46 kD and 48 kD. Several authors have shown that Cx45 can be phosphorylated mainly at serine residues but also on threonine and tyrosine residues [18-21]. In our samples, upon treatment with calf intestine phosphatase, the 48 kD band, which was of minor intensity compared to the strong 46 kD band, disappeared indicating that this band represented a phosphorylated form of the Cx45 protein. Co-incubation during the phosphatase treatment with phosphatase inhibitors prevented disappearance of the 48 kD signal thereby underpinning this conclusion. Laing *et al.*[21] also have shown that the (proposed proteolytic) 46 kD band was of unphosphorylated nature but that the mobility of the 48 kD form was not affected by dephosphorylation. The electrophoretic mobility of the protein as described in other studies shows some discrepancy. Some authors have separated Cx45 as a single band of 45 kD [12,18,20,29], or of 48 kD [15,16,30]. Others claim that the protein exists of both a 46 kD and a 48 kD band of which the 46 kD band was proposed to be a proteolytic product of the full protein [19,21]. Possible explanations for these contradictions might be: differences in used Cx45 antibody, percentage of the SDS-PAGE gel, quality of the protein markers, processing of the protein sample and nature of the Cx45 protein.

Western blot analysis was performed to elucidate which types of protein kinases were able to phosphorylate Cx45. Upon exposure to cAMP and pervanadate, the relative intensity of the phosphorylated form of mCx45 was significantly increased. Sequence analysis learns that the carboxyl terminus of Cx45 contains putative sites for phosphorylation by PKA. Preliminary results in our laboratory obtained with SKhep1 cells which endogenously express low amounts of hCx45, have indicated that upon stimulation with 8-Br-cAMP, phosphorylation of hCx45 channels is also increased.

Although it has been shown that pervanadate strongly activates MAPkinase [31], we could not exclude that the pervanadate-induced increase in phosphorylation of Cx45 we measured, is partly mediated by secondary effects. First, pervanadate is also known as a potent inhibitor of tyrosine phosphatase activity [32], and it has been shown that Cx45 can be phosphorylated on tyrosine residues [20]. Secondly, the PLS/TP motif, the most optimal sequence recognition site for both Erk1 and Erk2 [33], is not included in the carboxyl-terminus of mCx45.

To differentiate between these two mechanisms, we pre-inhibited the cells with 50  $\mu$ M PD90859, a specific inhibitor of MAPkinase, prior to stimulation with pervanadate. Specific inhibition of MAPkinase did not alter the increased phosphorylation induced by pervanadate. Furthermore, stimulation of the cells with Epidermal Growth Factor (EGF, an activator of MAPkinase) failed to increase phosphorylation as compared to control (data not shown). From this we have to conclude that the increase in phosphorylation of Cx45 upon stimulation of the cells with pervanadate is not mediated by activation of MAPkinase, but presumably by tyrosine phosphatase inhibition.

Incubation with PMA and cGMP did not significantly alter phosphorylation of Cx45 as compared to control. Even if exposure of the cells to PMA is prolonged to 15 or 25 minutes, phosphorylation is not altered (data not shown).

Because some evidence exists that expression of PKG in cultured cells may be lost during repeated passages of the cells [34], and because stimulation of this kinase seemed ineffective in altering Cx45 phosphorylation, we checked the expression of PKG in our HeLa cells. Both from WB analysis and immunocytochemical staining it can be concluded that PKG-1 is present in these

cells (data not shown). Therefore, stimulation of this kinase does not affect Cx45 phosphorylation.

### **Cx45 macroscopic junctional conductance is differentially modulated**

Macroscopic junctional conductance of Cx45 gap junction channels was significantly decreased after stimulation with cAMP and pervanadate, remained unaltered after stimulation with cGMP or using 4 $\alpha$ -PDD (the non-phosphorylating structural analogue of PKC activator PMA) but was increased after stimulation with PMA. Comparison of the electrophysiological results with those of the Western blot experiments implies that exposure to cGMP or 4 $\alpha$ -PDD does not affect phosphorylation and conductance of Cx45 gap junctions. Exposure to cAMP or pervanadate, which lead to increased phosphorylation of Cx45, both result in a decrease in junctional conductance. Perhaps surprisingly, PMA treatment which increased macroscopic conductance of Cx45 gap junctions, did not affect Cx45 phosphorylation. Phosphorylation by exposure to TPA or PMA was found for Cx32 [35], Cx40 [36], and Cx43 [37,38]. However, PKC induced phosphorylation of connexins is presumably not the only mechanism by which phorbol esters influence gap junction channels. Although Cx26 cannot be phosphorylated [35,39], exposure of SKHep1 cells transfected with rat Cx26 to TPA, reduced lucifer yellow dye transfer and junctional conductance and markedly decreased the amount of large channel conductances (140-150 pS) in favor of the smaller conductances (40-70 pS) [14]. This action of phorbol esters of unknown mechanism might also be responsible for the increase in junctional conductance of mCx45 channels in our experiments.

Macroscopic gap junctional conductance is determined by the number of channels, the open probability, and the conductance of one single gap junction channel. The timecourse of the modulatory effect was 1-2 minutes, making a change in the number of channels highly unlikely, also because the halflife of Cx45 was reported to be 4.2 hours [20]. This was confirmed by immunocytochemistry, showing no differences in subcellular localization, which would indicate rapid internalization of Cx45 protein (not shown). Reducing the open probability of the channels with halothane, allowed us to evaluate alterations in single channel conductance, but prohibited analysis of open probability itself.

### **Phosphorylation doesn't affect single channel conductance.**

Under control conditions, two channel conductances were measured. One large state of 39.0 pS and one small state of 21.9 pS. These channel conductances compare well to those previously reported in the literature. Using identical pipette solutions, Kwak *et al.* [14] showed that hCx45, endogenously expressed in SKHep1 cells, had only one channel conductance of 36 pS at  $V_j$ =25-50 mV. However, at larger  $V_j$  a second smaller conductance of 22 pS became apparent. Using the same cells, Moreno *et al.* [15] found only one conductance of 28 pS with pipette solutions similar to ours, and Hermans *et al.* [40] detected one conductance of 17.8 pS, but with a very dissimilar pipette solution. In N2A cells, single chick Cx45 (cCx45) gap junction channels had conductances of 32 pS and 35 pS, with 120 mM KCl and 140 mM CsCl as main pipette ion, respectively, at  $V_j$ <50 mV [17]. At larger  $V_j$ , a substate of 20 pS was detected (120 mM KCl as main ion in the pipette). In our experiments, the smaller conductance and the larger conductance state were measured both at  $V_j$  of 20 and 50 mV. Although independent openings and closures of the ~22 pS conductance were frequently observed, it is not clear whether it is an independent population of channels, or a substate of the larger conductance.

Pretreatment of the cells with (de)phosphorylating drugs did not result in significant

changes in the single channel conductances or distribution. The small hCx45 conductance of 22 pS was reported to shift towards 16 pS, after treatment with TPA, a phorbol ester very similar to PMA [14]. In our experiments, PMA did reduce the single channel conductance from 21.9 to 20.8 pS, although not significantly. Like in our experiments single channel distributions of hCx45 were insensitive to treatment with cGMP or cAMP [14]. By exclusion, since phosphorylation alters macroscopic conductance, and presumably not the number of channels or single channel conductance of Cx45 gap junction channels, we conclude that modulation occurs by changes in the open probability of mCx45.

In conclusion, this study demonstrates that phosphorylation of Cx45 is differentially regulated by various protein kinases and that the alterations evoked by phosphorylation differentially affect the electrical coupling between transfected cells expressing mCx45.

Immunocytochemistry has revealed that in the mouse heart, Cx45 gap junction channels are mainly located in the conduction system, and more specifically at the borderzone between the central core of the system and the working ventricular myocardium. In the conduction system, Cx45 is co-expressed with Cx40 and Cx43 [12,13], while in the working myocardium Cx43 is predominantly expressed (see [41] and references therein). From studies on transfected cells it is known that Cx45 is able to form functional gap junction channels with both Cx40 and Cx43 [22], while Cx40 and Cx43 fail to form functional channels [22,42,43]. In this position, Cx45 might function as an intermediate for impulse propagation between the conduction system and the myocardium.

Our results suggest that under (patho)physiological conditions, e.g. under ischemic conditions, when the propensity for arrhythmia's increases and an increased cAMP level in the Purkinje system has been measured [44], modulation of Cx45 channel properties might play an important role thereby affecting transmission of the electrical impulse from the conduction system to the working ventricular myocardium.

## **Acknowledgements**

A.A.B.v.V. and H.V.M.v.R. were financially supported by a project grant no. 97.184 from the Netherlands Heart Foundation (to H.J.J.). The authors wish to thank Prof. Dr. K. Willecke (Institute for Genetics, Bonn, Germany) for providing the Hela cells used in this study and Dr. T.H. Steinberg (Institute for Infectious Diseases, St.Louis, USA) for providing the Cx45 antibody.

## **References**

- [1] Bruzzone, R, White, TW, Paul, DL. Connections with connexins: The molecular basis of direct intercellular signaling. *Eur.J.Biochem.* 1996;238:127.
- [2] Verheule, S, Van Kempen, MJA, Te Welscher, PHJA, Kwak, BR, Jongsma, HJ. Characterization of gap junction channels in adult rabbit atrial and ventricular myocardium. *Circ.Res.* 1997.
- [3] Bastide, B, Neyses, L, Ganten, D, *et al.* Gap junction protein connexin40 is preferentially expressed in vascular endothelium and conductive bundles of rat myocardium and is increased under hypertensive conditions. *Circ.Res.* 1993;73:1138-1149.
- [4] Gros, D, Jarry-Guichard, T, Ten Velde, I, *et al.* Restricted distribution of Connexin40, a gap junctional protein, in mammalian heart. *Circ.Res.* 1994;74:839-851.
- [5] Gourdie, RG, Severs, NJ, Green, CR, *et al.* The spatial distribution and relative abundance of gap-junctional connexin40 and connexin43 correlate to functional properties of components of

the cardiac atrioventricular conduction system. *J.Cell Sci.* 1993;105:985-991.

[6] Van Kempen, MJA, Ten Velde, I, Wessels, A, *et al.* Differential connexin expression accommodates cardiac function in different species. *Micros.Res.Techn.* 1995;31:420-436.

[7] Davis, LM, Kanter, HL, Beyer, EC, Saffitz, JE. Distinct gap junction protein phenotypes in cardiac tissues with disparate conduction properties. *J.Am.Coll.Cardiol.* 1994;24:1124-1132.

[8] Davis, LM, Rodefeld, ME, Green, K, Beyer, EC, Saffitz, JE. Gap junction protein phenotypes of the human heart and conduction system. *J.Cardiovasc.Electr.* 1995;6:813-822.

[9] Van Kempen, MJA, Vermeulen, JLM, Moorman, AFM, *et al.* Developmental changes of connexin40 and connexin43 mRNA distribution patterns in the rat heart. *Cardiovasc.Res.* 1996;32:886-900.

[10] Kanter, HL, Saffitz, JE, Beyer, EC. Cardiac myocytes express multiple gap junction proteins. *Circ.Res.* 1992;70:438-444.

[11] Darrow, BJ, Laing, JG, Lampe, PD, Saffitz, JE, Beyer, EC. Expression of multiple connexins in cultured neonatal rat ventricular myocytes. *Circ.Res.* 1995;76:381-387.

[12] Coppen, SR, Dupont, E, Rothery, S, Severs, NJ. Connexin45 expression is preferentially associated with the ventricular conduction system in mouse and rat heart. *Circ.Res.* 1998;82:232-243.

[13] Coppen, SR, Severs, NJ, Gourdie, RG. Connexin45 ( $\alpha 6$ ) expression delineates an extended conduction system in the embryonic and mature rodent heart. *Dev.Genet.* 1999;24:82-90.

[14] Kwak, BR, Hermans, MMP, De Jonge, HR, *et al.* Differential regulation of distinct types of gap junction channels by similar phosphorylating conditions. *Mol.Biol.Cell* 1995;6:1707-1719.

[15] Moreno, AP, Laing, JG, Beyer, EC, Spray, DC. Properties of gap junction channels formed of connexin45 endogenously expressed in human hepatoma (SKHep1) cells. *Am.J.Physiol.* 1995;268:C356-C365.

[16] Steinberg, TH, Civitelli, R, Geist, ST, *et al.* Connexin43 and Connexin45 form gap junctions with different molecular permeabilities in osteoblastic cells. *EMBO J.* 1994;13:744-750.

[17] Veenstra, RD, Wang, HZ, Beyer, EC, Brink, PR. Selective dye and ionic permeability of gap junction channels formed by Connexin45. *Circ.Res.* 1994;75:483-490.

[18] Butterweck, A, Gergs, U, Willecke, K, Traub, O. Immunochemical characterization of the gap junction protein Connexin45 in mouse kidney and transfected human HeLa cells. *J.Membrane Biol.* 1994;141:247-256.

[19] Darrow, BJ, Fast, VG, Kléber, AG, Beyer, EC, Saffitz, JE. Functional and structural assessment of intercellular communication: Increased conduction velocity and enhanced connexin expression in dibutyryl cAMP-treated cultured cardiac myocytes. *Circ.Res.* 1996;79:174-183.

[20] Hertlein, B, Butterweck, A, Haubrich, S, Willecke, K, Traub, O. Phosphorylated carboxy terminal serine residues stabilize the mouse gap junction protein Connexin45 against degradation. *J.Membrane Biol.* 1998;162:247-257.

[21] Laing, JG, Westphale, EM, Engelmann, GL, Beyer, EC. Characterization of the gap junction protein, Connexin45. *J.Membrane Biol.* 1994;139:31-40.

[22] Elfgang, C, Eckert, R, Lichtenberg-Fraté, H, *et al.* Specific permeability and selective formation of gap junction channels in connexin-transfected HeLa cells. *J.Cell Biol.* 1995;129:805-817.

[23] Tyrode, MV. The mode of action of some purgative salts. *Arch.Int.Pharmacodyn.* 1910;20:205-223.

[24] Van Rijen, HVM, Van Kempen, MJA, Analbers, LJS, *et al.* Gap junctions in human umbilical cord endothelial cells contain multiple connexins. *Am.J.Physiol.* 1997;272:C117-C130.

[25] Lowry, OH, Rosebrough, NJ, Farr, AL, Randall, RJ. Protein measurement with the folin phenol reagent. *J.Biol.Chem.* 1951;193:265-275.

[26] Laemmli, UK. Cleavage of structural proteins during the assembly of the head of bacteriophage T4. *Nature* 1970;227:680-685.

[27] Van Rijen, HVM, Wilders, R, Van Ginneken, ACG, Jongsma, HJ. Quantitative analysis of dual whole-cell voltage-clamp determination of gap junctional conductance. *Pflug.Arch.* 1998;436:141-151.

[28] Eckert, R, Dunina-Barovskaya, A, Hülser, DF. Biophysical characterization of gap junction

channels in HeLa cells. *Pflug. Arch.* 1993;424:335-342.

- [29] Okuma, A, Kuraoka, A, Iida, H, *et al.* Colocalization of Connexin43 and Connexin45 but absence of Connexin40 in granulosa cell gap junctions of rat ovary. *J.Reprod.Fertil.* 1996;107:255-264.
- [30] Alcoléa, S, Théveniau-Ruissy, M, Jarry-Guichard, T, *et al.* Downregulation of Connexin45 gene products during mouse heart development. *Circ.Res.* 1999;84:1365-1379.
- [31] Zhao, Z, Tan, Z, Diltz, CD, You, M, Fischer, EH. Activation of mitogenactivated protein (MAP) kinase pathway by pervanadate, a potent inhibitor of tyrosine phosphatases. *J.Biol.Chem.* 1996;271:22251-22255.
- [32] Gordon, JA. Use of vanadate as protein-phosphotyrosine phosphatase inhibitor. *Method.Enzymol.* 1991;201:477-482.
- [33] Gonzalez, FA, Raden, DL, Davis, RJ. Identification of substrate recognition determinants for human ERK1 and ERK2 protein kinases. *J.Biol.Chem.* 1991;266:22159-22163.
- [34] Hoenderop, JGJ, Vaandrager, AB, Dijkink, L, *et al.* Atrial natriuretic peptide-stimulated  $Ca^{2+}$  reabsorption in rabbit kidney requires membrane targeted, cGMP-dependent protein kinase type II. *Proc.Natl.Acad.Sci.USA* 1999;96:6084-6089.
- [35] Sáez, JC, Nairn, AC, Czernik, AJ, *et al.* Phosphorylation of connexin32, a hepatocyte gap junction protein by cAMP-dependent protein kinase, protein kinase C and  $Ca^{2+}$ /calmodulin-dependent protein kinase. *Eur.J.Biochem.* 1990;192:263-273.
- [36] Traub, O, Eckert, R, Lichtenberg-Fraté, H, *et al.* Immunochemical and electrophysiological characterization of murine connexin40 and -43 in mouse tissues and transfected human cells. *Eur.J.Cell Biol.* 1994;64:1011-12.
- [37] Lampe, PD. Analyzing Phorbol ester effects on gap junctional communication: A dramatic inhibition of assembly. *J.Cell Biol.* 1994;127:1895-1905.
- [38] Berthoud, VM, Rook, MB, Traub, O, Hertzberg, EL, Sáez, JC. On the mechanisms of cell uncoupling induced by a tumor promotor phorbol ester in clone 9 cells, a rat liver epithelial cell line. *Eur.J.Cell Biol.* 1993;62:384-396.
- [39] Traub, O, Look, J, Dermietzel, R, *et al.* Comparative characterization of the 21-kD and 26-kD proteins in murine liver and cultured hepatocytes. *J.Cell Biol.* 1989;108:1039-1051.
- [40] Hermans, MMP, Kortekaas, P, Jongsma, HJ, Rook, MB. pH sensitivity of the cardiac gap junction proteins, connexin45 and 43. *Pflug.Arch.* 1995;431:138-140.
- [41] Gros, D, Jongsma, HJ. Connexins in mammalian heart function. *BioEssays* 1996;18:719-730.
- [42] Bruzzone, R, Haefliger, JA, Gimlich, RL, Paul, DL. Connexin40, a component of gap junctions in vascular endothelium, is restricted in its ability to interact with other connexins. *Mol.Biol.Cell* 1993;4:7-20.
- [43] Haubrich, S, Schwarz, HJ, Bukauskas, FF, *et al.* Incompatibility of Connexin40 and 43 hemichannels in gap junctions between mammalian cells is determined by intracellular domains. *Mol.Biol.Cell* 1996;7:1995-2006.
- [44] Sugiyama, A, McKnite, S, Wiegand, P, Lurie, KG. Measurement of cAMP in the cardiac conduction system of rats. *J.Histochem.Cytochem* 1995;43:601-605.



# Chapter 4

---

## **Electrophysiological and cellular characteristics of adrenergic stimulated neonatal cardiomyocytes cultured in a defined pattern**

Harold V.M. van Rijen, Toon A.B. van Veen, Jacques M.T. de  
Bakker, Marcel A.G. van der Heijden, Tobias Opthof, Habo J.  
Jongsma

## **Abstract**

**Background:** Neonatal rat ventricular cardiomyocytes can easily be isolated and cultured in defined geometrical patterns which enables determination of conduction velocity of the action potential under control conditions and upon adrenergic stimulation.

**Methods and Results;** Immunohistochemical comparison of isolated and cultured rat neonatal ventricular myocytes with similar cells in the intact ventricle revealed that they were largely comparable. Cells were predominantly coupled by gap junctions composed of Cx43 while Cx45 was expressed at a negligible level. Expression of Cx40 decreased upon ageing of the cultures and was lower when cells were cultured on collagen instead of laminin. Stimulation of cells with phenylephrine ( $\alpha$ -adrenergic, PE) or isoproterenol ( $\beta$ -adrenergic, ISO) did not induce marked alterations in expression and distribution of Cx43 but ISO slightly increased phosphorylation as shown by Western blotting. Preparations with a star shape pattern of 4-6 day old cultured cells expressing predominantly Cx43 were used to determine conduction velocity of the electric impulse. Conduction velocity was increased by 25% after 1 and 24 hour(s) of exposure to ISO while PE remained ineffective in changing conduction velocity. RT-PCR revealed that upon exposure to ISO, cells decreased expression of  $\alpha_{1C}$ , Kv4.3, RERG and KvLQT1 while upon exposure to PE only Kv4.3 decreased but  $\alpha_{1C}$  increased.

**Conclusions:**  $\alpha$ - and  $\beta$ -adrenergic stimulation differently affect propagation of the electric impulse which is most likely not caused by a differential effect on Cx43 expression, distribution or phosphorylation. Because RT-PCR data concerning the expression of ion channels which determine action potential size and shape are not providing a complete explanation for our findings additional experiment have to be performed.

## **Introduction**

In the heart, cell-to-cell propagation of the electrical impulse is enabled by specialized membrane structures named gap junctions. The composition of these structures and their expression in different mammals has been discussed in detail in Chapter 2 of this thesis. Expression of the different connexin isoforms is not uniform within cardiac tissue and is subject to developmental changes<sup>1-4</sup>. In ventricles of adult rat, Cx43 is expressed between virtually all working myocardial cells while expression of Cx40 and Cx45 is restricted to cells composing the specialized conduction system (Chapter 5 and 5.6). In contrast, rat neonatal ventricular myocytes express all three isoforms both *in vivo* and *in vitro*<sup>7,8</sup>.

Intercellular electrical coupling is determined by the number of expressed gap junction channels, the open probability of each channel ( $P_o$ ) and the single channel conductance ( $\gamma_j$ ). As discussed in Chapter 2,  $P_o$  and  $\gamma_j$  differ between isoforms and are subject to post-translational modulation (e.g. by phosphorylation). Stimulation of cultured myocytes with a variety of growth factors, including  $\alpha$ - and  $\beta$ -adrenergic agents, has been shown to affect single gap junction channel properties. During prolonged exposure, changes in expression of the connexin isoforms (number of channels) and induction of a hypertrophic phenotype of cultured cells have been reported (see Chapter 2).

In Chapter 7 we discuss an *in vivo* model of dilated cardiomyopathy in which during the onset of the disease, alterations in the expression and distribution of Cx43 results in an aberrant propagation of the electric impulse. In this chapter we have investigated, at a level of reduced complexity, the effect of  $\alpha$ - and  $\beta$ -

adrenergic stimulation on the conductive properties of rat neonatal cardiomyocytes in culture, where these cells form a confluent two dimensional layer of extensively coupled cells. We studied conduction velocity in sheets of myocytes cultured in a defined geometry, compared our cultured cells to cells in intact ventricles and adapted culture conditions to produce a system in which cultured myocytes are almost exclusively coupled by Cx43 gap junctions.

## **Materials and Methods**

### *Isolation and culture of neonatal rat ventricular cardiomyocytes*

Neonatal rat ventricular cardiomyocytes were isolated from hearts of 1-2 day old Wistar rats. Pups were decapitated, hearts were excised aseptically and large vessels and both atria were removed. Ventricular tissue was cut into ~1 mm<sup>3</sup> small pieces and remaining blood was washed out. Tissue fragments were transferred to a sterile glass container and shaken in Hanks medium supplemented with 0.125% trypsin and 20 µg/ml DNase for 12 minutes at 37°C. Next, the suspension was gently triturated, the supernatant was discarded from the sedimented tissue and replaced by fresh enzyme solution. This was repeated for 6 cycles of 15 minutes. Supernatants were collected and supplemented (1:1) with routine culture medium composed of Ham's F10, 5% Fetal Calf Serum, 5% Horse serum, 2 mM L-glutamine, 100 IU/ml penicillin/streptomycin. Sera were heat inactivated (56°C, 30 minutes). Cells were pelleted during 3 minutes centrifugation at 1100 rpm. To enrich the population of myocytes a differential attachment protocol was used<sup>9</sup>. Pellets were suspended in culture medium and plated for 2 hours on un-coated culture dishes (Falcon 3004). Non-myocytes rapidly adhere to uncoated plastic and thus removed from the suspension. The cells remaining in suspension were collected, pelleted and suspended in fresh culture medium, counted and plated on laminin (10 µg/ml, Boehringer) or collagen (25 µg/ml, Sigma) coated dishes or 12 mm (Ø) glass slides in a density of 10<sup>5</sup> cells/cm<sup>2</sup>. Culture medium was replaced every 24 or 48 hours. Next to routine culture medium, commercially available serum free PC-1 medium (Biowhittaker) was used in some experiments.

### *Determination of conduction velocity in vitro*

To measure conduction velocity *in vitro*, cells were seeded (1.2·10<sup>6</sup> cells/dish) onto custom made glass dishes (5x5 cm). The bottom side of these dishes is coated with a layer of indium-tin-oxide (translucent and electrically conductive) and platinum electrodes are integrated in the upper side of the dish, on top of which cells were grown in a defined pattern. This pattern was created by coating the dishes with collagen, followed by KTI Negative Resist KTFR coating (Cassio Chemicals, Wormerveer, NL) preventing cell attachment. Next, the KTFR coating was partially removed by UV radiation and Xylol, using a photo-lithographic mask. From this, a star shaped pattern with 8 legs (length 2mm, width 0.1mm) was produced exposing the collagen coating where myocytes can attach. Fig. 4.1 shows the preparation after attachment of the cells.

For electrophysiological experiments, the dish was mounted on a custom built stage on an inverted microscope (Leica) and connected to a custom built 64-channel amplifier. The electrically conductive coating of the bottom side of the dishes is used as a heating system by applying current through the coating, regulated by a thermostat (34°C). Measurements were performed in normal culture medium and gas exchange was prevented by layering of silicone-oil (2ml) on top of the culture medium. The preparation was paced at one of the legs (2x threshold)

at a cycle length of 400 ms using an extracellular bipolar electrode. Extracellular electrograms were recorded from 24 electrodes (3 electrodes/leg, inter-electrode distance 400 $\mu$ m) in unipolar mode at 2KHz. Local activation times were defined as the maximal negative  $dV/dt$  (see Fig.4.1) determined by custom made software based on MatLab (the Mathworks, Inc.). Conduction velocity between electrodes within one leg was calculated by dividing the inter-electrode distance by the difference in activation time.

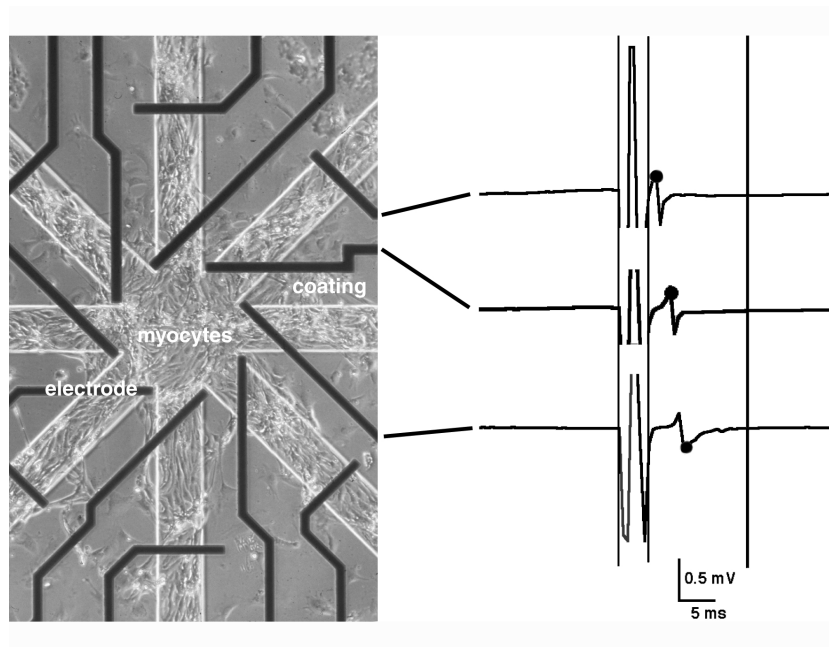


*Figure 4.1 Star shaped pattern with cultured myocytes covering the 'legs' and 'center' of the preparation while on the lacquer coating hardly cells have attached. In black the recording electrodes inserted in the bottom of the dish. The preparation was stimulated on the upper right leg. On the right, unipolar electrograms of the indicated electrodes. Local activation is determined by maximal negative  $dV/dt$  (dots).*

#### *Pharmalogical stimulation of the cells*

Adrenergic stimulation of cells (recordings made at 1 and 24 hours after application) was performed by adding 1  $\mu$ M phenylephrine (PE,  $\alpha$ -adrenergic, Sigma) or 50 nM isoproterenol (ISO,  $\beta$ -adrenergic, Sigma) to the culture medium. To determine the specificity of both agents, control incubations were performed in presence of 5  $\mu$ M prazosin ( $\alpha_1$ -antagonist, Sigma) or 10  $\mu$ M atenolol ( $\beta$ -antagonist, Sigma) which were added to the culture medium one hour prior to stimulation. To determine the effect of gap junction uncoupling on conduction velocity, palmitoleic acid (PA, Sigma) was added in concentrations from 10-40  $\mu$ M, diluted from a 2.5 mM stock solution (2 $\mu$ l PA/2.6 ml 100% Ethanol). After each experiment, the silicone oil was removed and the preparation was thoroughly rinsed with Hanks Balanced Salt Solution (HBSS), before new culture medium was applied. Since the conduction assay is non-invasive, the same preparation was used for control, 1h exposure and 24h exposure.

antibody	origin	Epitope *	company	Concen- tration IH	Concen- tration WB
Cx40	R	19 aa in C-terminus	Alpha Diagnostics	.5 µg/ml	-
Cx43	M	aa 236-382 of rCx43	Transduction Lab.	1 µg/ml	.5 µg/ml
Cx45	R	aa 259-396 of mCx45	Dr. TH Steinberg	1:4000	-
α-actinin	M	Rabbit skeletal muscle	Sigma	1:1000	1:2000
desmin	M	Human leiomyoma	Sanbio	.25 µg/ml	.06 µg/ml
N-cadherin	R	C-terminus chicken	Sigma	1:800	1:1000
α-SMA	M	10 aa mouse N-terminus	Sigma	1:1000	-
SMM	M	Human uterus	Sigma	1:500	-
titin	M	Chicken breast	Sigma	1:100	-
troponin-T	M	R. skeletal muscle	Sigma	1:100	-
β-MHC	M	Chicken heart	Dr.AFM Moorman	1:10	-
α-MHC	M	Chicken heart	Dr. AFM Moorman	1:10	-

*Table 7.I Specifications of used antibodies.\*= according to the manufacturer. α-SMA =α-Smooth Muscle Actin, SMM= Smooth Muscle Myosin, α,β-MHC=α,β-Myosin Heavy Chain, M= mouse monoclonal, R= rabbit polyclonal. Secondary antibodies were purchased from Jackson Laboratories; Texas Red (TR) conjugated donkey-anti-mouse IgG (IC, 13 µg / ml); Fluorescein Isothiocyanate (FITC)-conjugated goat-anti rabbit IgG (IC, 3 µg / ml); Horse Radish Peroxidase (HRP) conjugated antibodies, raised in goat against rabbit and mouse (both in WB, 1:8000). Dr.AFM Moorman, Dept.Anatomy / Embryology, Academic Medical Center, Amsterdam, The Netherlands; Dr. TH Steinberg, Washington University, St.Louis, USA.*

#### *Immunocytochemistry on cultured cells*

Coverslips with cultured cells were rinsed in PBS, fixed in methanol (-20°C) for 2 minutes and washed 3 times with PBS. Fixed cells were permeabilized with 0.2% Triton X-100 in PBS for 1 hour, and prior to the first antibody incubation, non-specific binding was blocked with 2% bovine serum albumin (BSA) for 30 min. Incubation with primary antibodies (Table 7.I) was performed overnight in PBS/

10% normal goat serum (NGS), in a total volume of 50  $\mu$ l/coverslip. Before secondary incubation, cells were incubated with 2% BSA in PBS. Immunolabeling was performed using Texas Red (TR)- or fluorescein isothiocyanate (FITC)-conjugated secondary antibodies against either mouse- or rabbit IgG. All incubation steps were performed at room temperature (20-23°C), and in between all incubation steps, cells were washed 3 times with PBS (except after blocking with BSA). Coverslips were mounted in Vectashield (Vector Laboratories) and examined with a Nikon Optiphot-2 light microscope equipped for epifluorescence. To test the specificity of the observed labeling patterns, coverslips were incubated either with 1) a mixture of primary antibody and a 500-fold excess of the synthetic peptide to which the antibodies were raised, 2) 10% NGS and 3) the second antibody alone.

#### *Immunocytochemistry on tissue sections*

Frozen hearts were serially sectioned in frontal plane with a cryostat, to produce 'four chamber view' sections of 10  $\mu$ m thickness which were mounted on aminopropyltriethoxysilane- (AAS) coated glass slides. Immunolabeling was performed as described for cultured cells on glass slides. Finally, sections were mounted in Vectashield (Vector Laboratories) and examined with a Nikon Optiphot-2 light microscope equipped for epifluorescence.

#### *Protein isolation, SDS-PAGE and Western Blotting*

Total cellular protein was isolated from confluent beating cultures by washing the cells with PBS and collecting them in lysisbuffer (400  $\mu$ l/ 10 cm dish; 50 mM Tris-HCl pH 7.4, 150 mM NaCl, 0.5% Nonidet-P40, 0.5% Sodium deoxycholate, 0.1% Sodium dodecyl sulfate (SDS), 2 mM Phenylmethylsulfonyl Fluoride (PMSF), protease-inhibitor-cocktail). Subsequently, the samples were sonicated on ice (3x10 seconds, 60W, Branson Sonic Power) and cellular debris was concentrated by centrifugation (5 min, 14000 rpm). Total cellular protein in the supernatant was determined using the Lowry protein assay.<sup>10</sup>

Aliquots were diluted with 4x Laemmli buffer and boiled for 5 minutes. Equal amounts (50  $\mu$ g/lane) of each sample were separated on 8% SDS-polyacrylamide gels,<sup>11</sup> and electrophoretically transferred to nitrocellulose membrane (0.45  $\mu$ m, Biorad). Protein transfer was assessed by Ponceau S staining. Prior to primary antibody incubation (Table II, overnight, 4°C, in 0.1% BSA/0.1% Tween20/PBS), the nitrocellulose membrane was blocked with 5% dried milk powder (1 hr, 20°C, in 0.1% Tween20/PBS). Next morning, the membrane was washed (3x5 minutes, 0.1% Tween20/PBS), incubated with Horse-Radish-Peroxidase conjugated secondary antibody (1 hr, 4°C, 0.1% BSA/0.1% Tween20/PBS), and washed again (6x5 minutes, 0.1% Tween20/PBS). Signals were visualized by 1 minute development in Enhanced Chemo Luminiscence reagent (ECL, Amersham) and exposure to XB-1 film (Kodak). Western blot signals were transferred to Adobe Photoshop software through high resolution scanning (Microtek ScanMaker 630) of the XB-1 films and digitized with Image Quant software.

#### *RNA isolation and semi-quantative RT-PCR*

After stimulation with PE and ISO for 24 hours, total RNA was isolated using Trizol (Gibco) according to the manufacturers protocol and 0.5  $\mu$ g RNA was reversed transcribed using M-MLV-RT (Gibco). PCR reactions were performed in 50  $\mu$ l reaction mixtures. DNA was denatured for 5 minutes at 94°C followed by a repetitive program used for x-cycli: 45 second denaturation at 94°C, 30 seconds annealing of primers at appropriate temperature and 1 minute DNA extension at 72°C. Reactions were terminated with 5 minutes extra DNA extension at 72°C

primer	Gene bank number	RNA sequence: sense antisense	Tem-plate (ng)	cycles	Anneal-ing temp (°C)	Size in bp	Con-tribute to
r $\alpha_{1C}$	M59786	TTCCAGATGAGACCCGCAGCAG TGTCTGCGGCGTTCTCCATCTC	33.3	30	58	750	I <sub>Ca-L</sub>
rERG	Z96106	AACATGATTCCTGGCTCCC GGGTTTCCAGCCTGTTTCAG	16.6	32	55	573	I <sub>KR</sub>
rKvLQT1	U92655	GCTCTGGCCACCGGGACCCT GATGCGGCCGGAATCATTCA	33.3	32	58	434	I <sub>KS</sub>
rKv4.3	U75448	GCTGGGTAGCACAGAGAAGG GTGTCCAGGCAGAAGAAAGC	33.3	31	58	497	I <sub>TO</sub>
GAPDH	M17701	ATGGTGAAGGTCGGTGTCAAC TTACTCCTTGGAGGCCATGTA	16.6	30	55	1002	-

Table 7.II: Reaction specifics of RT-PCR.

and cooling down to 20°C. Reaction specifics are collected in Table 7. II. Obtained PCR products were run on 1.5% agarose gels and stained with ethidium bromide.

#### Statistics

All values are given as mean $\pm$ S.E.M. Multiple group comparison was performed using ANOVA, followed by a Fishers Post-hoc test using StatView 4.5 for Macintosh. P-values $\leq$  0.05 were regarded as statistically significant.

## Results

### Isolation of cardiomyocytes and cell culture

From an optimal isolation approximately  $1.5 \times 10^6$  ventricular myocytes/heart were obtained. A seeding density of 100.000 cells/ml resulted within 24-36 hours in confluent monolayers of cells. Cultures were spontaneously active within 24 hours and showed synchronization of beating. Purity of the cultures was assessed by immuno-labeling against cardiac specific markers as desmin and  $\alpha$ -actinin which are strongly positive in cardiomyocytes but negative in non-myocytes. Co-staining with the dye Hoechst 33258 which labels the nuclei allowed for evaluation of the content of non-cardiac cells in the cultures. The differential attachment protocol (2 hours pre-plating), enriched the population in favor of myocytes and reduced content of non-myocytes to  $\leq 10\%$ . Addition of Cytosine Arabino-furanoside (Ara-C) to the cultures in order to suppress proliferation of non-myocytes was omitted because it negatively affected characteristics of the cardiomyocytes (cell shape, spontaneous activity). Routine culture medium contained 5% FCS and 5% horse serum (see methods). Serum deprivation induced arrest of spontaneous activity within 3-6 hours and cell-atrophy was observed after 24 hours. Use of commercially available serum free PC-1 medium prohibited the observed effects induced by serum deprivation of routine culture medium, although after more than three days, cell atrophy was induced as well.

Treatment of cultures with PE or ISO did not induce changes in cell shape but affected spontaneous beating of the cells differentially. PE did not change beating rate of the cultures compared to control (100 beats per minute (bpm)). ISO, on

the other hand, increased beating rate within minutes. A maximum rate of  $183 \pm 11.2$  bpm was reached after 6-24 hours of incubation. Pre-incubation with  $\beta$ -antagonist atenolol prevented the increase in beating rate. Interestingly, the phorbol-ester TPA which like PE activates PKC, reduced beating rate within 15 minutes and arrest of spontaneous contraction was observed within 24 hours. 4  $\alpha$ -PDD, a structural analogue of TPA not activating PKC, did not alter bpm.

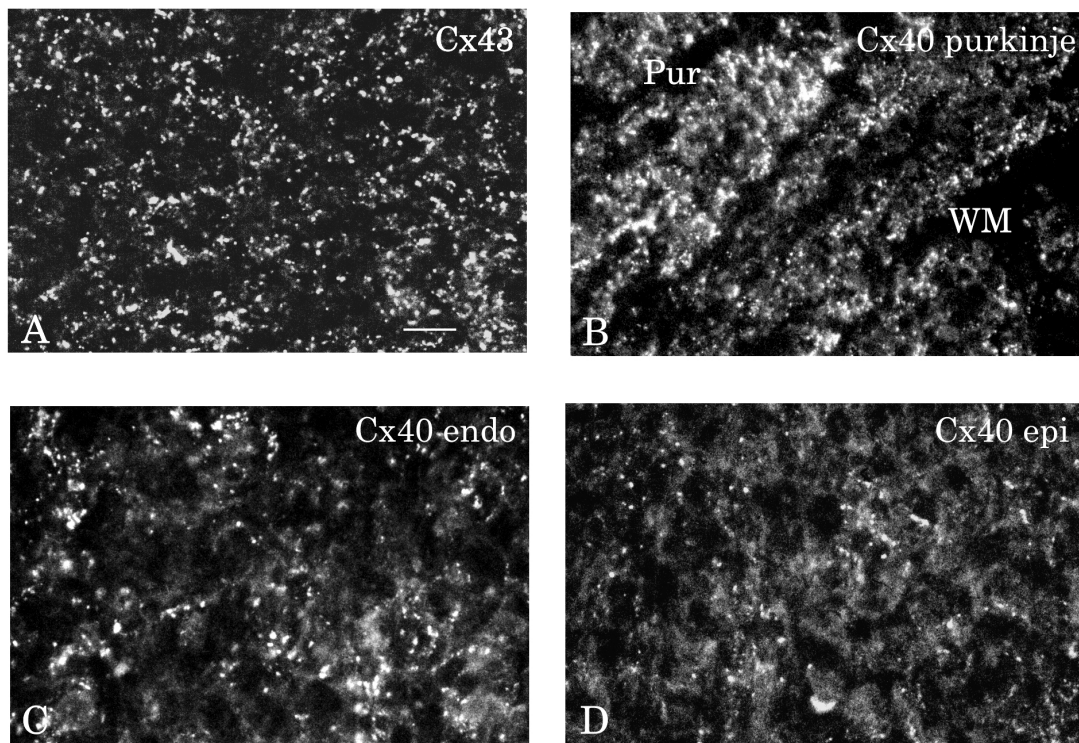


*Figure 4.2 A-D: Immunohistochemical labeling of ventricular sections from neonatal hearts. Pur = Purkinje fibers, WM= working myocardium. Bar (in A) = 50  $\mu$ m for A,B and 25  $\mu$ m for C,D.*

### **Immunohistochemistry**

To see to which extent cultured ventricular myocytes resembled cells in the intact ventricle, an immunohistochemical comparison was made. Thin sections of 2-day old neonatal rat hearts were labeled for presence of cardiac muscle cell markers (not shown) and expression of gap junction proteins. Labeling against desmin, SMA,  $\alpha$ -actinin and  $\beta$ -MHC revealed a cross-striated pattern in the ventricular working myocardium but not in the embedded vasculature. Other muscle markers like SMM,  $\alpha$ -MHC and titin were negative. Troponin-T labeled weakly positive. Uniform Cx43 labeling was observed in both ventricles (Fig.4.2A). No Cx45 labeling was detected but Cx40 was found in the endothelial lining of blood vessels and also, in contrast with adult hearts, between myocytes of the atrium and the ventricles. Whereas atrial expression was observed in virtually all myocytes, ventricular expression was heterogeneous. Highest levels of Cx40 expression were found in the ventricular conduction system (Fig 4.2B). In working ventricular myocardium, a gradient in Cx40 labeling exists from relatively high at the endocardial side (Fig.4.2C) which gradually declines in the direction of the epicardium where low levels were detected (Fig.4.2D). Regardless of the expression

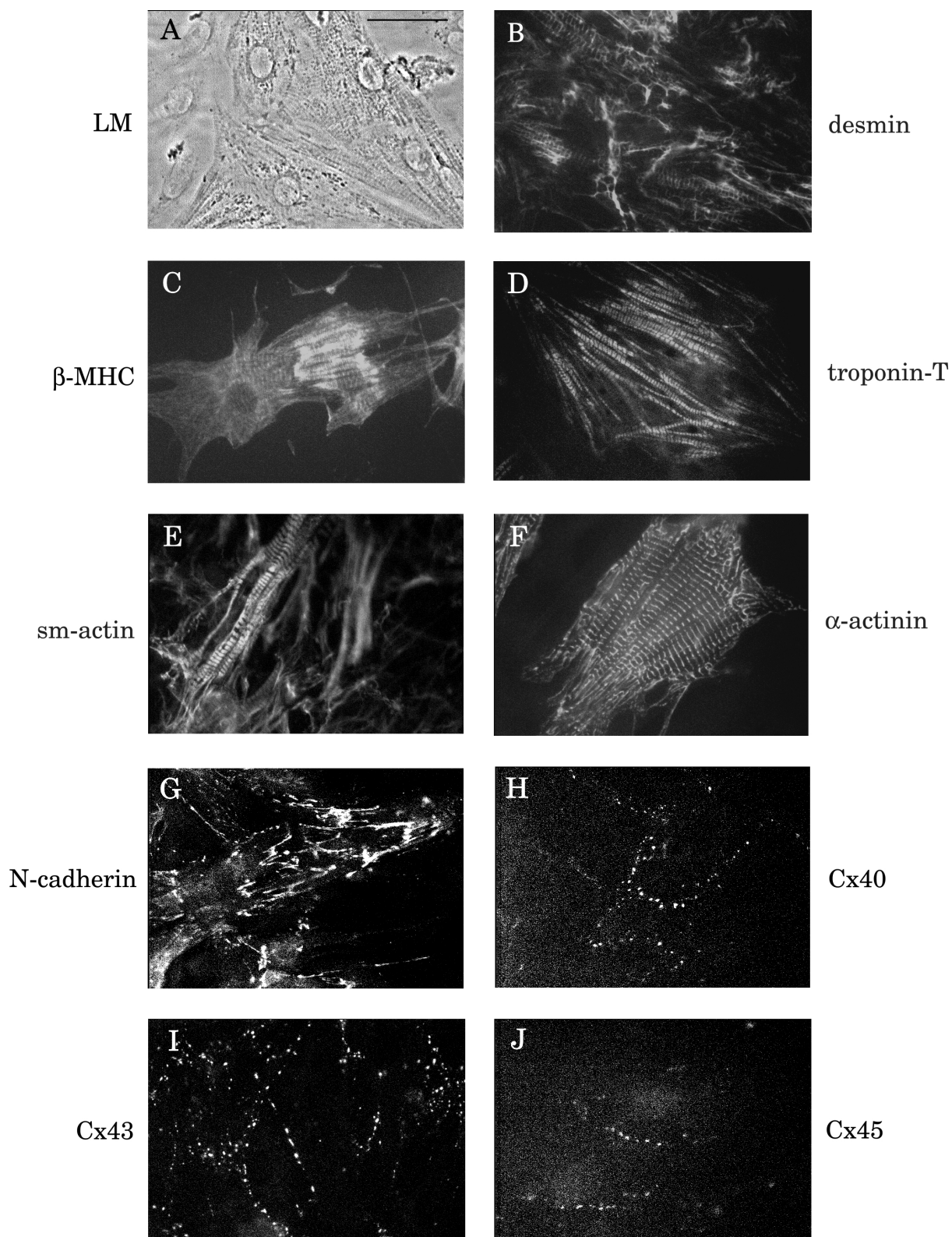
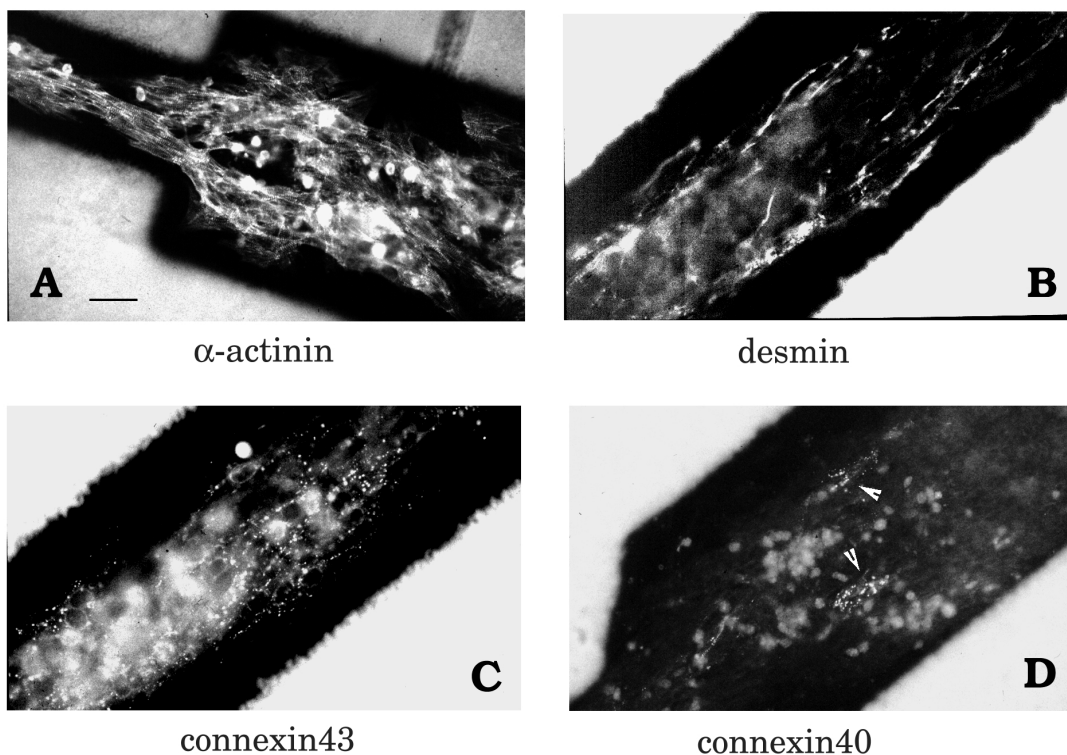


Figure 4.3 A: Light microscopy, and B-J: Immunohistochemical labeling of isolated and cultured neonatal ventricular myocytes grown on collagen coated slides. Bar (in A) = 40 µm in D,F,G, 30 µm in A,B,C,E,H,I and 20 µm in J.

level, some cells do express Cx40 while others appear to be negative which is another indication of heterogeneous expression. In neonatal hearts connexin expression is observed over the entire sarcolemma, while in adult hearts this expression is mainly restricted to the intercalated disks.

Isolated myocytes were grown on glass slides coated with laminin or collagen. Figure 4.3A shows a light-microscopy view of cultured cells on collagen coated glass slides. Labeling with antibodies against desmin (4.3B),  $\beta$ -MHC (4.3C), Troponin-T (4.3D),  $\alpha$ -SMA (4.3E) and  $\alpha$ -actinin (4.3F) revealed a clear pattern of striations. In contrast,  $\alpha$ -MHC, titin and SMM were negative (not shown). Cultures were positive for N-cadherin, a component of the adherens junction, which labeled the complete sarcolemma (4.3G). In a similar pattern, extensive Cx43 staining was found (4.3I). Cx40 was present at lower levels than Cx43 but heterogeneously distributed (4.3H). Cx45 was detected sparsely between some cells but only with use of high magnification (4.3J).

The Cx40 expression level was dependent on the age of the culture and the substrate used for coating. Cultures grown on laminin-coated slides contained more labeling compared to those grown on collagen coated slides. Additionally, Cx40 was more abundant in 2-day-old cultures than in 6-day-old cultures. Treatment of the cells with PE or ISO (1 or 24 h) in presence of serum, did not alter expression level or subcellular distribution of both Cx40 and Cx43. Serum deprivation for 24 hours, substantially reduced the total amount of Cx43 labeling and shifted the distribution from sarcolemmal to intracellular while Cx40 almost disappeared. Serum deprivation also reduced desmin and  $\alpha$ -actinin staining and cross-striations were less abundant. Analogue experiments using PC-1 serum free medium did not induce these changes.



*Figure 4.4 A-D: Immunohistochemical labeling of neonatal ventricular myocytes cultured on collagen in a star-shaped pattern. Bar (in A) = 50  $\mu$ m for A,D and 25  $\mu$ m for B,C.*

To minimize Cx40 expression (reduced by 4-6 days culture time) and to circumvent the unfavorable effects of serum deprivation (as observed in serum deprived routine medium and serum free PC-1), cells on preparations designed for the electrophysiological measurements of conduction velocity were cultured on collagen coating, for 4-6 days and in routine culture medium. Under these conditions, expression of connexins and muscle markers was analyzed on analogue prepared glass slides, but without the inserted electrodes. Figure 4.4 shows an example of a preparation labeled with antibodies raised against  $\alpha$ -actinin, desmin, Cx43 and Cx40. Immuno-positive staining is restricted to the collagen coated legs of the star since no cells adhered on the specific lacquer coating (see also Fig.4.1). Cells were strongly positive for  $\alpha$ -actinin (4.4A) and to a minor degree for desmin (4.4B), indicative for cardiomyocytes. Comparable to normal collagen coated glass slides, extensive Cx43 labeling was observed (4.4C) while Cx40 was hardly present (4.4D, arrowhead).

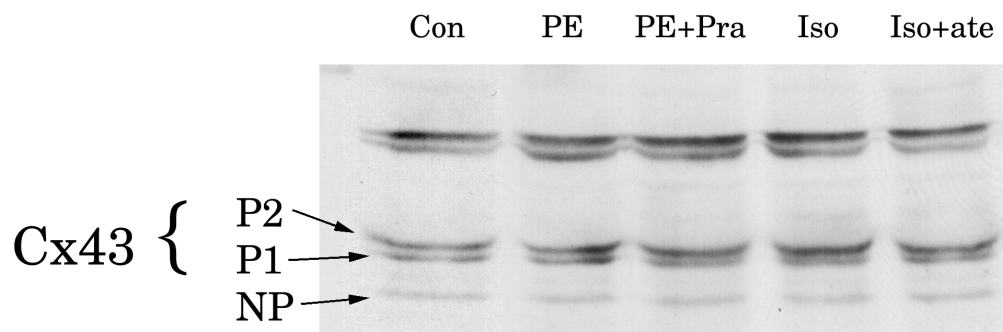


Figure 4.5 Western blot of (un)treated neonatal cardiomyocytes (total cellular protein) stained with antibodies raised against Cx43. Con=control, PE=phenylephrine, Pra=prazosin, ISO=isoproterenol, Ate=atenolol.

### Western blotting

In order to quantitate the effects of 24 hours adrenergic stimulation on the expression level of contractile proteins and gap junction proteins, Western analysis was performed on samples from cells cultured for 4-6 days on collagen coated dishes. Blots were incubated with antibodies raised against desmin,  $\alpha$ -actinin, N-cadherin and the gap junction proteins Cx40, Cx43 and Cx45. Probably due to the very low expression level, no signals were detected for Cx40 and Cx45 (not shown). Immunoblots of Cx43 (typical example in figure 4.5), exhibited the characteristic three-band pattern of 41-, 43- and 45 kD representing one non-phosphorylated (NP) and two phosphorylated forms (P1 and P2), respectively<sup>12</sup>. Upon adrenergic stimulation, no significant changes were found in the total density of the three bands. However, the P2 band of Cx43 in ISO treated cells consistently showed a higher density compared to the P2 band of control cells and of ISO treated cells pre-incubated with atenolol. Upon stimulation, no differences in expression level were found for the muscle markers desmin and  $\alpha$ -actinin, and the adherens junction component N-cadherin (data not shown).

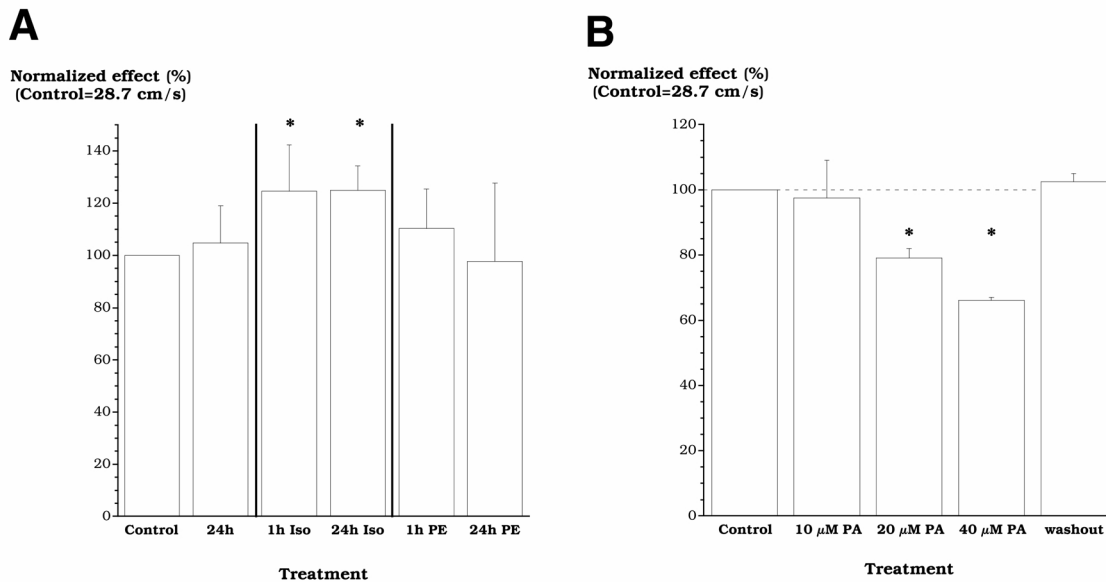


Figure 4.6 A: Bar plot showing the normalized effects on conduction velocity (control set on 100%) after stimulation of cells for 1 and 24 hours with ISO (N=6) and PE (N=4). B: Bar plot showing the effect of increasing concentrations of the gap junction blocker PA (N=2) on the normalized conduction velocity. Error bars are S.E.M. \* = significantly different from control.

### Effect of ISO and PE on impulse propagation

To correlate the expression and phosphorylation of gap junction channels with conduction velocity ( $\Theta$ ), identical experiments with 1 and 24h exposure to ISO and PE were performed with myocytes grown in a defined star-shaped pattern. Under control conditions, conduction velocity was  $28.7 \pm 2.1$  cm/s. Figure 4.6A shows that ISO significantly increased the conduction velocity ( $P=0.004$ ). After 1h exposure to ISO,  $\Theta$  was increased to  $124.6 \pm 7.3\%$  of control ( $P=0.003$ ), which persisted after 24h ( $124.9 \pm 4.2\%$ ,  $P=0.004$ ). PE did not significantly alter conduction velocity ( $P=0.64$ ), neither after 1h ( $110.4 \pm 7.5\%$ ,  $P=0.47$ ), nor after 24h ( $97.7 \pm 15.2\%$ ,  $P=0.87$ ).

Addition of Palmitoleic Acid (PA), a specific inhibitor of gap junction coupling<sup>13</sup> resulted in a reduction ( $P=0.019$ ) of conduction velocity (Fig. 4.6B). Exposure to  $10\mu\text{M}$  PA slightly reduced  $\Theta$  to  $97.3 \pm 11.6\%$  of control ( $P=0.74$ ). At 20 and  $40\mu\text{M}$ ,  $\Theta$  was increasingly and significantly reduced to  $79.3 \pm 3.1\%$  ( $P=0.04$ ) and  $65.7 \pm 1.0\%$  ( $P=0.068$ ), respectively. The effect of PA was reversible, since washout restored conduction velocity to control values ( $102.4 \pm 2.4\%$ ,  $P=0.77$ ).

### Expression of ion-channels

Since changes in expression and phosphorylation of Cx43 are probably not responsible for the observed changes in conduction velocity, we investigated the expression of ion channels contributing to excitability and shape of the conducted action potential. Results of (semi-quantitative) RT-PCR are shown in figure 4.7. PCR was performed with specific primers for  $\alpha_{1C}$  (L-type Calcium channel,  $I_{Ca-L}$ ), Kv4.3 ( $I_{TO}$ ), RERG ( $I_{Kr}$ ) and KvLQT1 ( $I_{Ks}$ ). Primers against GAPDH were used to assure that equal amounts of product were analyzed. As compared to control cells, expression of  $\alpha_{1C}$  decreased upon stimulation with ISO but increased after stimulation with PE. Both stimulation with ISO and PE slightly reduced expression

of Kv4.3. Expression of RERG and KvLQT1 was reduced upon stimulation with ISO but not affected by PE. Specificity of the reactions was indicated by the negative controls (no signals in right panel) in which the reverse transcriptase was omitted.

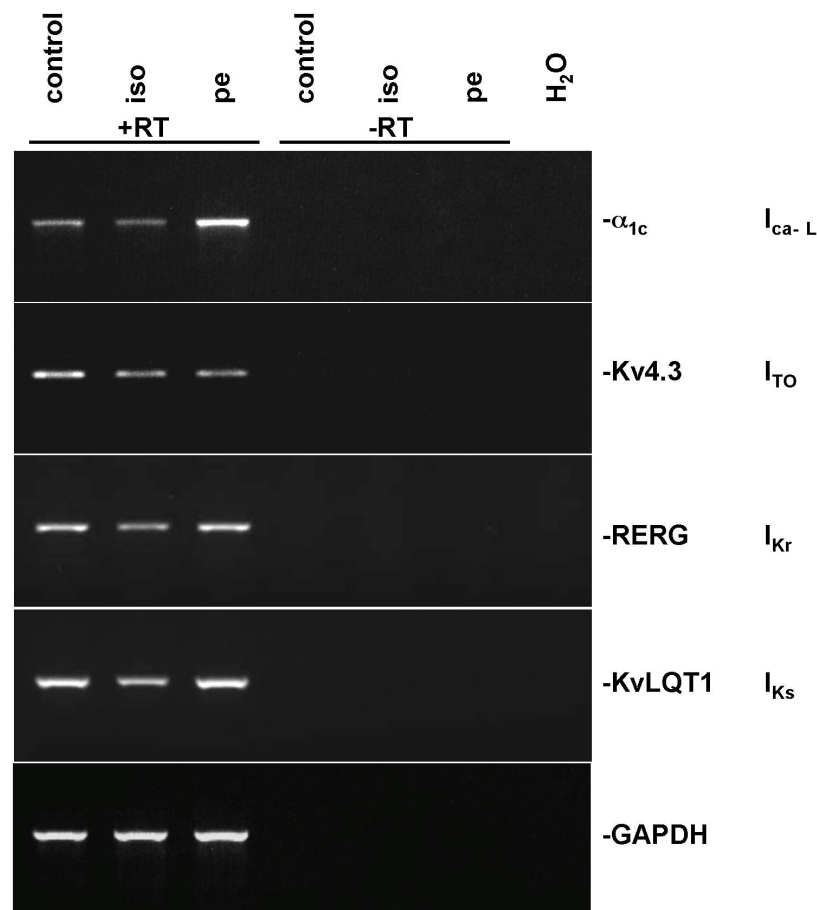


Figure 4.7 Overview of results obtained from RT-PCR. Equal amounts of DNA were separated as indicated by GAPDH signals. The first three lanes (from left) are showing the specific products obtained, the last 4 lanes are negative controls (RT omitted) and a water control. The legend on the right explains which product is shown and the current the product is associated with.

## Discussion

This study shows that; 1) 24 hours of stimulation with ISO and PE induced no marked alterations in expression, distribution and phosphorylation of Cx43. 2) Under these conditions, ISO but not PE increased conduction velocity by 25%. 3) Semi-quantitative RT-PCR showed a reduction in expression of α<sub>1c</sub>, RERG, KvLQT1 and Kv4.3 upon exposure to ISO while PE increased expression of α<sub>1c</sub>, decreased Kv4.3 leaving RERG and KvLQT1 unaffected.

### Characterization of our culture model.

Immuno-histochemical comparison between neonatal rat cardiomyocytes in culture and in intact ventricle showed that they were largely comparable.

Expression of cardiac muscle markers and of connexin isoforms in cultured preparations resembled that in the intact ventricle. In cultured cells, expression of Cx40 was as heterogeneous as in the ventricles. Furthermore, it was negatively affected by the substrate used for coating the slides and by the age of the cultures. Together with the negligible expression level of Cx45 this allowed us to create conditions where cells cultured in monolayers or in star shape patterns almost exclusively were coupled by Cx43 gap junctions: collagen coating of the substrate and 4-6 days culture time.

Exposure of the cells for 1 or 24 hours to ISO and PE did not markedly alter expression and distribution of Cx43, nor elevated it the expression levels of Cx40 and Cx45. ISO stimulation slightly increased Cx43 (P2) phosphorylation (Fig.4.5) by about 10%. It is doubtful whether this small increase can explain the increase in conduction velocity for it has been reported that, if anything, Cx43 phosphorylation mediated by PKA reduces gap junction channel conductance<sup>14</sup>. It has been shown before that long term stimulation of PKC (as PE does) or PKA (as ISO does) can change the expression and phosphorylation of Cx43 in cardiomyocytes<sup>7,15</sup>. A possible explanation for the absence of such effects in our cultures could be the inclusion of serum in the culture medium since the studies referred to used serum free PC-1 medium. Similarly, the inclusion of serum in our culture medium presumably prevented induction of hypertrophy in cultured myocytes because no differences in cell shape or in expression level of contractile proteins were observed. Serum deprivation did not solve this problem, however, because it caused the cells to atrophy, reduced expression of Cx43 and arrested spontaneous activity. Preliminary experiments with serum free PC-1 medium did not show these adverse effects, and experiments with ISO and PE stimulation in this medium are now in progress.

### **Measurements of conduction velocity and expression of ion channels.**

Conduction velocity ( $\Theta$ ) is dependent of action potential (AP) shape, action potential amplitude and on axial conductance composed of cytoplasmic conductance and gap junctional conductance. ISO but not PE exposure for 24 hours increased  $\Theta$  by 25%. As discussed, changes in gap junctional conductance are not involved and changes in cytoplasmic conductance are unlikely. Therefore we wondered whether changes in action potential size and shape could explain the observed effects. In a preliminary experiment (Fig.4.8), we found that ISO stimulation increased the rate of rise of the action potential and shortened its duration while PE had no effect on rate and rise but increased AP duration.

As shown in figure 4.7, ISO reduced expression of  $\alpha_{1C}$ , Kv4.3, RERG, and KvLQT1 mRNA, responsible for the membrane currents  $I_{Ca-L}$ ,  $I_{to}$ ,  $I_{Kr}$ , and  $I_{Ks}$ , respectively. Reduction of  $I_{Ca-L}$  would result in the observed shortening of the action potential by ISO, however, reducing  $I_{to}$ ,  $I_{Kr}$ , and  $I_{Ks}$  typically would increase action potential duration. On the other hand, in atrial fibrillation similar changes in mRNA levels and in accompanying currents were observed which resulted in shortening of the action potential duration<sup>16-18</sup>. The overall effect cannot be unequivocally explained by the PCR-data, which particularly do not include data on the sodium current ( $I_{Na}$ ). The rate of rise of the AP is primarily determined by the density of the sodium current ( $I_{Na}$ ). Data on the expression level of sodium channels have to be collected in order to evaluate whether an increase in number of sodium channels can explain the ISO induced increase ( $68 \pm 22\%$  increase as compared to control) in rate of rise of the action potential (Fig.4.8).

PE increased the expression of  $\alpha_{1C}$ , but reduced that of Kv4.3. An increased  $I_{Ca-L}$  and reduced  $I_{to}$  explain well an increased duration of the action potential and is typical for PE<sup>19,20</sup>. Modulation of expression of  $I_{Ca-L}$  by PE does not affect the

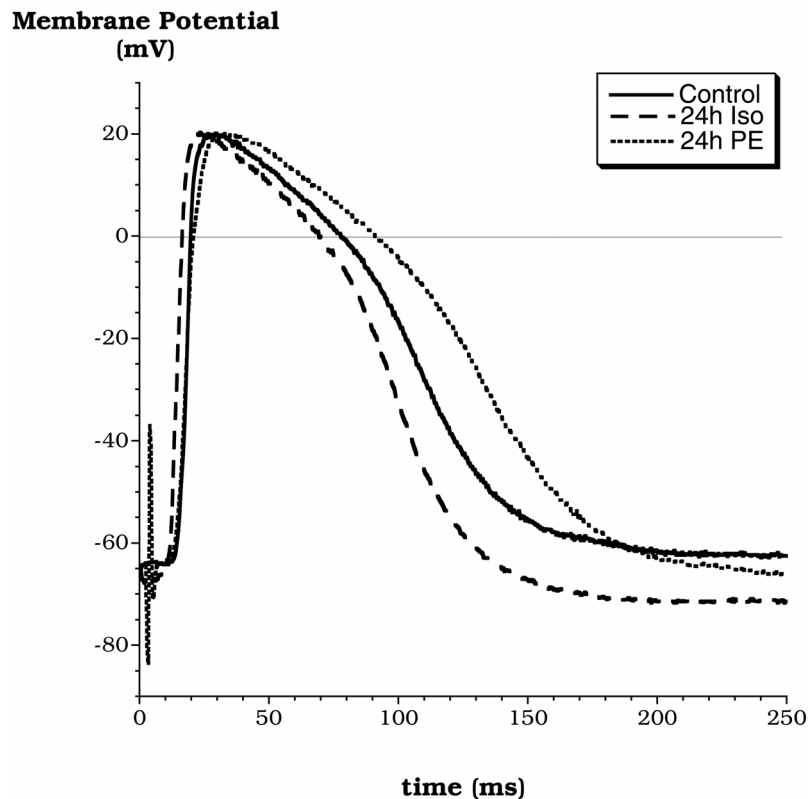


Figure 4.8 Examples of action potentials recorded from myocytes cultured on the star shaped preparations.

upstroke of the action potential, presumably because this is mainly determined by the sodium current.

Future experiments have to be performed to further unravel the effect of ISO and PE on the conduction of the action potential, preferably using the voltage clamp technique, which allows for direct measurement of membrane currents. Furthermore, it is necessary to elucidate whether changes in quantity of mRNA (revealed from RT-PCR) are a reliable prediction of functional changes at the protein level for all contributing ion channels. Finally, since the effect of ISO on conduction velocity is already significant after 1 hour, it is not unlikely that phosphorylation of ion channels (fast responses) could be a modulatory mechanism involved.

### **Acknowledgements**

Mw. SJA Tasserion (Dept.Experimental Cardiology, AMC, Amsterdam) is kindly acknowledged for her contribution in coating of the specific preparations and for isolation and culture of the myocytes on these preparations.

### **References**

1. Delorme B, Dahl E, Jarry-Guichard T, Marics I, Briand JP, Willecke K, Gros D, Théveniau-Ruissy M. Developmental regulation of Connexin40 gene expression in mouse heart correlates with the differentiation of the conduction system. *Developmental Dynamics*. 1995;204:358-371.

2. Van Kempen MJA, Vermeulen JLM, Moorman AFM, Gros D, Paul DL, Lamers WH. Developmental changes of connexin40 and connexin43 mRNA distribution patterns in the rat heart. *cardiovascular research*. 1996;32:886-900.
3. Delorme B, Dahl E, Jarry-Guichard T, Briand JP, Willecke K, Gros D, Theveniau-Ruissy M. Expression pattern of connexin gene products at the early developmental stages of the mouse cardiovascular system. *Circ Res*. 1997;81:423-437.
4. Alcoléa S, Théveniau-Ruissy M, Jarry-Guichard T, Marics I, Tzouanacou E, Chauvin JP, Briand JP, Moorman AFM, Lamers WH, Gros DB. Downregulation of Connexin45 gene products during mouse heart development. *Circulation Research*. 1999;84:1365-1379.
5. Coppen SR, Dupont E, Rothery S, Severs NJ. Connexin45 expression is preferentially associated with the ventricular conduction system in mouse and rat heart. *Circulation Research*. 1998;82:232-243.
6. Coppen SR, Severs NJ, Gourdie RG. Connexin45 ( $\alpha 6$ ) expression delineates an extended conduction system in the embryonic and mature rodent heart. *Developmental Genetics*. 1999;24:82-90.
7. Darrow BJ, Fast VG, Kléber AG, Beyer EC, Saffitz JE. Functional and structural assessment of intercellular communication: Increased conduction velocity and enhanced connexin expression in dibutyryl cAMP-treated cultured cardiac myocytes. *Circulation Research*. 1996;79:174-183.
8. Kwak BR, van Kempen MJA, Théveniau-Ruissy M, Gros DB, Jongsma HJ. Connexin expression in cultured neonatal rat cardiomyocytes reflects the pattern of the intact ventricle. *Cardiovascular Research*. 1999;44:370-380.
9. de Bruijne J, Jongsma HJ. Membrane properties of aggregate of collagenase-dissociated rat heart cells. *Adv Myocardiol*. 1980;1:231-242.
10. Lowry OH, Rosebrough NJ, Farr AL, Randall RJ. Protein measurement with the folin phenol reagent. *Journal of Biological Chemistry*. 1951;193:265-275.
11. Laemmli UK. Cleavage of structural proteins during the assembly of the head of bacteriophage T4. *Nature*. 1970;227:680-685.
12. Musil LS, Cunningham BA, Edelman GM, Goodenough DA. Differential phosphorylation of the gap junction protein connexin43 in junctional communication-competent and -deficient cell lines. *J Cell Biol*. 1990;111:2077-2088.
13. Burt JM, Massey KD, Minnich BN. Uncoupling of cardiac cells by fatty acids: Structure-activity relationships. *ajp*. 1991;260:C439-C448.
14. Kwak BR, Jongsma HJ. Regulation of cardiac gap junction channel permeability and conductance by several phosphorylating conditions. *Molecular and Cellular Biochemistry*. 1996;157:93-99.
15. Dodge SM, Beardslee MA, Darrow BJ, Green KG, Beyer EC, Saffitz JE. Effects of angiotensin II on expression of the gap junction channel protein connexin43 in neonatal rat ventricular myocytes. *J Am Coll Cardiol*. 1998;32:800-807.
16. Yue L, Feng J, Gaspo R, Li GR, Wang Z, Nattel S. Ionic remodeling underlying action potential changes in a canine model of atrial fibrillation. *Circ Res*. 1997;81:512-525.
17. Yue L, Melnyk P, Gaspo R, Wang Z, Nattel S. Molecular mechanisms underlying ionic remodeling in a dog model of atrial fibrillation. *Circ Res*. 1999;84:776-784.
18. van der Velden HMW, van der Zee L, Wijffels MC, van Leuven C, Dorland R, Vos MA, Jongsma HJ, Allessie MA. Atrial fibrillation in the goat induces changes in monophasic action potential and mRNA expression of ion channels involved in repolarization. *J Cardiovasc Electrophysiol*. 2000;11:1262-1269.
19. Tomaselli GF, Marbán E. Electrophysiological remodeling in hypertrophy and heart failure. *Cardiovascular Research*. 1999;42:270-283.
20. Zhang TT, Takimoto K, Stewart AF, Zhu C, Levitan ES. Independent regulation of cardiac Kv4.3 potassium channel expression by angiotensin II and phenylephrine. *Circ Res*. 2001;88:476-482.

# Chapter 5

---

## **Electrical activation of rodent ventricular conduction systems: correlation with expression of cardiac connexins and tissue morphology.**

Toon A.B. van Veen, Harold V.M. van Rijen, Marjan J.A. van Kempen, Jacques M.T. de Bakker, Tobias Opthof, Habo J. Jongsma

*To be submitted*

## **Abstract**

**Background:** Gap junction channels facilitate propagation of the action potential from one cell to another. Connexin40 (Cx40) and Connexin45 (Cx45) are the prominent gap junction proteins in the specific conduction system of mammals. We studied the expression/distribution of connexins in relation to propagation of the electric impulse in the ventricular conduction system of mice and rats.

**Methods:** Isolated hearts of 6 adult mice (C57B6) and 6 rats (Wistar) were Langendorff perfused with modified tyrode solution at 2 respectively 10 ml/min. After removing the right and left ventricular free wall, extracellular activity was determined with a multiterminal electrode harboring 247 terminals. Connexin distribution was determined with antibodies raised against Cx40, Cx43 and Cx45. Collagen distribution was assessed by Sirius Red staining.

**Results:** In mice, myocytes of the common bundle and bundle branches labeled positive for Cx40 and Cx45 but not for Cx43. Only in the very distal parts of the branches, Cx40, Cx43 and Cx45 colocalized. In contrast, Cx43 is co-expressed with Cx40 and Cx45 in the proximal branches of the rat heart. In both species, size of the intercalated disks and expression of muscle markers differ between the conduction system and the septal working myocardium. In mice, myocytes of the proximal branches are morphologically different from those in the distal branches with respect to the organization of the intercalated disks. In the proximal branches of the mouse heart, conduction velocity of the electrical impulse was significantly higher as compared to the distal branches while in rat, conduction velocity was independent of the recording position.

**Conclusion:** In mice, connexin expression, distribution and conduction velocity differ between the proximal and distal bundle branches. Comparison with connexin data and conduction velocity in the rat bundle branches suggest that differences in the connexin distribution are not responsible for the differences in conduction velocity in the proximal and distal bundle branches of mouse heart.

## **Introduction**

In the heart, the action potential is propagated from cell to cell by current flow through specialized membrane structures named gap junctions; agglomerates of intercellular channels connecting the cytoplasm of adjacent cells. In mammals, at least 15 different gap junction proteins (connexins, Cxs) have been cloned (for a review see<sup>1</sup>). In between cardiac myocytes, gap junction channels composed of Cx40, Cx43 and Cx45, have been identified. Expression is primarily located on the end-to-end cell-edges in specialized structures called intercalated disks (IDs). In most mammalian hearts, Cx40 is expressed in the atrial working myocardium, the vascular endothelium, the sinoatrial node and the ventricular conduction system<sup>2-9</sup>. Cx43 is ubiquitously expressed in the atrial and ventricular working myocardium, but also in the peripheral parts of the ventricular conduction system<sup>4,5,8,10</sup>. Cx45 is expressed in the atrio-ventricular conduction system (including the atrio-ventricular node), and probably also at low levels in the atria and ventricles<sup>11,12</sup>.

Recent studies stress the importance of different gap junction isoforms for propagation of the electrical impulse through the conduction system. Lack of Cx40 results in impaired conduction and conduction block in the bundle branches<sup>13,14</sup>. Depletion of Cx45, the other prominent isoform expressed in the conduction system causes mice to die at day 9.5 pc *in utero* probably due to conduction block<sup>15,16</sup>.

Although the significance of the different gap junction isoforms for propagation of the cardiac impulse has been noted, data on the distribution of connexins in the conduction system in relation to conduction velocity are lacking. We therefore determined the expression of cardiac connexins in the ventricular conduction system of mice and rats. Connexin expression was correlated with the electrical activation pattern of the inter ventricular septum (IVS), impulse propagation in the conduction system and morphology of the tissue involved.

## **Materials and Methods**

### *Animals*

Commercially available OLA-C57B/6 mice and Wistar rats were bred at the GDL, Utrecht University, Utrecht, The Netherlands. Mice and rats between 4 and 6 months of age were used for experiments. The study was performed conform the guiding principles of the American Physiological Society.

### *Preparation of the hearts*

Mice and rats were anaesthetized by an intraperitoneal injection of urethane (1.5 g/kg bodyweight). The chest was opened and the heart was excised and submerged in ice-cold Tyrode's solution<sup>17</sup>. With the help of a binocular microscope the heart was dissected from the lungs and other tissue, the aorta was cannulated and the heart was connected to a Langendorff-perfusion setup and retrogradely perfused at 37°C with a perfusion pressure of 80 cm H<sub>2</sub>O. Perfusion buffer composition was (in mM): NaCl 90, KCl 3.6, KH<sub>2</sub>PO<sub>4</sub> 0.92, MgSO<sub>4</sub> 0.92, NaHCO<sub>3</sub> 19.2, CaCl<sub>2</sub> 1.8, glucose 22, creatin 6, taurine 6, insulin 0.1 µM, gassed with 95% O<sub>2</sub> and 5% CO<sub>2</sub>. In all experiments the heart started to beat immediately after initiating perfusion. Flow rate was approximately 2 ml/min (mice) and 10 ml/min (rats). To prevent heat loss to the surroundings, the heart was placed against a heated (37°C) and continuously moisturized support.

### *Recording of electrograms*

Extracellular electrograms were recorded with a 247 (19 by 13 electrode-grid inter-electrode distances of 0.3 mm) or 208 (16 by 13 electrode-grid, inter-electrode distances of 0.4 mm) multi terminal electrode, mounted in a micromanipulator. Electrodes were silver wires with a diameter of 0.1 mm which were isolated except at the tip. Recordings were made in unipolar mode with regard to a reference electrode connected to the support of the heart. Electrograms were acquired using a custom built 256-channel data-acquisition system. Signals were bandpass filtered (low cut-off 0.16 Hz (12dB), high cut-off 1 kHz (6 dB)), and digitized with 16 bits resolution at a bit step of 2 µV and a sampling frequency of 2 kHz. The input noise of the system was 4 µV (peak-peak). For septal measurements, the right and left ventricular free walls were removed and the electrode grid was positioned on the IVS just below the atrio-ventricular valves.

### *Data Analysis*

Activation maps were constructed from activation times, determined with custom written software based on Matlab (The Mathworks Inc.). The moment of maximal negative dV/dt in the unipolar electrograms was selected as the time of local activation. Statistical comparisons were performed using an unpaired students *t*-test, using StatView 4.5. P-values ≤ 0.05 were considered as statistically significant.

### *Immunohistochemistry and histology*

Following the electrophysiological recordings, hearts were rapidly frozen in liquid nitrogen and stored at  $-80^{\circ}\text{C}$  until use. Frozen hearts were serially sectioned in a frontal plane to produce 'four chamber view' sections of  $10\text{ }\mu\text{m}$  thickness which were mounted on aminopropyltriethoxysilane- (AAS) coated glass slides. Sections at the level of the conduction system were permeabilized in 0.2% Triton X-100 (1 hour), blocked in 2% bovine serum albumin (BSA, 30 min.) and incubated overnight in presence of 10% normal goat serum (NGS) with primary antibodies directed against Cx40, Cx43, Cx45,  $\alpha$ -actinin,  $\beta$ -catenin, desmin and Pan-cadherin. After blocking again with 2% BSA (30 min.), secondary labeling was performed with appropriate Texas Red (TR) or fluorescein isothiocyanate (FITC)-conjugated antibodies (2 hours in presence of 10% NGS). All chemicals were dissolved in phosphate buffered saline (PBS) which was also used to wash the sections in between the subsequent incubations. Finally, sections were mounted in Vectashield (Vector Laboratories) and examined using a light microscope equipped for epifluorescence (Nikon Optiphot-2) or by confocal laser scanning microscopy (Nikon RCM-8000 Real Time Laser Confocal Microscope). Additionally, sections were fixed in 4% paraformaldehyde/PBS (30 min), stained with picro-sirius red and examined by light microscopy for assessment of connective tissue<sup>18</sup>.

### *Antibodies*

The following antibodies were used; a rabbit polyclonal antibody (crude serum, 1:4000) raised against aminoacids 259-396 of mCx45, kindly provided by Dr. T.H. Steinberg, Washington University, St.Louis; a rabbit polyclonal antibody (0.5  $\mu\text{g/ml}$ ) raised against 19 aminoacids in the carboxyterminus of mCx40 (Alpha Diagnostics), a mouse monoclonal antibody (1  $\mu\text{g/ml}$ ) raised against aminoacids 236-382 of rat Cx43 (Transduction Laboratories); a mouse monoclonal antibody (0.25  $\mu\text{g/ml}$ ) raised against human desmin (Sanbio); a mouse monoclonal antibody (1:1000) raised against rabbit skeletal  $\alpha$ -actinin (Sigma); a mouse monoclonal antibody (1:1000) raised against the C-terminus of mouse  $\beta$ -catenin (Transduction Laboratories) and a rabbit polyclonal antibody (1:800) raised against the C-terminus of chicken N-cadherin (Sigma).

Secondary antibodies were purchased from Jackson Laboratories; TR conjugated donkey-anti-mouse IgG (13  $\mu\text{g/ml}$ ), TR conjugated donkey-Anti-Rabbit IgG (13  $\mu\text{g/ml}$ ), FITC-conjugated goat-anti-rabbit IgG (3  $\mu\text{g/ml}$ ) and FITC-conjugated donkey-anti-mouse IgG (13  $\mu\text{g/ml}$ ).

## **Results**

### ***Connexin expression in the atrial and ventricular myocardium***

As reviewed in<sup>19</sup>, both in rat and mouse hearts, Cx43 labeling was observed between myocytes of the atrial and ventricular working myocardium while Cx40 was detected between myocytes of the conduction system and between mouse atrial myocytes. Cx45 staining was exclusively found in myocytes of the conduction system. In working myocardial cells, Cx40 and Cx43 are clustered in IDs forming the longitudinal cell borders where they prominently co-localized with N-cadherin, a component of the adherence junctions, and  $\beta$ -catenin which anchors the cytoskeleton to the adherence junctions. In both species, atrial IDs are much smaller compared to ventricular IDs.

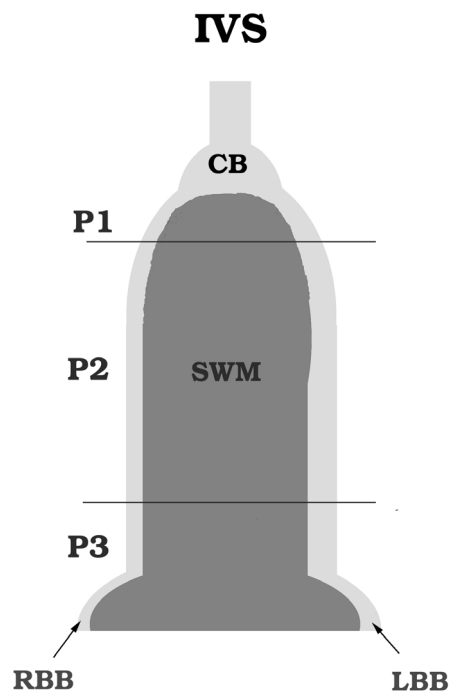


*Figure 5.1 Scheme of the inter ventricular septum indicating the different regions of the conduction system. IVS=interventricular septum, CB= common His bundle, LBB=left bundle branch, RBB=right bundle branch, SWM=septal working myocardium. P1, P2, P3 are the proximal, midseptal and distal regions of the bundle branches.*

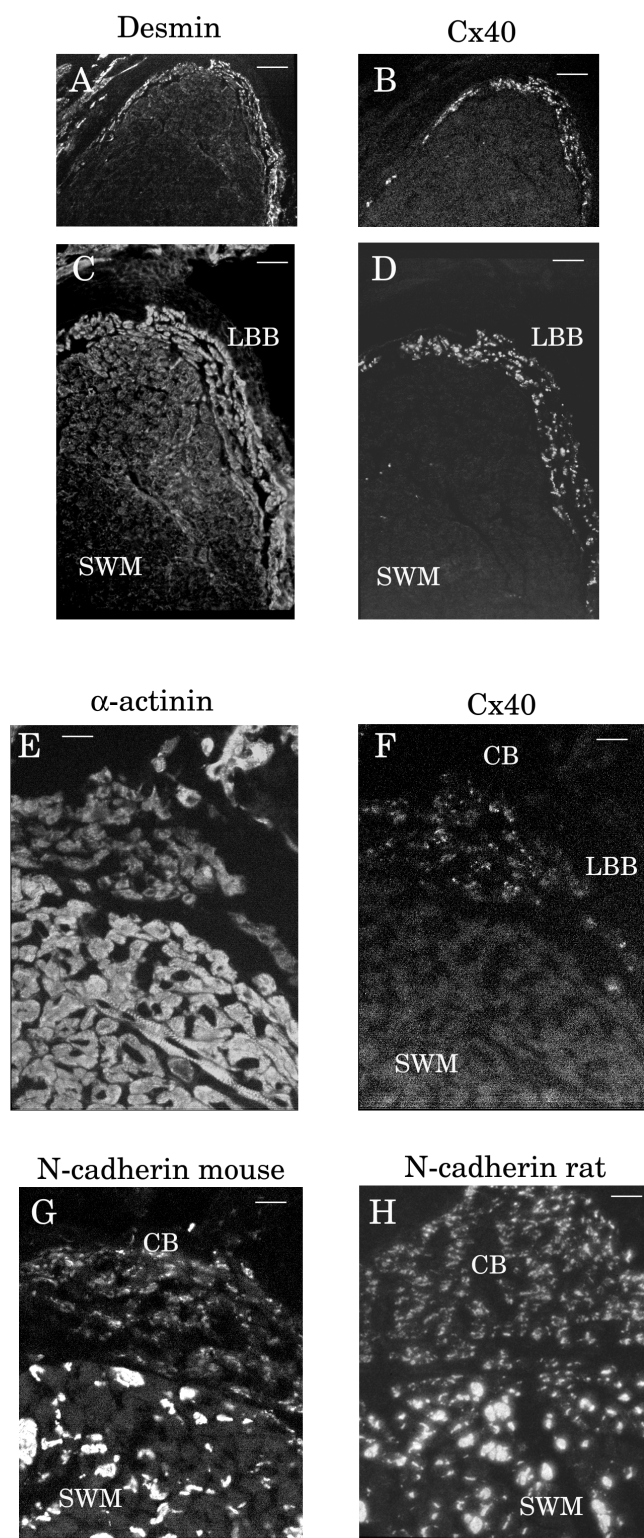
### **Expression of cardiac muscle markers in the ventricular conduction system.**

Figure 5.1 schematizes the IVS with the different regions of the conduction system. We arbitrary divided the bundle branches (BB) in three regions; P1 directly apical from the bifurcation, P2 comprises the midsection and P3 the distal part of both BB and the Purkinje-fibers.

Both in mice and rats desmin proved to be a potent marker to delineate the ventricular conduction system. In mouse heart e.g., desmin labeling of the ventricular conduction system is more intense compared to labeling of the septal working myocardium (Fig. 5.2A,C). Double labeling of the same sections with Cx40 (Fig. 5.2B,D) shows that highest intensity of desmin labeling is observed in Cx40 positive cells of the conduction system. Figure 5.2A,C additionally show that the proximal left bundle branch (LBB, P1) measures 4 to 6 endocardial cell-layers which is about twice the thickness of the right bundle branch (RBB). On the other hand, double labeling of  $\alpha$ -actinin (Fig. 5.2E) and Cx40 (Fig. 5.2F) revealed a lower intensity of  $\alpha$ -actinin labeling in the ventricular conduction system compared to the septal working myocardium. Control incubations using only the fluorescent secondary antibody excluded that the increased intensity is caused by aspecific binding of the secondary antibody (not shown). N-cadherin labeling in mice (Fig. 5.2G) and rats (Fig. 5.2H), revealed that IDs between myocytes of the ventricular conduction system are much smaller compared to IDs between septal working myocardial cells.

### **Connexin expression in the ventricular conduction system.**

*Expression in the mouse.* Serial sections of the IVS were labeled with antibodies raised against Cx40, Cx43 and Cx45. Septal working myocardial cells show



*Figure 5.2 Immunolabeling of the mouse IVS (A-G). Double labeling with antibodies raised against desmin (A and enlarged in C) and Cx40 (B and enlarged in D), and of  $\alpha$ -actinin (E) and Cx40 (F). N-cadherin labeling of the HIS - IVS transition in mouse heart (G) and rat heart (H). Bar = 80  $\mu$ m in A,B, 40  $\mu$ m in C,D,H, 20  $\mu$ m in E, F and G. SWM= septal working myocardium, CB= common His-bundle, LBB= left bundle branch.*

abundant Cx43 labeling but are negative for Cx40. In the common bundle double labeling of Cx40 and Cx45 can be detected while Cx43 is absent (Fig.5.5, left panel P1, Fig.5.3A, 5.3C). Following the labeling of Cx45 from the central core of the common bundle, where it colocalizes with Cx40, towards the borderzone between the common bundle and the septal working myocardium, intensity of Cx45 labeling increases. In between this central core and the top of the septal working myocardium, one or two transitional cell-layers exist which are exclusively positive for Cx45. More apical, the first layers of septal working myocytes are positive for Cx43 and Cx45, but further in apical direction Cx45 labeling rapidly declines to the level of very rare and small spots until it is undetectable after about five cell layers apical from the top of the septal working myocardium. The co-localization of Cx43 and Cx45 at the interface between the common bundle and the septal working myocardium (Fig.5.3C, arrowheads), and the absence of an isolating sheet of connective tissue at this level (Fig.5.3E, arrow-heads), result in activation of the septum in a baso-apical direction (Fig.5.3G).

No co-localization of Cx40 and Cx43 (Fig.5.4A, 5.4C) nor of Cx45 and Cx43 (Fig.5.4B) was observed in cells forming the borderzone of both proximal BB (Fig.5.5 left panel, P1 and P2) and the septal working myocardium. In this area, cells are either positive for Cx40 and Cx45 (BB) or for Cx43 (working myocardium). Further apically, in the distal parts of the BB (Fig.5.5 left panel P3, Fig.5.4D), colocalization of Cx40 and Cx43 and of Cx45 and Cx43 is present. Here, cells positive for Cx40 and Cx45 are occasionally found to be neighbored by cells positive for Cx40, Cx43 and Cx45. However, no labeling of Cx45 is found in cells besides those which are positive for Cx40 indicating them to be part of conductive tissue.

*Expression in rat heart.* Cx43 is the exclusively observed isoform in the septal working myocardium. Cx40 and Cx45 labeling in the common bundle was comparable with that in mice. However, Cx45 is absent in the first basal cell-layers of the septal working myocardium and most important, at the transition of the common bundle and the septal working myocardium, Cx43 does not colocalize with Cx40 nor with Cx45 (Fig.5.5 right panel P1, Fig.5.3B, 5.3D). Here, a narrow immunonegative space separates both regions. Sirius Red staining showed that in rats, in contrast to the mouse, the common bundle is isolated from the basal part of the septal working myocardium by a thin sheet of connective tissue (Fig.5.3F, arrow heads). Additionally, more connective tissue is found, as compared to mice, surrounding the myocytes of the proximal BB. These observations suggest that in contrast to mice, in rats no direct electrical communication exist between the common bundle and the top of the septal working myocardium. This is substantiated by septal activation maps made during sinus rhythm which revealed that earliest activation is found in the midseptal region from which the activation spreads over the septum with latest activation found at the base (Fig.5.3H).

In the BB, double-labeling of Cx43 with Cx40 is already detectable just apical from the bifurcation (Fig.5.5 right panel P1, Fig. 5.4E) where in addition Cx45 labeling is observed in the BB but not in the septal working myocardium (Fig.5.4F).

### **Cellular organization of gap junction expression in the bundle branches.**

In both rat and mice, myocytes of the proximal BB (P1 and P2) differ in several aspects from septal working myocardial cells. Firstly, ID labeling profiles in cells of the BB are smaller than neighboring septal working myocardial cells (see Fig. 5.4B,E). Secondly, myocytes of the BB and those of the septal working myocardium express different connexins. Thirdly, the subcellular distribution of Cx40 and Cx45 (and in rat also of Cx43) in myocytes forming the proximal part (P1 and P2)

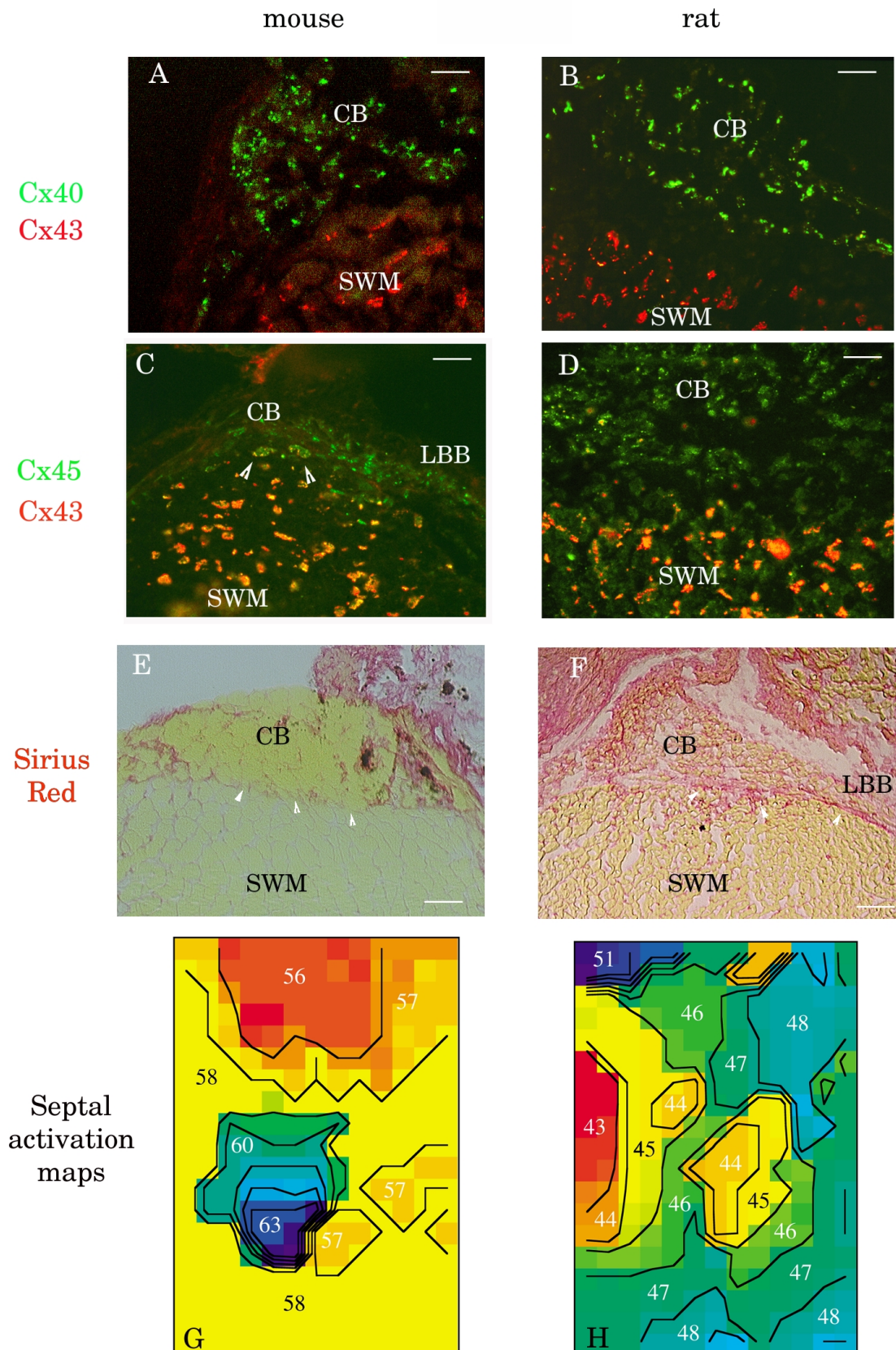


Figure 5.3 Left panels: mouse heart, right panels: rat heart. Double labeling of the CB-SWM transition with: Cx40/Cx43 in A and B, Cx45/Cx43 in C and D. Sirius red staining of the CB-SWM transition in E and F. Bar = 20  $\mu$ m in A, 40  $\mu$ m in B, C, D, E, and 100  $\mu$ m in F. Septal activation maps in G and H. Numbers indicate activation time in ms. SWM= septal working myocardium, CB= common His-bundle, LBB= left bundle branch.

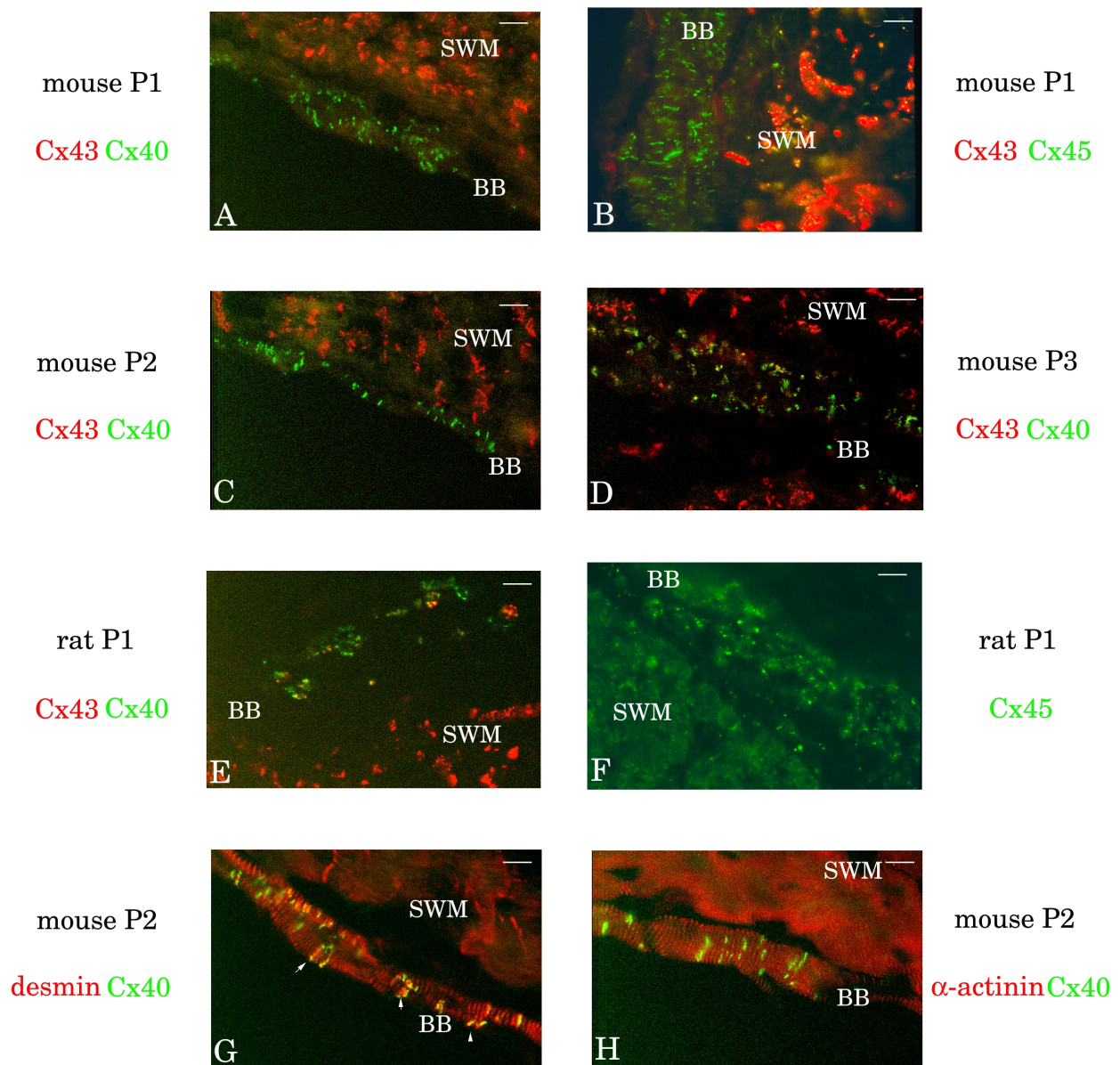
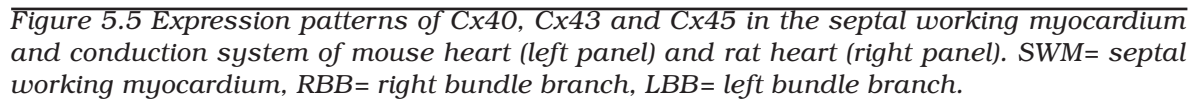


Figure 5.4 Immunofluorescence labeling of the mouse (A,B,C,D,G,H) and rat (E,F) bundle branches. Bar = 10  $\mu$ m in H, 20  $\mu$ m in A,B, C, D,E, F, G. SWM= septal working myocardium, BB= bundle branch.

of both the LBB and RBB, differs substantially from the distribution of Cx43 gap junctions between septal working myocardial cells.

Between ventricular and atrial cardiomyocytes, gap junctions are fairly exclusively located in the IDs forming the longitudinal cell borders. In contrast, in P1 and P2 of the mouse heart, labeling with Cx40 (Fig.5.4A,C) and Cx45 (Fig.5.4B) reveals a pattern of small 'steps' (like a staircase) over the entire cell membrane. Double-labeling of Cx40 with desmin (Fig.5.4G) or of Cx40 and  $\alpha$ -actinin (Fig.5.4H) shows that Cx40, not only co-localizes at the longitudinal IDs where desmin staining shows highest intensity (arrow heads), but is also found in between these longitudinal cell borders. This suggests that ID like structures in the ventricular conduction system are not exclusively located at the longitudinal cell borders. Staining against other ID associated proteins like  $\beta$ -catenin (Fig.5.7A) and N-cadherin (Fig.5.7B) confirmed this hypothesis.

Confocal analysis (stacks of 0.2  $\mu$ m optical sections) of the cellular organization



### ***Conduction of the electric impulse in the bundle branches.***

To investigate whether differences in connexin expression patterns within the BB functionally reflect on action potential propagation, we mapped the electrical activity of the specific conduction system with the multi-electrode positioned 0.5 mm below the atrio-ventricular valves. Figure 5.7E shows a typical example of a LBB recording in mouse heart. Both in the RBB and the LBB, proximal conduction (P1 and early P2) velocity appeared significantly higher than in more distal parts (remainder P2 and P3). Conduction velocity in the LBB was  $71.6 \pm 8.9$  cm/s (mean  $\pm$  SEM) in the proximal part and  $27.7 \pm 4.9$  cm/s in the distal part ( $P < 0.001$ ).

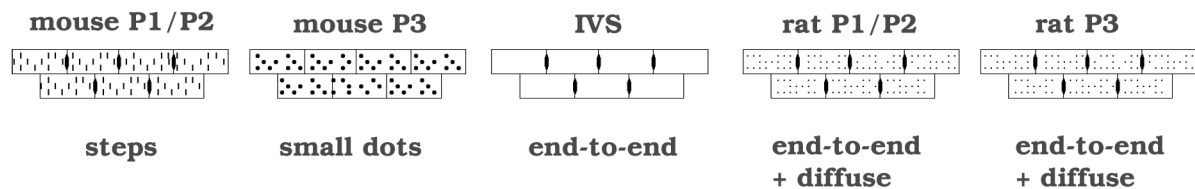


*Figure 5.7 Schematic illustration indicating the subcellular distribution of intercalated disk proteins in the different regions of the ventricular conduction system of adult mouse and rat heart.*

In the RBB, conduction velocity in the proximal part was  $57.7 \pm 6.1$  cm/s and in the distal part  $30.0 \pm 10.0$  cm/s ( $P < 0.04$ ).

Similar recordings in rat heart (Fig. 5.7F) revealed that there were no significant differences in conduction velocity ( $n=3$ ,  $P=0.82$ ) over the entire recorded distance (P1 and first half of P2). Unfortunately, we were unable to map electrical activity in the distal parts (apical part P2 and P3) of the BB. When the recorded distance was divided in two equal parts, conduction velocity in the LBB was  $56 \pm 4.9$  cm/s in the basal part and  $49 \pm 10.5$  cm/s in the apical part. Conduction velocity in the RBB was  $55 \pm 4.3$  cm/s in the basal part and  $54 \pm 3.5$  cm/s in the apical part.

## Discussion

This study shows that: 1) Similar connexin isoforms are expressed within the conduction system of mice and rats. 2) In mouse but not rat co-localization of Cx45 and Cx43 exists at the interface between the common-bundle and the septal working myocardium, resulting in a basal-apical activation of the septum in mice. 3) Co-localization of Cx43 with Cx40 and Cx45 already commences in the basal parts of the BB in rat hearts, whereas this only occurs in the very distal parts in mice. 4) Subcellular distribution of Cx40 and Cx45 in the proximal part of the mouse BB differs from that in the distal part, which is associated with differences in the conduction velocity in these parts. In contrast, in rats the distribution of these connexins is uniform along the entire BB as is the conduction velocity (as far as recorded).

### **Connective tissue, expression of connexin isoforms and septal activation.**

Both in mice and rats, Cx40 and Cx45 are expressed in the complete conduction system (this study and<sup>11,12</sup>). However, in mouse BB expression of Cx43 does not colocalize with Cx40 and Cx45 until the level of P3, the very distal parts of the BB and the purkinje fibers while in rats, Cx43 is already co-expressed at the very basal parts of the BB (P1, just apical from the bifurcation). This proximal expression of Cx43 has previously been shown for human and cow where in cow the proximal BB are separated from the septal working myocardium by an isolating sheath of connective tissue<sup>20</sup>. In this respect, the connective tissue surrounding the proximal BB in rats is more pronounced compared to that in mice.

The amount of connective tissue and expression of connexins at the transition between the common bundle and the top of the septal working myocardium also differs between rats and mice. In both species, Cx40 expression is exclusively found in the BB and not in septal working myocytes. In contrast, in mouse hearts

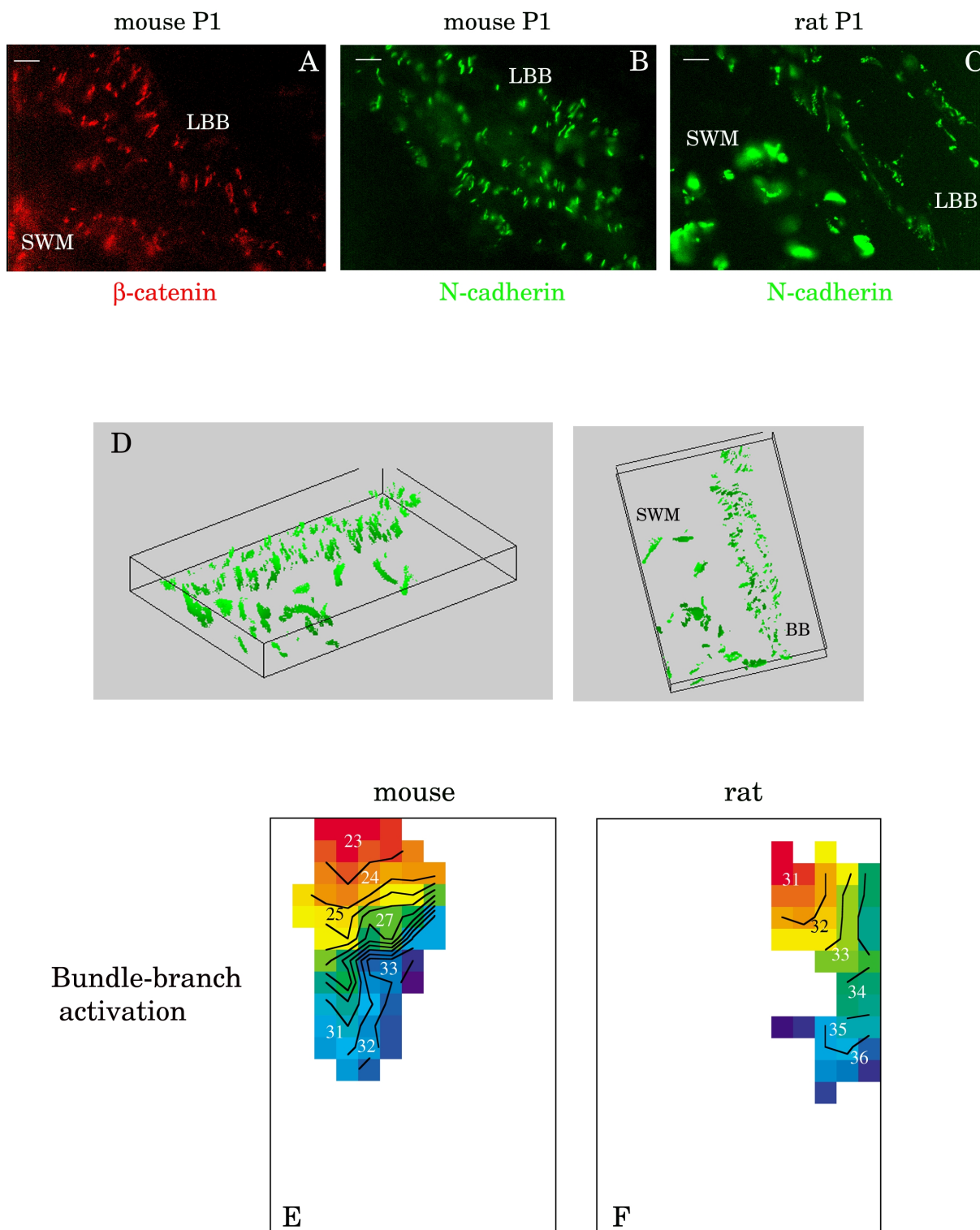


**Figure 5.6** Immuno-labeling of the mouse (A,B) and rat (C) proximal bundle branches. Bar = 10  $\mu$ m in A,B, and 20  $\mu$ m in C. D: Immunofluorescence reconstruction of difference in ID structure between the cells of the bundle branches and the septal working myocardium. E and F: Representative electrical activation maps of the mouse (E) and rat (F) left bundle branch. Earliest activation is shown in red, latest activation in blue. Numbers indicate activation time in ms. SWM= septal working myocardium, LBB= left bundle branch.

Cx43 and Cx45 co-localize in the mentioned borderzone while in rats such a colocalization could not be detected since the common bundle (Cx45 positive) is separated from the septal working myocardium by an thin immuno-negative space, representing a sheet of connective tissue. In mice, the thin sheet of connective tissue is discontinuous and penetrated by myocytes which are physically connected to each other. In larger mammals, a sheet of connective tissue electrically isolates the common bundle from the septal working myocardium which prevents premature activation of the septal myocardium at the basis. Consequently the action potential is propagated from the common bundle through the BB in order to activate the ventricles and septum by the Purkinje system (P3) from left to right and from apex to base <sup>21,22</sup>. In rat, electrical activation of the septal myocardium revealed that earliest activation occurred midseptal and latest activation at the basis while in mice, earliest activation was observed at the basis and latest at the apex (this study and <sup>14</sup>). Thus, septal activation and morphology in rats conforms more to that of larger mammals than to a closely related family member as the mouse is. Since it has been shown that Cx43 and Cx45 can form functional heterotypic channels<sup>23</sup>, in mice electrical coupling of the common bundle and the septal working myocardium likely is mediated by gap junctions co-expressing Cx43 and Cx45.

### ***Subcellular distribution of connexins and ID associated proteins.***

In adult mouse working myocardial cells, Cx43 (atria and ventricles) and Cx40 (atria) are predominantly expressed in IDs at the longitudinal cell borders where they colocalize with N-cadherin and desmoplakin<sup>24,25</sup>. This polarized distribution favors longitudinal over transverse conduction and thus gives rise to anisotropic conduction <sup>26</sup>. In the conduction system however, the expression pattern of Cx40 and Cx45 seems to extend like multiple step-like regions over the entire sarcolemma. This divergent labeling pattern was also observed for N-cadherin and  $\beta$ -catenin but not for desmin. More apical in the mouse BB (P3), the remarkable ID structures are not so pronounced compared to those in P1 and P2 but at this site labeling covers the entire cell surface in small dots.

This organization of the IDs in mice BB seems not specific for rodents because in the rat BB it could not be detected although the nature of expressed connexins (Cx45 and Cx40) was not different. However, also in rat BB, organization of the IDs is different from that in septal working myocytes since labeling both for connexins and other ID associated proteins revealed a rather diffuse labeling over the entire sarcolemma with highest intensity found at the longitudinal cell borders. This labeling pattern, together with the already mentioned sheath of connective tissue surrounding the proximal conductive cells conforms to the organization in human and cow <sup>20</sup>.

In addition to the specific organization of IDs in the BB, more observations indicate that these myocytes are phenotypically different from working myocardial cells: 1) The diffuse labeling for Cx40, Cx43, Cx45 and N-cadherin in myocytes of the rat conduction system (this study), has been described before in other cardiomyocyte phenotypes like neonatal and maturing myocytes<sup>25,27</sup>, dedifferentiating adult myocytes in culture<sup>28</sup> and in cardiomyopathic hearts<sup>26</sup>. 2) Similar to embryonic stages of mouse heart<sup>29</sup> and adult bovine heart<sup>20</sup>, also in adult mice and rats differences exist between the expression levels of desmin and  $\alpha$ -actinin in the conduction system and the septal working myocardium. Whether the phenotypical differences originate from differences in cellular differentiation during cardiac development<sup>30</sup>, or from differences in the origin of the tissue (two different germ layers<sup>31</sup>), is still unresolved.

***Impulse propagation and connexin expression.***

Conduction velocity of the electric impulse is high over the recorded distance in rat BB. In mice, propagation in the proximal BB is similar to rat, but velocity is reduced by half in the distal BB. In general, conduction velocity is determined by several factors: Electrical coupling<sup>32-34</sup>, cell shape and size<sup>35</sup> and excitability<sup>33</sup>. Unlike in rabbits and pigs, where differences in cell size and shape between myocytes in the BB and those in the septal working myocardium have been reported<sup>36</sup>, neither in mice or rats we, and others<sup>37</sup>, could detect this with exception of the myocytes forming the common His-bundle which indeed seemed to be smaller. Staining of the sections with Hoechst 33258 did not reveal differences between the BB and the septal working myocardium in the number of stained nuclei/distance (data not shown).

Connexin expression patterns, distribution and cell shape along the entire rat BB are very similar which fit well to the continuous impulse conduction found in rat bundle branches. In mice however, labeling intensities in the proximal BB are high and clustered in many IDs, firmly connecting adjacent myocytes electrically, while in the distal part labeling is diffuse and not mainly clustered in intercalated disks (shown schematically in Fig.5.6). According to Jongsma & Wilders, to reduce conduction velocity by halve, a decrease in coupling from 3500 nS to 500 nS (85% reduction) is needed<sup>34</sup>. Although the observed labeling pattern strongly suggests reduced longitudinal coupling in the distal bundle branches, it is debatable whether this is primary responsible for the reduction in conduction velocity. In addition, modulation of gap junction distribution *per se* proved to have only little effect on conduction velocity<sup>35</sup>.

More likely, reduced conduction velocity in the distal BB results from different electrical interactions of the proximal and distal BB with the septal working myocardium. In the proximal BB Cx40 and Cx45 are expressed, while in the distal region Cx40, Cx43, and Cx45 are found. Furthermore, we did observe that fiber orientation especially in the proximal BB is perpendicular to that of the septal working myocardium. Since the septal working myocardium exclusively expresses Cx43, electrical coupling between the septal working myocardium and BB will be most prominent in the distal BB. In this part the small bundle will electrically interact with the large IVS, and conduction slowing may be induced here by current loss and activation delay due to load mismatch<sup>38</sup>. In contrast, load mismatch in the rather broad proximal bundle will be minimal since interaction with the septal working myocardium is hampered by the absence of Cx43 in the BB and the perpendicular fiber orientation.

In summary, our results demonstrate that expression patterns of cardiac connexins and conduction velocities are similar in rat BB. Conduction velocities in the proximal BB of rat and mice are similar. Although different distribution patterns of connexins were observed, longitudinal coupling was present in both. In mice, however, conduction velocities as well as connexin expression patterns differ in the proximal and distal parts of the conduction system. Reduced longitudinal coupling and the degree of interaction between cells in the distal part of the BB and the septal working myocardium may contribute to the reduced conduction velocity in the distal part of the conduction system.

**Acknowledgements**

A.A.B. Van Veen and H.V.M. Van Rijen were financially supported by a project grant no.97.184 from the Netherlands Heart Foundation (to H.J.J.). The authors

wish to thank Dr. T.H. Steinberg for providing the Cx45 antibody.

## **References**

1. Bruzzone R, White TW, Paul DL. Connections with connexins: The molecular basis of direct intercellular signaling. *European Journal of Biochemistry*. 1996;238:1-27.
2. Bastide B, Neyses L, Ganten D, Paul M, Willecke K, Traub O. Gap junction protein connexin40 is preferentially expressed in vascular endothelium and conductive bundles of rat myocardium and is increased under hypertensive conditions. *Circulation Research*. 1993;73:1138-1149.
3. Gros D, Jarry-Guichard T, Ten Velde I, De Mazière AMGL, Van Kempen MJA, Davoust J, Briand JP, Moorman AFM, Jongsma HJ. Restricted distribution of Connexin40, a gap junctional protein, in mammalian heart. *Circulation Research*. 1994;74:839-851.
4. Gourdie RG, Severs NJ, Green CR, Rothery S, Germroth P, Thompson RP. The spatial distribution and relative abundance of gap-junctional connexin40 and connexin43 correlate to functional properties of components of the cardiac atrioventricular conduction system. *Journal of Cell Science*. 1993;105:985-991.
5. Van Kempen MJA, Ten Velde I, Wessels A, Oosthoek PW, Gros D, Jongsma HJ, Moorman AFM, Lamers WH. Differential connexin expression accomodates cardiac function in different species. *Microscopy Research and Technique*. 1995;31:420-436.
6. Davis LM, Kanter HL, Beyer EC, Saffitz JE. Distinct gap junction protein phenotypes in cardiac tissues with disparate conduction properties. *Journal of the Americal College of Cardiology*. 1994;24:1124-1132.
7. Davis LM, Rodefeld ME, Green K, Beyer EC, Saffitz JE. Gap junction protein phenotypes of the human heart and conduction system. *Journal of Cardiovascular Electrophysiology*. 1995;6:813-822.
8. Van Kempen MJA, Vermeulen JLM, Moorman AFM, Gros D, Paul DL, Lamers WH. Developmental changes of connexin40 and connexin43 mRNA distribution patterns in the rat heart. *cardiovascular research*. 1996;32:886900.
9. Verheule S, van Kempen MJ, Postma S, Rook MB, Jongsma HJ. Gap junctions in the rabbit sinoatrial node. *Am J Physiol Heart Circ Physiol*. 2001;280:H2103-2115.
10. Van Kempen MJA, Fromaget C, Gros D, Moorman AFM, Lamers WH. Spatial distribution of Connexin43, the major cardiac gap junction protein, in the developing and adult rat heart. *Circulation Research*. 1991;68:16381651.
11. Coppén SR, Dupont E, Rothery S, Severs NJ. Connexin45 expression is preferentially associated with the ventricular conduction system in mouse and rat heart. *Circulation Research*. 1998;82:232-243.
12. Coppén SR, Severs NJ, Gourdie RG. Connexin45 ( $\alpha 6$ ) expression delineates an extended conduction system in the embryonic and mature rodent heart. *Developmental Genetics*. 1999;24:82-90.
13. Tamaddon HS, Vaidya D, Simon AM, Paul DL, Jalife J, Morley GE. High-resolution optical mapping of the right bundle branch in connexin40 knockout mice reveals slow conduction in the specialized conduction system. *Circ Res*. 2000;87:929-936.
14. van Rijen HV, van Veen TA, van Kempen MJ, Wilms-Schopman FJ, Potse M, Krueger O, Willecke K, Opthof T, Jongsma HJ, de Bakker JM. Impaired conduction in the bundle branches of mouse hearts lacking the gap junction protein connexin40. *Circulation*. 2001;103:1591-1598.
15. Kumai M, Nishii K, Nakamura K, Takeda N, Suzuki M, Shibata Y. Loss of connexin45 causes a cushion defect in early cardiogenesis. *Development*. 2000;127:3501-3512.
16. Krüger O, Plum A, Kim J, Winterhager E, Maxeiner S, Hallas G, Kirchhoff S, Traub O, Lamers WH, Willecke K. Defective vascular development in connexin 45-deficient mice. *Development*. 2000;127:41794193.
17. Tyrode MV. The mode of action of some purgative salts. *Arch.Int.Pharmacodyn*. 1910;20:205-

223.

18. Sweat F, Puchter H, Rosenthal SI. Sirius Red F3Ba as a stain for connective tissue. *Arch Pathol.* 1964;1964:69-72.

19. Gros D, Jongsma HJ. Connexins in mammalian heart function. *BioEssays.* 1996;18:719-730.

20. Oosthoek PW, Viragh S, Lamers WH, Moorman AF. Immunohistochemical delineation of the conduction system. II: The atrioventricular node and Purkinje fibers. *Circ Res.* 1993;73:482-491.

21. Burchell HB, Essex HE, Pruitt RD. Studies on the spread of excitation through the ventricular myocardium. II. The ventricular septum. *Circulation.* 1952;6:161-171.

22. Durrer D, van Dam RT, Freud GE, Janse MJ, Meijler FL, Arzbaeher RC. Total excitation of the isolated human heart. *Circulation.* 1970;41:899-912.

23. Elfång C, Eckert R, Lichtenberg-Fraté H, Butterweck A, Traub O, Klein RA, Hülser DF, Willecke K. Specific permeability and selective formation of gap junction channels in connexin-transfected HeLa cells. *Journal of Cell Biology.* 1995;129:805-817.

24. Peters NS, Severs NJ, Rothery SM, Lincoln C, Yacoub MH, Green CR. Spatiotemporal relation between gap junctions and fascia adherens junctions during postnatal development of human ventricular myocardium. *Circulation.* 1994;90:713-725.

25. Angst BD, Khan LUR, Severs NJ, Whitely K, Rothery S, Thompson RP, Magee AI, Gourdie RG. Dissociated spatial patterning of gap junctions and cell adhesion junctions during postnatal differentiation of ventricular myocardium. *Circulation Research.* 1997;80:88-94.

26. Uzzaman M, Honjo H, Takagishi Y, Emdad L, Magee AI, Severs NJ, Kodama I. Remodeling of gap junctional coupling in hypertrophied right ventricles of rats with monocrotaline-induced pulmonary hypertension. *Circ Res.* 2000;86:871-878.

27. Kwak BR, van Kempen MJA, Théveniau-Ruissy M, Gros DB, Jongsma HJ. Connexin expression in cultured neonatal rat cardiomyocytes reflects the pattern of the intact ventricle. *Cardiovascular Research.* 1999;44:370-380.

28. Kostin S, Hein S, Bauer EP, Schaper J. Spatiotemporal development and distribution of intercellular junctions in adult rat cardiomyocytes in culture. *Circ Res.* 1999;85:154-167.

29. Franco D, Icardo JM. Molecular characterization of the ventricular conduction system in the developing mouse heart: topographical correlation in normal and congenitally malformed hearts. *Cardiovasc Res.* 2001;49:417-429.

30. Moorman AF, de Jong F, Denyn MM, Lamers WH. Development of the cardiac conduction system. *Circ Res.* 1998;82:629-644.

31. Gorza L, Vitadello M. Distribution of conduction system fibers in the developing and adult rabbit heart revealed by an antineurofilament antibody. *Circ Res.* 1989;65:360-369.

32. Shaw RM, Rudy Y. Ionic mechanisms of propagation in cardiac tissue: Roles of the sodium and L-type calcium currents during reduced excitability and decreased gap junction coupling. *Circulation Research.* 1997;81:727-741.

33. Rohr S, Kucera JP, Kléber AG. Slow conduction in cardiac tissue, I. Effects of a reduction of excitability versus a reduction of electrical coupling on microconduction. *Circulation Research.* 1998;83:781-794.

34. Jongsma HJ, Wilders R. Gap junctions in cardiovascular disease. *Circ.Res.* 2000;86:1193-1197.

35. Spach MS, Heidlage JF, Dolber PC, Barr RC. Electrophysiological effects of remodeling cardiac gap junctions and cell size. Experimental and model studies of normal cardiac growth. *Circulation Research.* 2000;86:302-311.

36. Tranum-Jensen J, Wilde AA, Vermeulen JT, Janse MJ. Morphology of electrophysiologically identified junctions between Purkinje fibers and ventricular muscle in rabbit and pig hearts. *Circ Res.* 1991;69:429-437.

37. Lev M, Thäemert JC. The conduction system of the mouse heart. *Acta Anat (Basel).* 1973;85:342-352.

38. Kucera JP, Kléber AG, Rohr S. Slow conduction in cardiac tissue, II. Effects of branching

tissue geometry. *Circulation Research*. 1998;83:795-805.



# Chapter 6

---

## **Impaired conduction in the bundle branches of mouse hearts lacking the gap junction protein Connexin40**

Harold V.M. van Rijen, Toon A.B. van Veen, Marjan J.A. van Kempen, Francien J. G. Wilms-Schopman, Mark Potse, Olaf Krueger, Klaus Willecke Tobias Opthof, Habo J. Jongsma, Jacques M.T. de Bakker

*Circulation (2001) 103: 1591-1598*

**Abstract:***Background:*

Connexin 40 (Cx40) and 45 (Cx45) are the major protein subunits of gap junction channels in the conduction system of mammals. In order to determine the role of Cx40 we correlated cardiac activation with connexin distribution in normal and Cx40 deficient mice hearts.

*Methods and Results:*

Epicardial and septal activation was recorded in Langendorff perfused adult mice hearts with a 247 point compound electrode (interelectrode distance 0.3 mm). Following electrophysiologic measurements hearts were prepared for immunohistochemistry and histology to determine connexin distribution and fibrosis.

In both wildtype and Cx40-deficient animals, epicardial activation patterns were similar. The right and left ventricular septum was invariably activated from base to apex. Histology revealed a continuity of myocytes from the common bundle to the septal myocardium. Within this continuity colocalization was found of Cx43 and Cx45 but not of Cx40 and Cx43. Both animals showed similar His-bundle activation.

In Cx40 deficient mice, the proximal bundle branches expressed Cx45 only. The absence of Cx40 in the proximal bundles correlated with right bundle branch block. Conduction in the left bundle branch was impaired as compared to wildtype animals.

*Conclusions:*

Our data show that 1) in mice a continuity exists between the common bundle and the septum 2) Cx40 deficiency results in right bundle branch block and impaired left bundle branch conduction.

**Introduction**

Electrical coupling of myocytes by gap junctions permits intercellular current flow, a prerequisite for cardiac conduction. Gap junctions are agglomerates of individual channels that directly connect the cytoplasm of adjacent cells. Gap junction channels are formed by head-to-head alignment of two hexameric hemichannels, each composed of six connexin (Cx) molecules. At least four different cardiac connexins have been reported. Cx37 is found in rabbit endocardium <sup>1</sup>, Cx40 is mainly found in the atrium and conduction system <sup>2-8</sup>, Cx43 is located in the atrial and ventricular myocardium and in the distal parts of the conduction system <sup>4,5,8</sup>. Finally, Cx45 is present throughout the heart in small amounts <sup>6,7,9,10</sup>, with some overexpression in the conduction system <sup>11,12</sup>.

Mice lacking the gene for Cx40 exhibit reduced atrial, but not ventricular conduction velocity <sup>13</sup>. The ECGs of Cx40 knockout mice have prolonged P waves, in agreement with reduced atrial conduction velocity. Moreover, the PR-interval is prolonged, suggestive for atrioventricular (AV) nodal dysfunction <sup>14-16</sup>. Also, QRS-complexes of these animals are prolonged <sup>14-16</sup>. Impaired function of the specific conduction system probably explains the prolonged QRS duration because Cx40 is normally not expressed in working ventricular myocardium.

The purpose of this study is to determine the role of Cx40 in propagation of the electrical impulse in the specific conduction system of the mouse heart.

## **Materials and Methods**

### *Animals*

All mice of mixed genetic background (Cx57BL/6 and 129Sv) were generated and bred at the Institute of Genetics, University of Bonn, Bonn, Germany and genotyped by PCR as described<sup>15</sup>. In total, 12 wildtype and 12 Cx40 -/- littermates between 4 and 6 months of age were used for experiments. The study conformed to the guiding principles of the American Physiological Society.

### *Preparation of the hearts*

Mice were anaesthetized by intraperitoneal injection of urethane (2 g/kg bodyweight). The chest was opened and the heart was excised and submerged in Tyrode solution<sup>17</sup> at 4 °C. With the help of a binocular microscope the heart was dissected from the lung as well as other tissue and the aorta was cannulated. Subsequently, the heart was connected to a Langendorff perfusion setup and perfused at 37 °C and perfusion pressure of 80 cm H<sub>2</sub>O. Perfusion buffer composition (in mM): NaCl 90, KCl 3.6, KH<sub>2</sub>PO<sub>4</sub> 0.92, MgSO<sub>4</sub> 0.92, NaHCO<sub>3</sub> 19.2, CaCl<sub>2</sub> 1.8, glucose 22, creatin 6, taurin 6, insulin 0.1 μM, gassed with 95% O<sub>2</sub> and 5% CO<sub>2</sub>. In all experiments the heart started to beat immediately after initiating perfusion. Flow rate was approximately 2 ml/min. To ensure proper temperature of the preparation, the heart was placed against a heated (37°C) and continuously moisturized support.

### *Recording of electrograms*

Extracellular electrograms were recorded with a 247 point multi terminal electrode, mounted in a micromanipulator. Electrodes were silver wires with a diameter of 0.1 mm that were isolated except at the tip. Electrode terminals were arranged in a 19 by 13 grid at interelectrode distances of 0.3 mm. Recordings were made in unipolar mode with regard to a reference electrode connected to the support of the heart. Electrograms were acquired using a custom built 256-channel data-acquisition system. Signals were bandpass filtered (low cut-off 0.16 Hz (12dB), high cut-off 1 kHz (6 dB)), and digitized with 16 bits resolution at a bit step of 2 μV and a sampling frequency of 2 kHz. The input noise of the system was 4 μV (peak-peak). Data were acquired at a sample rate of 2 kHz.

Epicardial recordings of the ventricles were made in sinus and paced rhythm [wildtype(knockout): left ventricle N=12(11), right ventricle N=12(11)]. For the latter a bipolar silver wire (diameter of poles 0.1 mm, interelectrode distance 0.2 mm) was positioned on one of the atria. Pacing was performed with a Grass bipolar isolated stimulator. Stimulus trains were generated by a Macintosh computer, equipped with an AD-board and custom written software.

For septal measurements, the right and left ventricular free walls were removed. Surgical resection of the free wall sometimes resulted in AV-block, thus prohibiting the recording of bundle activation. The electrode grid was positioned in basal position on the interventricular septum. Reliable determination of conduction velocity required electrograms at 4 adjacent electrodes [wildtype(knockout): left bundle branch N=4(3), right bundle branch N=6(12)]. AV nodal conduction curves were determined [wildtype(knockout): N=5(5)]. The atrium was stimulated at a cycle-length of 100 ms. Every sixteenth stimulus was followed by one premature stimulus. Starting at 90 ms the coupling interval of the extra stimulus was reduced in steps of 5 ms until AV block occurred. We used the time constant of the conduction curve fitted to a mono-exponential function as a measure for progressively increasing AH-delay. His-bundle measurements were made after opening of the right atrium. Subsequently, the center of the electrode grid was

positioned on the coronary sinus and recordings were made [wildtype(knockout): N=3(2)].

### *Data Analysis*

Activation maps were constructed from the activation times, determined with custom written software based on Matlab (The Mathworks Inc.). The moment of maximal negative  $dV/dt$  in the unipolar electrograms was selected as the time of local activation.

Activation times of the ventricular epicardia were corrected for sinus rhythm frequency using the conduction curves of the His-bundle.

### *Statistics*

All numerical values are given as mean  $\pm$  standard error of mean. Statistical comparisons were performed using an unpaired students *t*-test, using StatView 4.5. P-values  $\leq 0.05$  were regarded as statistically significant.

### *Immunohistochemistry and histology*

Connexin expression was compared between Cx40 deficient (n=5) and wildtype littermates (n=5). The hearts were connected to the Langendorff setup for several minutes, to remove blood. The hearts were rapidly frozen in liquid nitrogen and stored at  $-80^{\circ}\text{C}$ .

The hearts were serially sectioned in frontal plane with a cryostat, to produce 'four chamber view' sections. Sections incorporating the conduction system were incubated with primary antibodies directed against Cx40, Cx43, Cx45. Desmin was used as a marker for the conduction system. Primary antibodies were visualized with fluorescent secondary antibodies as described previously<sup>18</sup>. Sections were stained with picro-sirius red and examined by light microscopy for assessment of fibrosis<sup>19</sup>.

## **Results**

Wildtype and Cx40 deficient mouse hearts did not differ in morphology or heart weight. In wildtype mice, gap junctions between atrial myocytes were composed of Cx40 and Cx43, while only Cx43 was detected in ventricular myocytes. In Cx40 deficient animals, only Cx43 was found in atrial myocardium.

### ***Epicardial connexin expression and activation patterns***

Epicardial activation patterns were determined during sinus rhythm (RR interval  $172 \pm 6.8$  and  $188 \pm 13.8$  ms in wildtype and knockout hearts, respectively) and were not significantly different between wildtype and knockout ( $P=0.3$ ). In 10 of 12 wildtype hearts, earliest epicardial activation of the right ventricle was found at the basal site, of which 8 had a second early activated area at the apex or the septal/lateral wall (Fig. 6.1A). In the other 2 hearts, breakthrough activation was found in the mid free wall. Similarly, 10 of 11 Cx40 deficient hearts showed earliest activation at the basal site, 8 of which also had second early sites at the apex of the septal/lateral wall (Fig. 6.1B). In the remaining hearts apical activation was found. Left epicardial activation was similar to right ventricular activation of both wildtype and knockout, also showing predominant basal earliest activation. In wildtype animals, average corrected right ventricular activation occurred 4.8 ms earlier than left ventricular activation, while in knockout animals the opposite was found. Right ventricular activation was 2.6 ms later than left ventricular activation ( $P=0.01$ ).

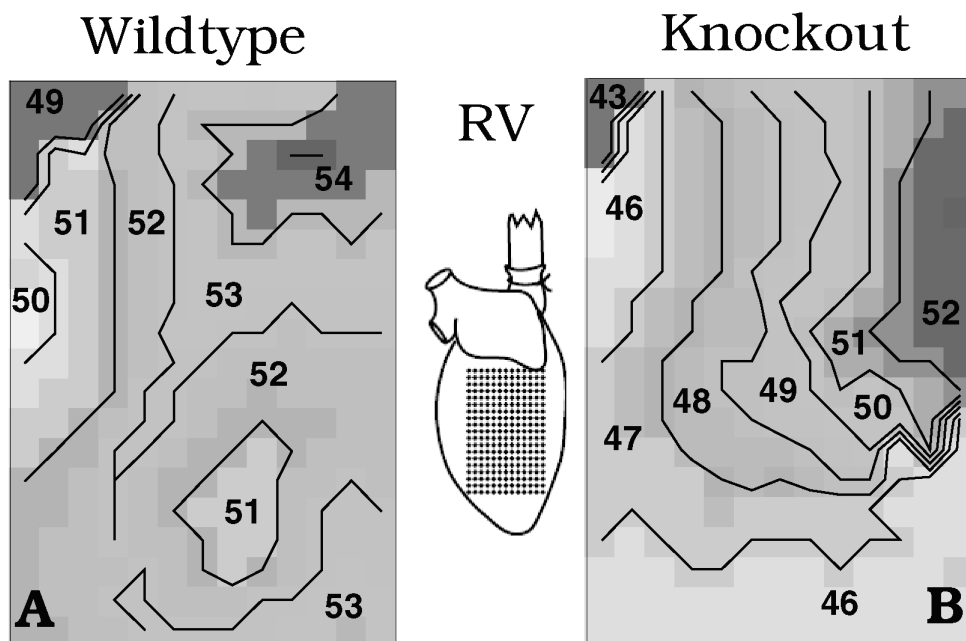


Figure 6.1 Epicardial activation patterns of the right ventricle of wildtype (A) and Cx40 deficient (B) mouse hearts in sinus rhythm. Activation times are calculated with respect to first atrial activation. In wildtype, earliest epicardial activation was found at a basal site (A). In the Cx40 deficient heart, earliest activation was also found at the basal site (B).

### Bundle branch conduction and septal activation

After removal of the left and right ventricular free walls, the electrode grid was positioned against the left or right septal wall. The stimulation electrode was placed on one of the atria, to pace the heart at a constant rate. Figure 6.2 shows typical examples of activation patterns of the conduction system. Left bundle branch deflections (marked by asterisk in right panels) were found in all experiments on both wildtype and Cx40 deficient animals. Right bundle branch signals (asterisk in left panels) were recorded in all wildtype animals. However, in only 1 of 12 Cx40 deficient hearts, full RBB activation was measured. In 3 (of 12) Cx40 deficient hearts RBB activation blocked at 0.3 or 0.6 mm from the AV groove (as shown in Fig.2), while in the other 8 hearts, no RBB signals could be detected.

In wildtype hearts, conduction velocities in the left (LBB) and right bundle branch (RBB) were  $0.42 \pm 0.03 \text{ m} \cdot \text{s}^{-1}$  and  $0.31 \pm 0.04 \text{ m} \cdot \text{s}^{-1}$ , respectively. Conduction velocity in the His-bundle ( $0.52 \pm 0.15 \text{ m} \cdot \text{s}^{-1}$ ) was always faster than in the bundle branches. In Cx40 knockout mice (Fig. 2 lower panels), the conduction velocity in the LBB was  $0.28 \pm 0.02 \text{ m} \cdot \text{s}^{-1}$ , significantly lower as compared to wildtype ( $P=0.01$ ). RBB activation conducted at  $0.32 \text{ m} \cdot \text{s}^{-1}$ . In Cx40 knockout hearts, conduction velocity in the His-bundle was high ( $0.64 \pm 0.37$ ) and not significantly different from wildtypes ( $P=0.76$ ).

Figure 6.3 shows typical examples of right septal activation patterns in wildtype (Fig. 6.3A) and Cx40 deficient hearts (Fig. 6.3B). In both the wildtype and Cx40 deficient mice, earliest septal activation was seen invariably at the base. Activation patterns of the left interventricular septum were identical to the right septum.

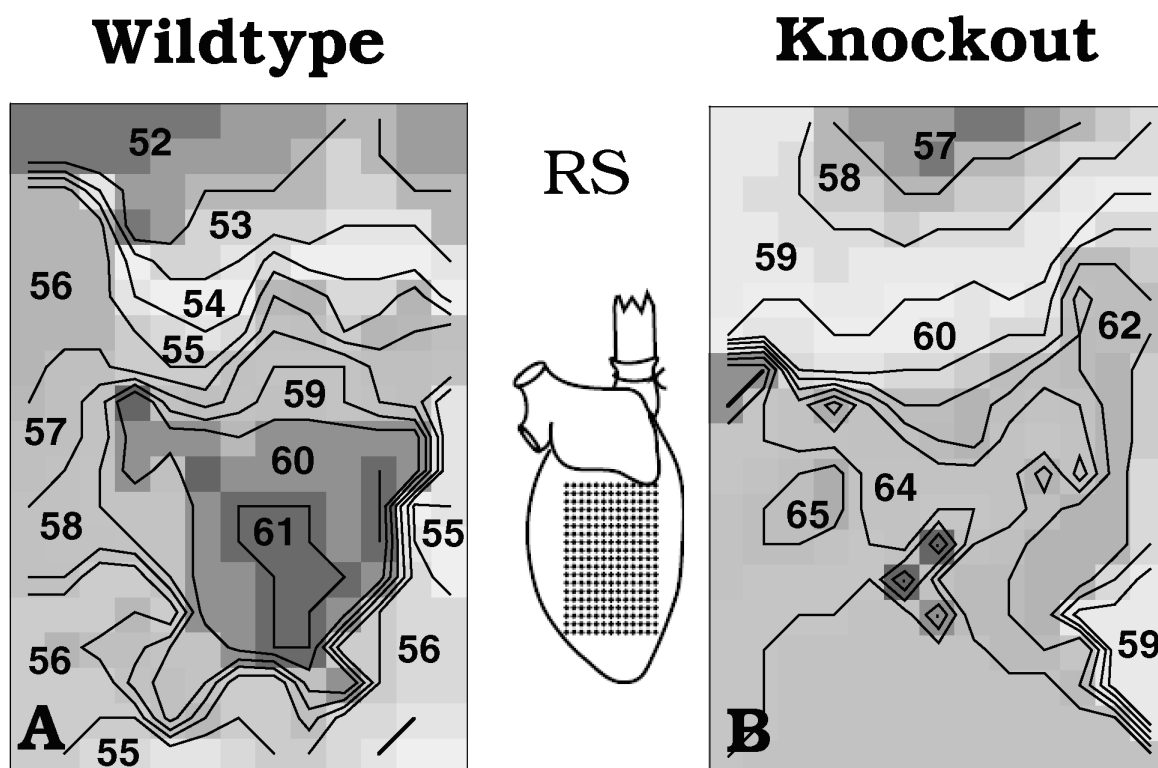


Figure 6.3 Activation patterns of the right interventricular septum in wildtype (A) and Cx40 knockout animals (B). Septal activation is always observed from base (top) to apex (bottom).

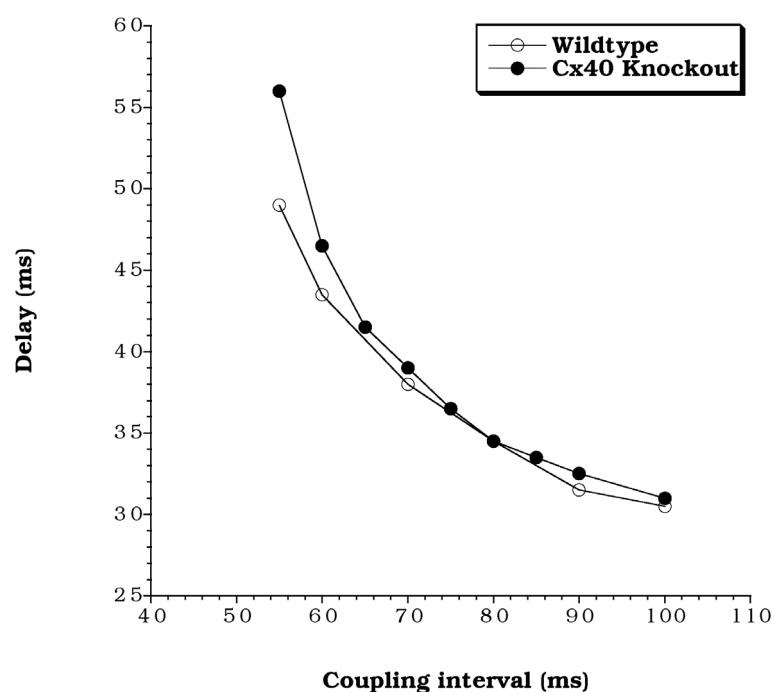


Figure 6.4 Typical example of the A-H delay of wildtype (open circles) and Cx40 knockout (closed circles) mice. No statistical significant differences were found between knockout and wildtype animals.

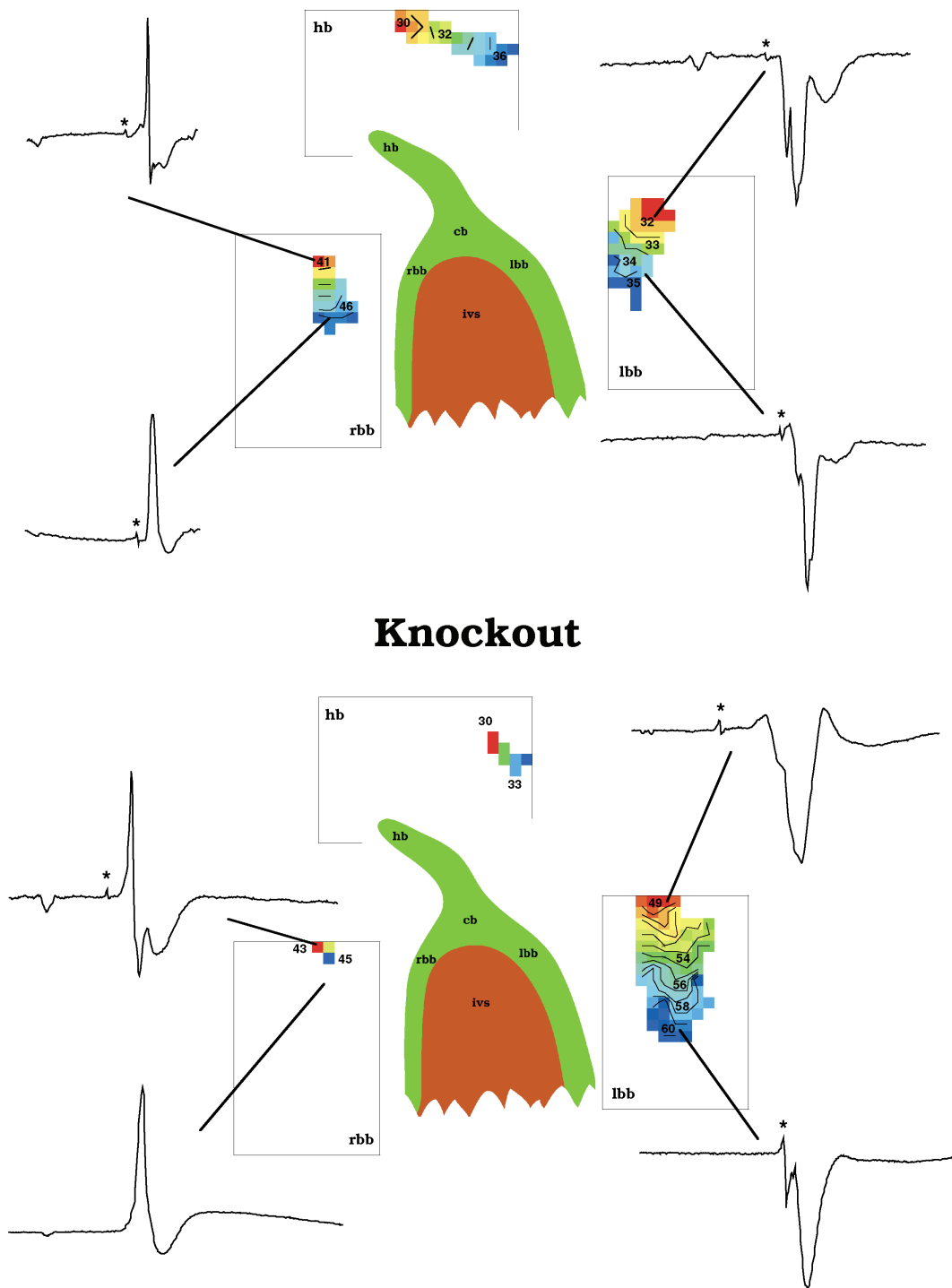
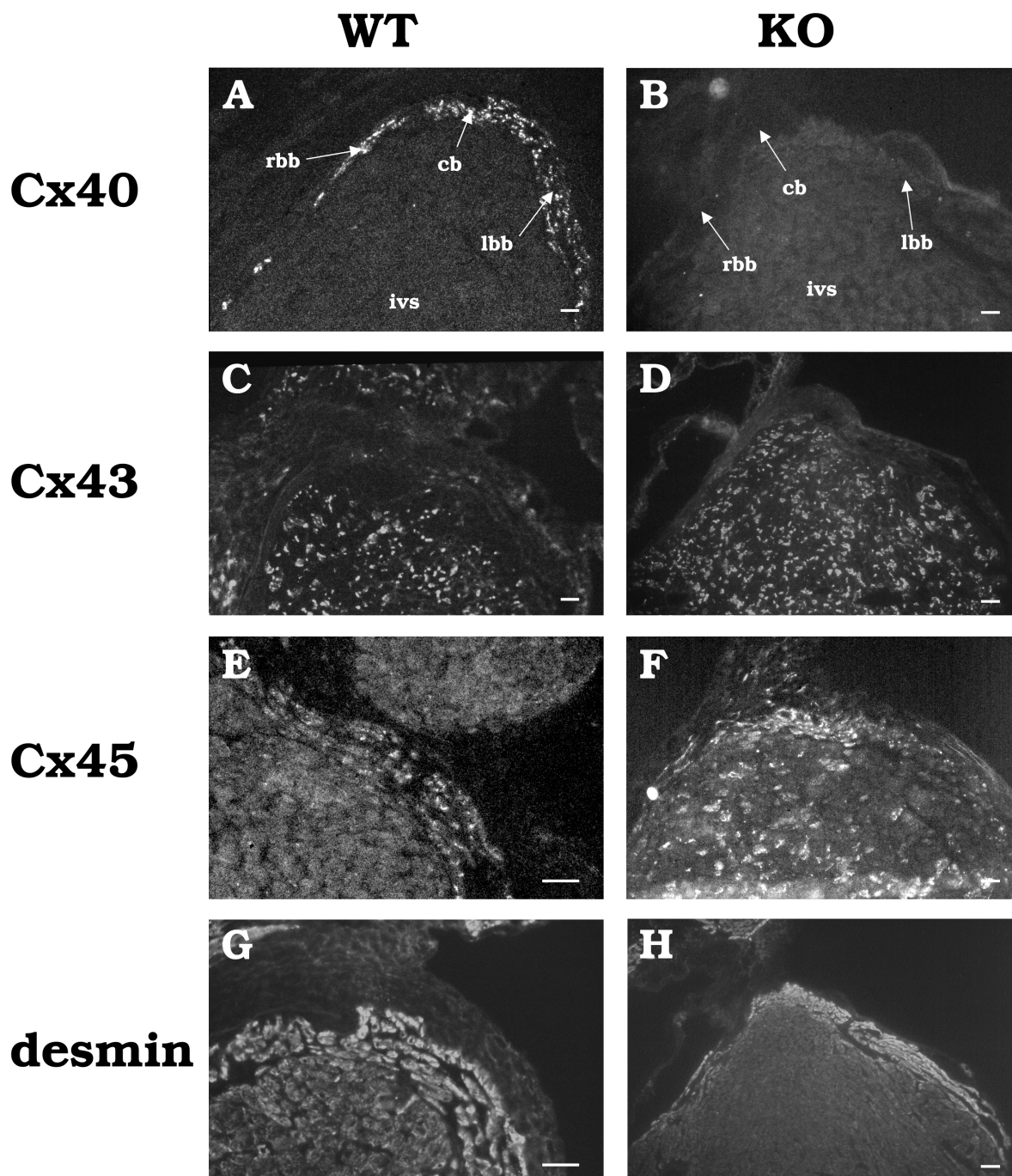


Figure 6.2 Typical examples of bundle branch activation on both the left and right septum in wildtype (upper panels) and Cx40 knockout animals (lower panels). After removal of the ventricular free walls, the electrode grid was positioned on the septum, while the heart was paced on the atrium using a separate stimulus electrode. The top panels show the activation of the His bundle (hb). Electrograms of representative individual electrodes show a remote P-wave ( $t=0$  at onset of P-wave), followed by the bundle branch signal (marked by asterisk). The large complex reflects activation of the interventricular septum. Note the premature block of the right bundle branch (rbb) in Cx40 knockout animals. Left bundle branch (lbb) activation is significantly slower in knockout animals while His bundle activation is not altered.



*Figure 6.5 Immunohistochemical analysis of frontal serial sections of wildtype (left) and Cx40 knockout (right) hearts, stained for Cx40, Cx43, Cx45, and desmin. Cx40 is located in the common bundle and bundle branches and clearly shows the difference in size of the right (small) and left (wide) bundle branch (A). Cx40 is absent in Cx40 animals (B) Cx43 is located in the working myocardium only of both wildtype and Cx40 knockout (C&D). Cx45 is located in the His bundle, common bundle and proximal bundle branches (E&F). Desmin labeling showed a clear demarcation of the conduction system (G&H). rbb, right bundle branch; lbb, left bundle branch, ivs, interventricular septum. Scalebar=20  $\mu$ m.*

### **AV conduction characteristics**

Figure 6.4 shows a typical example of a conduction curve. The AH-delay increases exponentially with decreasing coupling interval, being almost identical in wildtype and Cx40 deficient animals. The time constants of the conduction curves in both wildtype and Cx40 deficient animals were similar and not statistically different (wildtype  $20.8 \pm 3.9$  ms, Cx40 knockout  $20.7 \pm 4.5$  ms;  $P=0.99$ ). Also, the maximal increase in delay was not different as well (wildtype  $21.5 \pm 3.7$  ms, Cx40 knockout  $23.6 \pm 2.7$  ms;  $P=0.68$ ).

Even though activation in the RBB blocks after 0.3-0.6 mm below the AV groove in Cx40 deficient animals, the activation times recorded at these proximal electrodes are not different from control.

### **Connexin distribution in and histology of the septum & common bundle**

Figure 6.5 shows sections of the septum containing the conduction system, of both wildtype (left panels) and Cx40 deficient hearts (right panels) illustrating the distribution of Cx40, Cx43, Cx45, and desmin.

**Cx40 expression:** In wildtype mice, Cx40 is abundantly expressed in the Hisbundle, common bundle and bundle branches (Fig. 6.5A). The Cx40 distribution indicates that the left bundle branch (lbb) is much wider than the right bundle branch (rbb). Cx40 was absent in the bundle branches of Cx40 deficient mice (Fig. 6.5B).

**Cx43 expression:** In both wildtype and Cx40 deficient hearts, Cx43 was expressed in the septal region of the heart, but not in the proximal conduction system (Fig. 6.5C, 6.5D).

**Cx45 expression:** In both wildtype and Cx40 deficient hearts, Cx45 staining was found in the His-bundle, the common bundle, proximal bundle branches and Purkinje system, but not in the septal regions (Fig. 6.5E, 6.5F).

**Coexpression of Cx40, Cx43, and Cx45:** Figure 6.6A shows a double labeling of Cx40 (green) and Cx43 (red). Cx40 was found in the common bundle and bundle branches (marked by desmin in consecutive section in fig. 6.6C) and Cx43 in the septum. No co-localization of Cx43 and Cx40 was found. Figure 6.6B shows that the expression of Cx45 (green) extended from the common bundle towards the septum where Cx43 (red) is expressed. Cx43 and Cx45 colocalize in the cells between the common bundle and the septum (arrows). In both wildtype and Cx40 deficient animals electrical continuity is likely from the common bundle to the septum and mediated by Cx45.

**Connective tissue in the septum:** Figure 6.6D shows a consecutive section of Fig 6.6B stained for connective tissue (red). Thin septae of connective tissue are present between the bundle branches and the septum but connective tissue is virtually absent at the common bundle-septum interface (arrow). There is a clear continuity of myocytes from the common bundle into the septum. Such continuity was found in both wildtype and knockout mice and correlates with baso-apical activation of the ventricular septum (Fig. 6.3).

## **Discussion**

### **Right but not left bundle branch block in Cx40 deficient mice**

The electrophysiological data showed RBB block in Cx40 deficient hearts. The immunohistochemical data show that no differences in morphology or Cx expression, other than Cx40, are found, excluding any developmental changes. Therefore, our data are highly suggestive for functional block in the RBB of Cx40 deficient mice. The absence of Cx40 also significantly decreases conduction

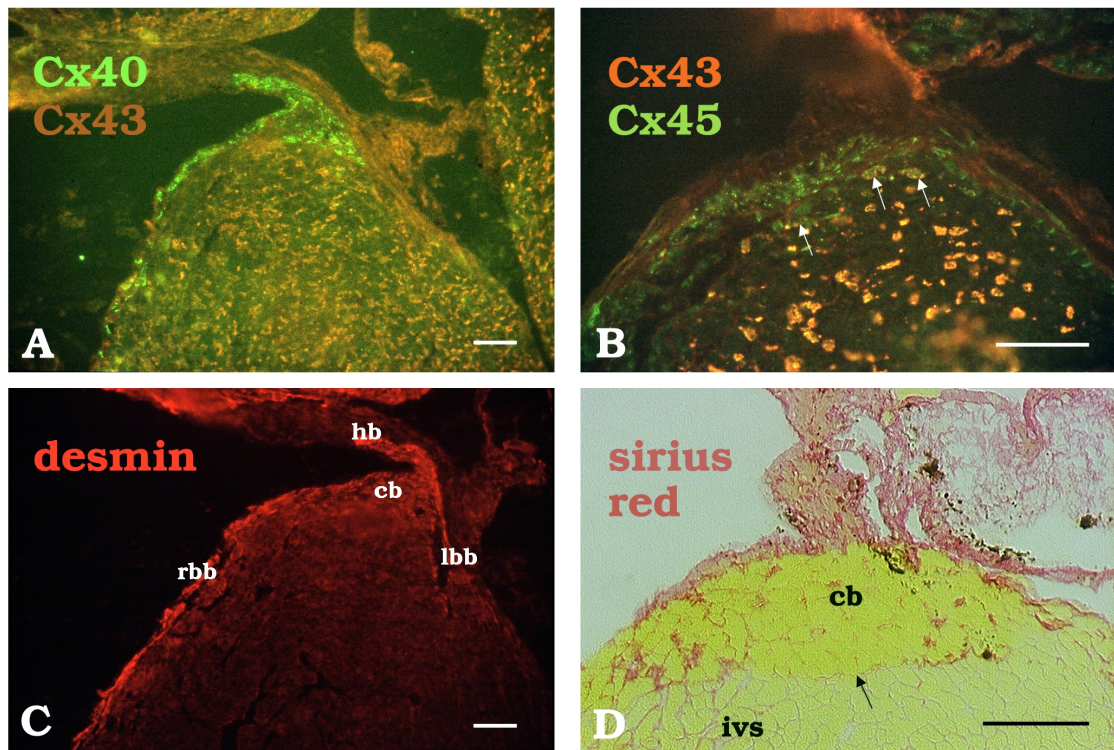


**Figure 6.6** Histochemical analysis of the transition zone between common bundle and basal septum. A. Wildtype animal, showing the expression of Cx40 and Cx43. In the septum and conduction system these expression patterns are mutually exclusive. B. Double labeling of Cx43 and Cx45 in Cx40 knockout animals, showing co-expression of Cx43 and Cx45 at the interface between common bundle and septum (marked by arrows). C. Sister section of A stained for desmin showing the conduction system. D: Sirius red staining showing fibrotic tissue. cb: common bundle, ivs: interventricular septum. The arrow marks strands of myocytes connecting the common bundle and the interventricular septum. Scale bar=50 $\mu$ m.

velocity in the LBB from 0.42 to 0.28 m·s<sup>-1</sup>. Presumably, conduction along the LBB occurs exclusively by gap junctions formed of Cx45. The reduced conduction velocity in the LBB is in accordance with observations in model studies and experiments on linear strands of cardiomyocytes. In these systems, a decrease of gap junctional coupling results in reduction of conduction velocity<sup>20-22</sup>. In these model studies a reduction of conduction velocity from 0.43 to 0.28 m·s<sup>-1</sup> (66% reduction) resulted from a reduction in coupling of ~1.1 to 0.5  $\mu$ S (~65%)<sup>20,22</sup>. The absence of Cx40 in the RBB results in conduction block. However, Cx45 labeling is similar in the LBB and RBB, suggesting similar degree of intercellular coupling. We can only speculate about the reason why right bundle branch block occurs while the left bundle is still conducting, albeit with reduced conduction velocity. Reduced coupling between myocytes alone is not sufficient to explain this discrepancy. Simulations of impulse propagation in strands of myocytes have shown that the electrical coupling between cells must be reduced by at least a factor of 100 to result in conduction block<sup>20,22</sup>. On the other hand, clinical studies have shown that the vulnerability of the right bundle for conduction block is greater than that of the left bundle<sup>23-25</sup>. The smaller diameter of the right bundle may play a role because minor discontinuities are more prominent in such bundles for generating activation block by load mismatch<sup>26,27</sup>. Right bundle

branch block was also reported as a result of longitudinal dissociation in the His-bundle<sup>28</sup>. This RBB-block could be normalized by pacing of the His-bundle. It is, however, unlikely that longitudinal dissociation was present in our experiments. No conduction abnormalities of fractionated potentials were found in the His-bundle activation measurements. Secondly, the RBB-block was located 0.3-0.6 mm distal from the AV-groove and finally, the conduction curves measured at the site of the common bundle in Cx40 knockout hearts were not different from control. If a longitudinal dissociation were present in the His-bundle, premature stimulation of the atria would have uncovered a progressive AH-delay.

Conduction velocity in the His-bundle was not different between wildtype and Cx40 knockout. The absence of Cx40, leaving Cx45 as the only Cx in the His-bundle does presumably not reduce intercellular conductance to a level at which conduction velocity is also reduced (cf. Ref 22).

The measured RBB-block and reduced conduction velocity in the LBB fit well in the previously reported phenotype of the Cx40 deficient mice. One overall finding is that the delay between atrial and ventricular activation (PR interval) is increased<sup>13-16</sup>, probably caused by the decreased conduction velocity in the working atrial myocardium<sup>13</sup> and in the conduction system (this study).

Secondly, an increased QRS duration has been reported in Cx40 knockout mice<sup>13-16</sup>. Impaired ventricular activation can be due to slow conduction along the ventricle, which is unlikely, since Cx40 is normally not expressed in the ventricle, or results from abnormal ventricular activation by the conduction system. Impairment of the conduction system in Cx40 knockout mice was suggested by Simon *et al.*<sup>16</sup> based on the long and split QRS complexes, and frontal axis deviation in Cx40 deficient mice. We previously reported that the QRS-duration in Cx40 deficient mice was only prolonged in sinus rhythm, but not during ventricular pacing, indicating that activation of the ventricles rather than ventricular conduction itself is impaired<sup>13</sup>. Our experimental results confirm these hypotheses by direct demonstration of RBB activation block in Cx40 deficient mice.

### **Septal activation in wildtype and Cx40 deficient mice**

In larger mammals, intraventricular septal activation occurs from left to right and from apex to base<sup>29,30</sup>. The proximal conduction system is electrically insulated from the septal myocardium by a fibrotic sheet, to ensure ventricular activation after dispersal of the impulse through the conduction system<sup>31</sup>. Our experiments show that ventricular activation does not follow this pathway in mouse hearts, either wildtype or Cx40 deficient.

Septal measurements of both wildtype and Cx40 deficient hearts always showed a baso-apical activation sequence, suggesting a direct electrical connection between the common bundle and the septum. This direct electrical connection indeed seems present, because the fibrotic sheet between the septum and conduction system shows large fenestrations, as reported by Lev and Thaemert<sup>32</sup>. Furthermore, coexpression of Cx45 and Cx43 was found in the transitional region. A previous study by Coppen *et al.*<sup>12</sup> reported that in the proximal conduction system Cx45 is not only coexpressed with Cx40, but that this expression extends through several cell layers in septal and lateral direction. Coexpression of Cx45 with Cx43 in this region was, however, not reported.

In conclusion, our study shows that in mice, a continuity exists between the common bundle and the septum, both histological and electrical, and that absence of Cx40 results in right bundle branch block and impaired left bundle branch conduction.

Our observation of an electrical continuity between the common bundle and the septum prohibits comparison of global activation patterns in the mouse and human heart. Our results show, however, that the vulnerability of the RBB is greater than that of the LBB, which is in line with data in patients<sup>23-25</sup>. This might also be the case for the preferred site of block which is at a basal site in the RBB rather than at the muscle Purkinje junction.

### **Acknowledgements**

This study was financially supported by the Netherlands Heart Foundation (grant 97.184) and the Netherlands Organization for Scientific Research (grant 902-16-193).

Work in the Bonn laboratory was supported by the German Research Organization (SFB, grant number 284 (C1)) and the Foundation for Chemical Industry (K.W). The laboratories of H.J.J. and K.W. acknowledge common financial support of the European Community (Biomed QLGl-CT1999-00516).

### **References**

1. Verheule S, Van Kempen MJA, Te Welscher PHJA, Kwak BR, Jongsma HJ. Characterization of gap junction channels in adult rabbit atrial and ventricular myocardium. *Circ Res.* 1997;80:673-681.
2. Bastide B, Neyses L, Ganten D, Paul M, Willecke K, Traub O. Gap junction protein connexin40 is preferentially expressed in vascular endothelium and conductive bundles of rat myocardium and is increased under hypertensive conditions. *Circ Res.* 1993;73:1138-1149.
3. Gros D, Jarry-Guichard T, Ten Velde I, De Mazière AMGL, Van Kempen MJA, Davoust J, Briand JP, Moorman AFM, Jongsma HJ. Restricted distribution of Connexin40, a gap junctional protein, in mammalian heart. *Circ Res.* 1994;74:839-851.
4. Gourdie RG, Severs NJ, Green CR, Rothery S, Germroth P, Thompson RP. The spatial distribution and relative abundance of gap-junctional connexin40 and connexin43 correlate to functional properties of components of the cardiac atrioventricular conduction system. *J Cell Sci.* 1993;105:985-991.
5. Van Kempen MJA, Ten Velde I, Wessels A, Oosthoek PW, Gros D, Jongsma HJ, Moorman AFM, Lamers WH. Differential connexin expression accommodates cardiac function in different species. *Microsc Res Tech.* 1995;31:420-436.
6. Davis LM, Kanter HL, Beyer EC, Saffitz JE. Distinct gap junction protein phenotypes in cardiac tissues with disparate conduction properties. *J Am Coll Cardiol.* 1994;24:1124-1132.
7. Davis LM, Rodefeld ME, Green K, Beyer EC, Saffitz JE. Gap junction protein phenotypes of the human heart and conduction system. *J Cardiovasc Electrophysiol.* 1995;6:813-822.
8. Van Kempen MJA, Vermeulen JLM, Moorman AFM, Gros D, Paul DL, Lamers WH. Developmental changes of connexin40 and connexin43 mRNA distribution patterns in the rat heart. *Cardiovasc res.* 1996;32:886-900.
9. Kanter HL, Saffitz JE, Beyer EC. Cardiac myocytes express multiple gap junction proteins. *Circ Res.* 1992;70:438-444.
10. Darrow BJ, Laing JG, Lampe PD, Saffitz JE, Beyer EC. Expression of multiple connexins in cultured neonatal rat ventricular myocytes. *Circ Res.* 1995;76:381-387.
11. Coppen SR, Dupont E, Rothery S, Severs NJ. Connexin45 expression is preferentially associated with the ventricular conduction system in mouse and rat heart. *Circ Res.* 1998;82:232-243.
12. Coppen SR, Severs NJ, Gourdie RG. Connexin45 ( $\alpha 6$ ) expression delineates an extended conduction system in the embryonic and mature rodent heart. *Dev Genet.* 1999;24:82-90.

13. Verheule S, van Batenburg CA, Coenjaerts FE, Kirchhoff S, Willecke K, Jongsma HJ. Cardiac conduction abnormalities in mice lacking the gap junction protein connexin40. *J Cardiovasc Electrophysiol*. 1999;10:1380-1389.
14. Hagendorff A, Schumacher B, Kirchhoff S, Lüderitz B, Willecke K. Conduction disturbances and increased atrial vulnerability in Connexin40 deficient mice analyzed by transesophageal stimulation. *Circulation*. 1999;99:1508-1515.
15. Kirchhoff S, Nelles E, Hagendorff A, Kruger O, Traub O, Willecke K. Reduced cardiac conduction velocity and predisposition to arrhythmias in connexin40-deficient mice. *Curr Biol*. 1998;8:299-302.
16. Simon AM, Goodenough DA, Paul DL. Mice lacking connexin40 have cardiac conduction abnormalities characteristic of atrioventricular block and bundle branch block. *Curr Biol*. 1998;8:295-298.
17. Tyrode MV. The mode of action of some purgative salts. *Arch.Int.Pharmacodyn*. 1910;20:205-223.
18. Van Kempen MJA, Jongsma HJ. Distribution of connexin37, connexin40 and connexin43 in the aorta and coronary artery of several mammals. *Histochem Cell Biol*. 1999;112:479-486.
19. Sweat F, Puchter H, Rosenthal SI. Sirius Red F3Ba as a stain for connective tissue. *Arch Pathol*. 1964;69:72.
20. Shaw RM, Rudy Y. Ionic mechanisms of propagation in cardiac tissue: Roles of the sodium and L-type calcium currents during reduced excitability and decreased gap junction coupling. *Circ Res*. 1997;81:727-741.
21. Rohr S, Kucera JP, Kléber AG. Slow conduction in cardiac tissue. I. Effects of a reduction of excitability versus a reduction of electrical coupling on microconduction. *Circ Res*. 1998;83:781-794.
22. Jongsma HJ, Wilders R. Gap junctions in cardiovascular disease. *Circ.Res*. 2000;86:1193-1197.
23. Golshayan D, Seydoux C, Berguer DG, Stumpe F, Hurni M, Ruchat P, Fischer A, Meuller X, Sadeghi H, von Segesser L, Goy JJ. Incidence and prognostic value of electrocardiographic abnormalities after heart transplantation. *Clin Cardiol*. 1998;21:680-684.
24. Tuzcu EM, Emre A, Goormastic M, Loop FD, Underwood DA. Incidence and prognostic significance of intraventricular conduction abnormalities after coronary bypass surgery. *J Am Col Cardiol*. 1990;16:607-610.
25. Newby KH, Pisano E, Krucoff MW, Green C, Natale A. Incidence and clinical relevance of the occurrence of bundle-branch block in patients treated with thrombolytic therapy. *Circulation*. 1996;94:2424-2428.
26. Rohr S, Kucera JP. Involvement of the calcium inward current in cardiac impulse propagation: induction of unidirectional conduction block by nifedipine and reversal by Bay K 8644. *Biophys J*. 1997;72:754-766.
27. Rohr S, Kucera JP, Fast VG, Kléber AG. Paradoxical improvement of impulse conduction in cardiac tissue by partial cellular uncoupling. *Science*. 1997;27:841-844.
28. El-Sherif N, Amay YLF, Schonfield C, Scherlag BJ, Rosen K, Lazzara R, Wyndham C. Normalization of bundle branch block patterns by distal His bundle pacing. Clinical and experimental evidence of longitudinal dissociation in the pathologic his bundle. *Circulation*. 1978;57:473-483.
29. Burchell HB, Essex HE, Pruitt RD. Studies on the spread of excitation through the ventricular myocardium. II. The ventricular septum. *Circulation*. 1952;6:161-171.
30. Durrer D, van Dam RT, Freud GE, Janse MJ, Meijler FL, Arzbaecher RC. Total excitation of the isolated human heart. *Circulation*. 1970;41:899-912.
31. Anderson RH, Becker BE, Trantum-Jensen J, Janse MJ. Anatomicoelectrophysiological correlations in the conduction system-a review. *Br Heart J*. 1981;45:67-82.
32. Lev M, Thaemert JC. The conduction system of the mouse heart. *Acta Anat*. 1973;85:342-352.



# Chapter 7

---

## **Remodeling of gap junctions in mouse hearts hypertrophied by forced retinoic acid signaling.**

Toon A.B. van Veen, Harold V.M. van Rijen, Rob F. Wiegelerinck,  
Jacques M.T. de Bakker, Melissa C. Colbert, Sophie Clement,  
Tobias Opthof, Habo J. Jongsma

*Submitted*

## **Abstract**

*Background:*  $\beta$ -MHC-hRAR $\alpha$  transgenic mice express a constitutively active (truncated) form of the human retinoic acid receptor (primarily) in the left ventricle of the heart and consequently, develop a biventricular dilated cardiomyopathy. Severity of the pathologic changes depends on the number of copies of the transgenic construct inserted.

*Methods and Results:* As compared to wildtype mice (no inserted hRAR $\alpha$  copies), hearts of 4-6 month old mice with 7-12 inserted hRAR $\alpha$  copies show ventricular dilatation and occasionally atrial remodeling due to left atrial thrombosis. These structural alterations are reflected by an increased heart weight/body weight- and heart weight/tibia length ratio. 3-Lead body surface ECG's revealed prolongation of the Q-j interval suggesting delayed ventricular activation. Mapping of electrical activity of epi- and endocardial left ventricular free wall revealed activation delay with regional conduction block and ectopic activity. Ventricular tachycardia's did not occur spontaneously nor could be induced by ventricular pacing. Immunohistochemical analysis of hearts showed profound and heterogeneous down-regulation of the gap junction protein connexin43 in the left ventricular free wall, where hRAR $\alpha$  expression induced re-expression of the hypertrophic markers  $\alpha$ -skeletal actin and  $\beta$ -MHC. Concomitant with changes in subcellular distribution of Cx43, changes in expression and distribution of  $\beta$ -catenin and N-cadherin (two other intercalated disk associated proteins) were observed. In 3 out of 10 severely affected mice, ventricular re-expression of Cx40 was found in regions nearly devoid of Cx43 expression.

*Conclusions:*  $\beta$ -MHC-hRAR $\alpha$  transgenic mice show heterogeneous re-expression of (early) sarcolemmal gene products and simultaneously, a severe impairment of connexin43, N-cadherin and  $\beta$ -catenin expression which suggests structural remodeling of involved myocytes. Consequently ventricular activation is delayed with areas of block but no lethal arrhythmias occurred.

## **Introduction**

Dilated cardiomyopathy (DCM) is a multifactorial cardiac disease, characterized by cardiac dilatation and myocardial dysfunction, which has a poor clinical prognosis<sup>1</sup>. Although the onset of the disease can be diverse, cellular changes in expression/function of sarcomeric proteins, ion channels and gap junction channels are consistently reported<sup>2-4</sup>. Previously, Colbert *et al.* described the generation of transgenic mice expressing a constitutively active form of the human retinoic acid receptor (hRAR $\alpha$ ) under control of the  $\beta$ -MHC promoter<sup>5</sup>. RARs belong to the nuclear receptor superfamily which act upon binding of steroid-like molecules, like retinoic acid, as ligand activated transcription factors. Upon activation, RARs dimerize and regulate expression of genes which contain retinoic acid responsive elements in their proximal promoter<sup>6</sup>. Retinoic acid (RA) signalling is important for both cardiac development and differentiation into adult muscle cells<sup>7,8</sup>. Evidence is accumulating showing that changes in RA homeostasis, e.g. induced by retinoic acid embryopathy, evoke severe malformations during cardiogenesis<sup>9</sup>. Additionally, RA dependent signal transduction appears to preserve the normal differentiated phenotype of cardiomyocytes by antagonizing the effect of various hypertrophic stimuli<sup>10</sup>.

In  $\beta$ -MHC-hRAR $\alpha$  mice, forced activity of hRAR $\alpha$  induced a DCM with pathophysiological characteristics as found in classical forms of DCM; severe impairment of cardiac function and a reduced contractility while endstage failing

hearts showed biventricular chamber dilatation and left atrial thrombosis<sup>5</sup>. However, before cardiac dysfunction becomes overt, early alterations were observed in the mRNA levels of genes associated with cardiac hypertrophy<sup>11</sup>. One of the differentially expressed genes is connexin43 (Cx43), a gap junction protein. Gap junctions are agglomerates of multiple intercellular channels which directly connect the cytoplasms of adjacent cells. Each individual gap junction channel consists of 12 connexin (Cx) molecules, assembled from two head to head aligned hexameric hemichannels (neighboring cells both deliver one hemichannel). In mammals, up till now at least 15 different connexin genes have been cloned and named after their theoretical molecular mass (for review see<sup>12</sup>). In heart, gap junction channels are responsible for propagation of the electric impulse from cell to cell. They may be composed of Cx40, Cx43 and Cx45 and are primarily located on the longitudinal cell-edges in specialized structures called intercalated disks (IDs), (for review<sup>13</sup>).

Alterations in expression level of connexins and subcellular redistribution of gap junctions have been reported in various forms of cardiac disease<sup>14-16</sup>, and are associated with an increased propensity to develop cardiac arrhythmias<sup>17</sup>. In this study we show that in  $\beta$ -MHC-hRAR $\alpha$  mouse ventricles, Cx43 is subcellularly redistributed prior to severe heterogeneous down-regulation in regions where the transgene is expressed. In those regions, cellular differentiation is changed as shown by re-expression of fetal sarcomeric proteins and down-regulation of ID associated markers. Also, we show that electrical activation of the left ventricle is delayed and regional conduction block occurs as a consequence of this redistribution.

## **Materials and Methods**

### *Animals*

$\beta$ MHC-hRAR $\alpha$ -LacZ transgenic mice express a constitutively active (by truncation) human retinoic acid receptor under control of a  $\beta$ -MHC promoter. Mice were generated in a FVB/N background at the Children's Hospital Research Foundation, Cincinnati, USA as described previously<sup>5</sup>. Breeding of mice originating from line 30 (12 inserted hRAR copies) was performed at the animal facility, Utrecht University, Utrecht, The Netherlands. Imported transgenic mice were crossed to maintain high copy numbers of the transgene in the litters. To exclude uncontrolled genetic disorders blurring the effects induced by the transgene, primary litters were back-crossed with FVB/N wildtype mice. Animals were used between 4 and 6 months of age. The study conformed to the guiding principles of the American Physiological Society.

### *Experimental design*

Mice were genotyped by Southern/Dot blotting of genomic DNA (tail tips). After anaesthesia, body weight was determined, body surface ECG's were recorded and tibia length was measured. Next, the heart was excised, prepared and mounted on a Langendorff perfusion system to perform epicardial and endocardial mapping. At the end of the experiment, heart wet weight was assessed and hearts were snap frozen for histochemistry (complete hearts) or for protein isolation (hearts separated into compartments). Thin sections were used for immunofluorescence microscopy or fixed and stained to determine  $\beta$ -Galactosidase activity. Separated ventricles were minced and protein was isolated for SDS-PAGE and Western blotting.

### *Genotyping*

Genomic DNA was isolated from tail-tips according to Laird *et al.*<sup>18</sup>, overnight digested with BamHI/Bgl-II and subsequently 10 µg was separated on a 0.8% agarose gel. By Southern blotting, DNA was transferred to Z-probe membrane (Biorad), fixed and probed with a <sup>32</sup>P labeled 1 kB probe raised against the LacZ insert. Since the probe used produced one specific band (see Fig.7.1A), further characterization of mice was performed using Dot-blot analysis. After primary development, blots were stripped and incubated with a probe raised against GAPDH. Signals were visualized (phospho-imager, STORM 820, Molecular Dynamics, Sunnyvale, CA, USA) and quantified with Image Quant software (Molecular Dynamics). Copynumbers were calculated from samples with defined amounts of Bgl-II digested vector DNA (modified pKS vector with a 3 kB LacZ fragment cloned in between two Bgl-II sites) representing increasing amounts of inserted copies (samples supplemented with 10 µg wildtype mouse DNA). Calculated copynumbers were corrected for differences in GAPDH.

### *Preparation of the hearts*

Mice were anaesthetized by a intraperitoneal injection of urethane (2 g/kg bodyweight). Body weight (BW) was measured and corrected for the volume of injected anesthetics. 3-Extremity lead ECG's were recorded and signals were analyzed using custom-made software. Preparation of the hearts and Langendorff perfusion was performed as described before<sup>19</sup>. Finally, heart (wet) weight (HW) and tibia length (TL) of the left hind limb were measured, hearts were snap frozen in liquid nitrogen and stored at -80°C until use.

### *Recording of electrograms*

Extracellular electrograms were recorded with a 247 point multi-terminal electrode as described before<sup>19</sup>. In brief, electrode terminals were arranged in a 19 by 13 grid at inter-electrode distances of 0.3 mm. Unipolar electrograms were acquired using a custom built 256-channel data-acquisition system. Epicardial recordings of the ventricles were made in sinus and paced rhythm. To determine spread of electrical activation during basic and premature stimulation, the epicardium was stimulated from two adjacent central electrodes in the grid at a cycle-length of 100 ms. Every sixteenth stimulus was followed by one premature stimulus. Starting at 90 ms the coupling interval of the extra stimulus was reduced in steps of 10 ms until conduction block occurred. To measure conduction velocity, the left atrium was removed and a custom built grid with 8 linear electrodes was inserted through the mitral valves. The electrode terminals were positioned against the endocardial surface of the left ventricular free wall (LVFW) and unipolar recordings were made during programmed stimulation from the two most apical electrodes of the grid.

### *Data Analysis*

Activation maps were constructed from the activation times using custom written software based on Matlab (The Mathworks Inc.). Maximal negative dV/dt in the unipolar electrograms was selected as the time of local activation. Statistical comparisons were performed using ANOVA with Fischer's post-hoc analysis. Values are mean ± S.E.M. P-values ≤ 0.05 were considered as statistically significant.

### *Immunohistochemistry and histology*

Frozen hearts were serially sectioned in frontal plane with a cryostat, to produce 'four chamber view' sections of 10- and 12 µm thickness. They were mounted on aminopropyltriethoxysilane- (AAS) coated glass slides. Sections were permeabilized

in 0.2% Triton X-100 (1 hour), blocked in 2% bovine serum albumin (BSA, 30 min.) and incubated overnight in presence of 10% normal goat serum (NGS) with primary antibodies. After blocking again with 2% BSA (30 min.) secondary labeling was performed with appropriate Texas Red (TR)- or fluorescein isothiocyanate (FITC)-conjugated antibodies (2 hours in presence of 10% NGS). All chemicals were dissolved in phosphate buffered saline (PBS) which was also used to wash the sections in between the subsequent incubations. Finally, sections were mounted in Vectashield (Vector Laboratories) and examined with a Nikon Optiphot-2 light microscope equipped for epifluorescence.

#### *LacZ staining*

Expression of the transgene could be assessed by LacZ staining because of the insertion of  $\beta$ -galactosidase DNA in the transgenic construct. Thin sections were post-fixed with 2% paraformaldehyde/0.2% glutaraldehyde (5 minutes, 4°C), rinsed in PBS, and incubated with 1 mg/ml X-Gal, 5 mM  $\text{K}_4\text{Fe}(\text{CN})_6 \cdot 3\text{H}_2\text{O}$ , 5 mM  $\text{K}_3\text{Fe}(\text{CN})_6$ , 2 mM  $\text{MgCl}_2 \cdot 6\text{H}_2\text{O}$  in PBS (overnight, 37°C). Finally, thin sections were dehydrated, embedded in Entellan and analyzed by classical light microscopy.

#### *Protein isolation, SDS-PAGE and Western Blotting*

Total cellular protein was isolated from 4 separated fractions: left ventricular free wall (LVFW), right ventricular free wall (RVFW), interventricular septum (IVS) and pooled atria (A). Tissue was pulverized in a liquid nitrogen cooled mortar and rapidly transferred to RIPA-buffer (50 mM Tris pH7.4, 150 mM NaCl, 1% nonidet P40, 1% DOC, 0.1% SDS, 2 mM PMSF and a cocktail of protease inhibitors). After 15 minutes at room temperature samples were sonicated, centrifuged and protein content of the supernatant was assessed according to Lowry<sup>20</sup>. Aliquots were diluted with 4x Laemmli buffer and boiled for 5 minutes. Equal amounts (50  $\mu\text{g}$ /lane) of each sample were separated on 10% SDS-polyacrylamide gels and electrophoretically transferred to nitrocellulose membrane (0.45  $\mu\text{m}$ , Biorad). Protein transfer was assessed by Ponceau S staining. Prior to primary antibody incubation (overnight, 4°C, in 0.1% BSA/0.1% Tween20/PBS), the nitrocellulose membrane was blocked with 5% dried milk powder (1 hr, RT, in 0.1% Tween20/PBS). Next morning, the membrane was washed (3x5 minutes, 0.1% Tween20/PBS), incubated with Horse-Radish-Peroxidase conjugated secondary antibody (1 hr, 4°C, 0.1% BSA/0.1% Tween20/PBS), and washed again (6x5 minutes, 0.1% Tween20/PBS). Signals were visualized using an Enhanced Chemo Luminiscence reagent (ECL, Amersham) according to the instructions of the manufacturer and exposure to XB-1 film (Kodak) .

#### *Antibodies*

The following commercially available antibodies were used; rabbit polyclonal Cx40 (Alpha Diagnostics), mouse monoclonal Cx43 and mouse monoclonal  $\beta$ -catenin (Transduction Laboratories), rabbit polyclonal Cx43 (Zymed), mouse monoclonal desmin (Sanbio), rabbit polyclonal N-cadherin and mouse monoclonal  $\alpha$ -actinin (Sigma), rabbit polyclonal ANF (Biotrend)). A mouse monoclonal antibody against  $\beta$ -MHC was a kind gift of Dr. AFM Moorman, Dept. Anatomy/Embryology, Academic Medical Center, Amsterdam, The Netherlands. A rabbit polyclonal antibody against  $\alpha$ -skeletal actin was produced at the Department of Pathology, University of Geneva, Switzerland<sup>21</sup>. Secondary antibodies (Texas red (TR) or Fluorescein-Isothiocyanate (FITC)-conjugated) were purchased from Jackson Laboratories.

## Results

### Characterization of the mice.

In our mouse breeding program, no differences within the population were observed in number of offspring nor in loss of animals after birth that could be associated with expression of high amounts of inserted transgenic construct. Genotyping of the offspring was initially performed with Southern hybridization. In figure 7.1A genotyping of 5 mice is shown. A 3.3 kB signal of predicted size<sup>22</sup> was found in lane 1,3 and 5 while the positive control (pKS vector with LacZ insert) revealed as

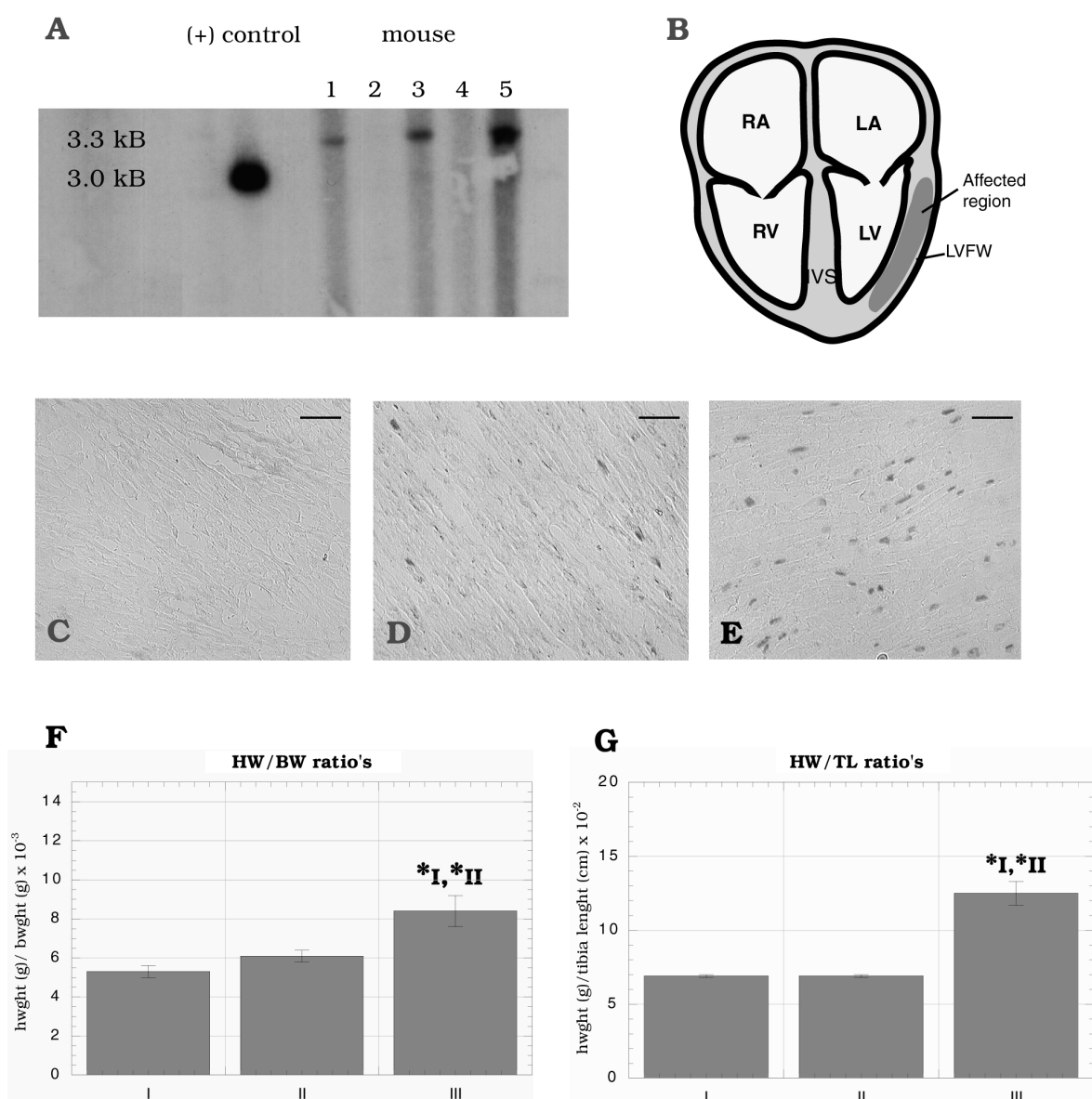


Figure 7.1 A: Genotyping of the mice with Southern blot analysis. B: Cartoon of the heart with indicated the affected region in the LVFW. C-E: bar = 20  $\mu$ m, LacZ staining of thin sections from the LVFW of hearts in group I (C), group II (D) and group III (E). F-G: Bar plots of HW/BW ratio's (F), HW/TL ratio's (G), error bars indicate S.E.M. \*I, \*II = significantly different from group I and group II.

calculated, a 3 kB band. Since the probe appeared to be specific, genotyping was simplified using Dot-blot analysis. Transgenic constructs appeared to be inserted in the range from 0-12 copies.

Mice were divided in three groups ( $n \geq 10$  in each group) based on the copy number and LacZ staining: group I (control): 0 copies, no LacZ, group II: 3-5 copies, low LacZ and group III: 7-12 copies, high LacZ. Functional expression of the inserted transgene was assessed by lacZ staining of post fixed thin cryosections. No staining was found in control hearts (7.1C) nor in atrial tissue of group II and III (not shown). Both group II (7.1D) and III (7.1E) show characteristic blue staining of nuclei (due to the endogenous nuclear localization signal (NLS)), especially in myocytes of the affected area in the left ventricular free wall (LVFW, 7.1B). The number of stained nuclei in group III was much larger than in group II. In areas of group III LVFW which were heavily stained with LacZ, nuclear staining was accompanied by diffuse perinuclear staining due to excessive expression of the transgene. In those animals, a few myocytes of the right ventricular free wall (RVFW) stained positive as well.

Heart weight/body weight ratio's (HW/BW) as well as heart weight/tibia length ratio's (HW/TL) of the three groups are shown in figure 7.1E, 7.1F and summarized in table 7.I. HW/BW ratio's of group I ( $5.3 \pm 0.3 \times 10^{-3}$ ) and group II ( $6.1 \pm 0.3 \times 10^{-3}$ ) were not statistically different ( $P=0.63$ ) but the ratio of group III ( $8.4 \pm 0.8 \times 10^{-3}$ ) was significantly larger than ratio's of both group I ( $P=0.0007$ ) and group II ( $P=0.0036$ ). HW/TL ratio's of group I ( $6.9 \pm 0.1 \times 10^{-2}$ ) and II ( $6.9 \pm 0.1 \times 10^{-2}$ ) were not different ( $P=0.95$ ) but the ratio of group III ( $12.5 \pm 1.5 \times 10^{-2}$ ) was significantly larger than the ratio's of group I ( $P=0.0089$ ) and II ( $P=0.0077$ ). Sometimes (2 out of 10), hearts in group III weighted more than 400 mg (average HW group I; 160 mg, group III; 270 mg) and showed strong biventricular dilatation and left atrial thrombosis.

### **Extremity leads (ECG) and epicardial mapping.**

After anesthesia with urethane which minimally affects cardiac electrophysiology<sup>23</sup>, 3-extremity lead ECG's were recorded. Figure 7.2A shows typical examples of group I, II and III ECG's. Statistical analysis is summarized in table 7.I. Duration of P-Q interval (figure 7.2B) was significantly longer in group III ( $39.7 \pm 3.0$ ) compared to group I ( $33.9 \pm 0.3$ ,  $P=0.01$ ) and II ( $33.6 \pm 1.0$ ,  $P=0.011$ ). Duration of R-R interval (figure 7.2C) was not significantly different between the three groups (I;  $106.8 \pm 2.8$ , II;  $102.7 \pm 3.0$ , III;  $101.1 \pm 2.7$ ,  $P=0.39$ ). Q-j interval (figure 7.2D) was significantly

Table I	Group I	Group II	Group III
HW/BW( $\times 10^{-3}$ )	$5.3 \pm 0.3$	$6.1 \pm 0.3$	$8.4 \pm 0.8$
HW/TL ( $\times 10^{-2}$ )	$6.9 \pm 0.1$	$6.9 \pm 0.1$	$12.5 \pm 1.5$
RR (ms)	$106.8 \pm 2.8$	$102.7 \pm 3.0$	$101.1 \pm 2.7$
PQ (ms)	$33.9 \pm 0.3$	$33.6 \pm 1.0$	$39.7 \pm 3.0$
Qj (ms)	$10.8 \pm 0.3$	$10.6 \pm 0.2$	$19.5 \pm 3.0$

Table 7.I: Statistics of ECG analysis and HW/BW, HW/TL ratio's. Group I = control, Group II = mildly affected, Group III = severely affected. Data are mean  $\pm$  S.E.M.

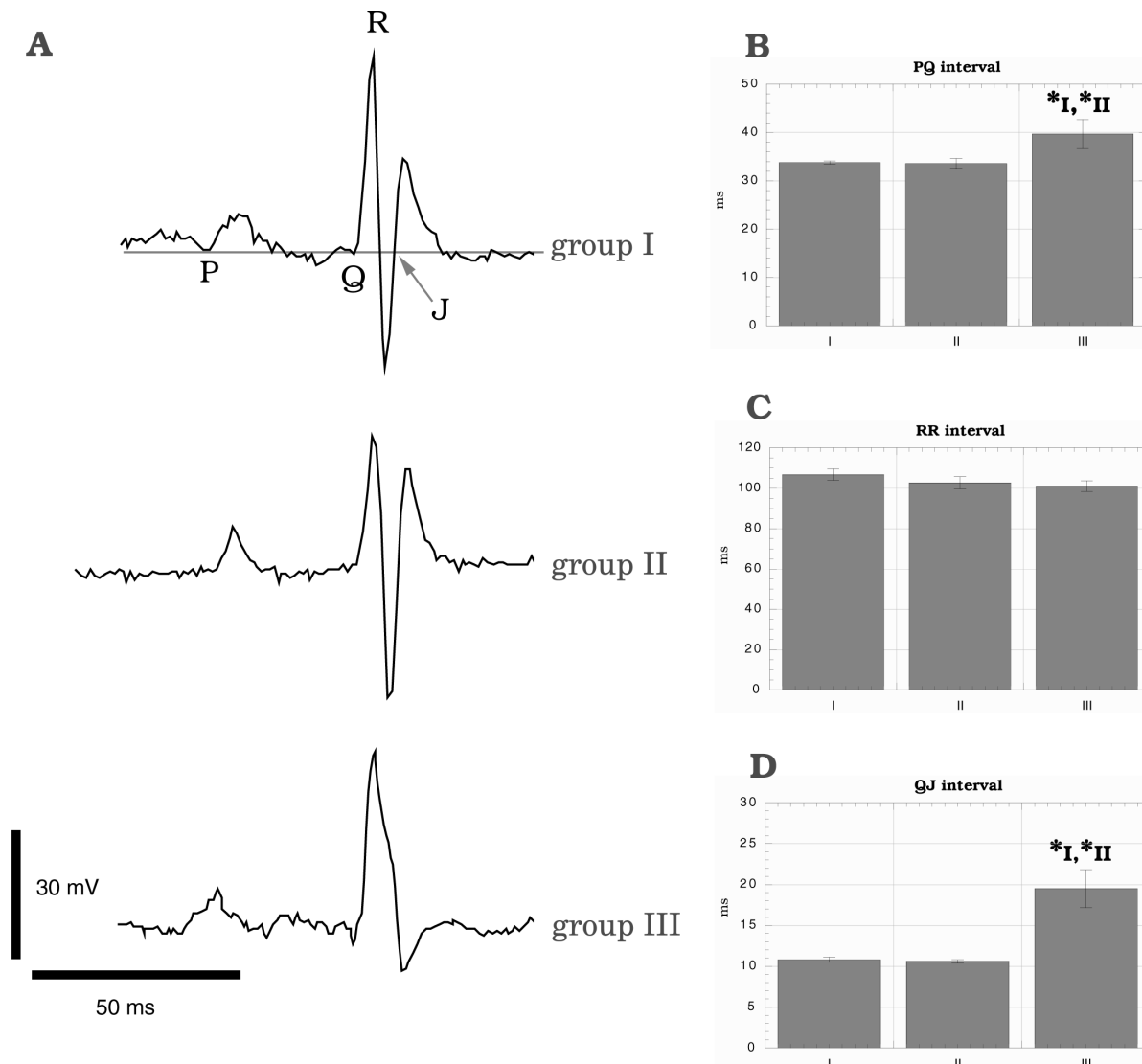


**Figure 7.2** A: ECG complexes of Einthoven-2 recordings from group I, II and III. B-D: Bar plots of P-Q interval-length (B), R-R interval-length (C) and Q-j interval-length (D) of group I, II and III. Average is given in table 7.1, error bars indicate S.E.M. \*I, \*II = significantly different from group I and group II.

prolonged in group III animals ( $19.5 \pm 2.3$ ) as compared to group I ( $10.8 \pm 0.3$ ,  $P < 0.0001$ ) and group II ( $10.6 \pm 0.2$ ,  $P < 0.0001$ ). In 3 out of 10 group III mice, a split morphology of the QRS complex was found (not shown).

Epicardial maps of the LVFW are shown in figure 7.3A,B. Spontaneous ventricular arrhythmia could not be detected either in hearts of group I, II or III. LVFW epicardial maps of group I and III were comparable in SR (figure 7.3A, left panel), and during programmed stimulation from the center of the electrode grid at basic cycle length (figure 7.3A, mid-panel). However, profound conduction delay and regional block were detected in group III after premature stimulation (figure 7.3A, right panel). Programmed stimulation (3 extra stimuli) of the hearts to assess vulnerability for ventricular arrhythmias resulted in ectopic activity in 3 out of 10 group III mice (figure 7.3B), but never in mice of group I and II. RVFW epicardial

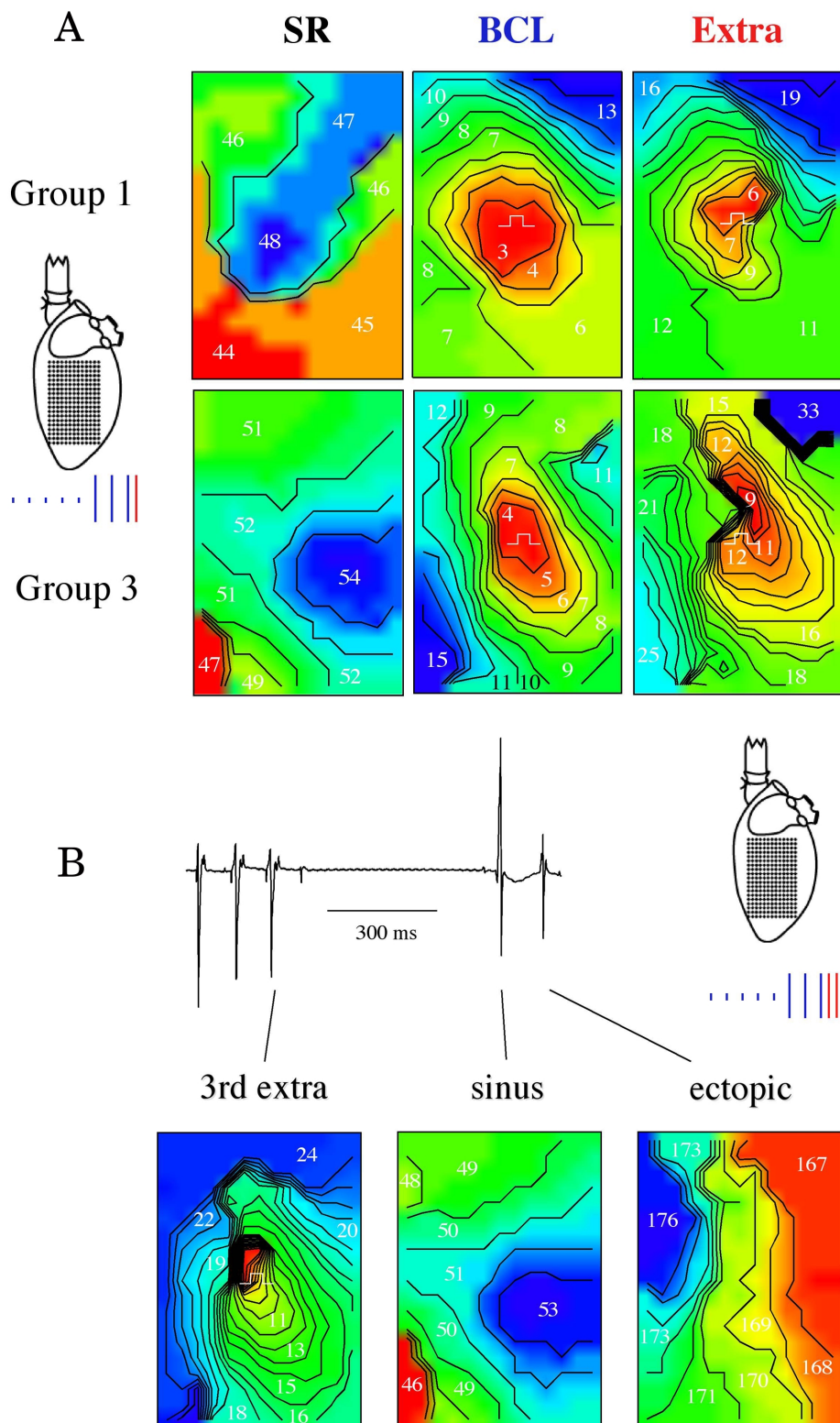
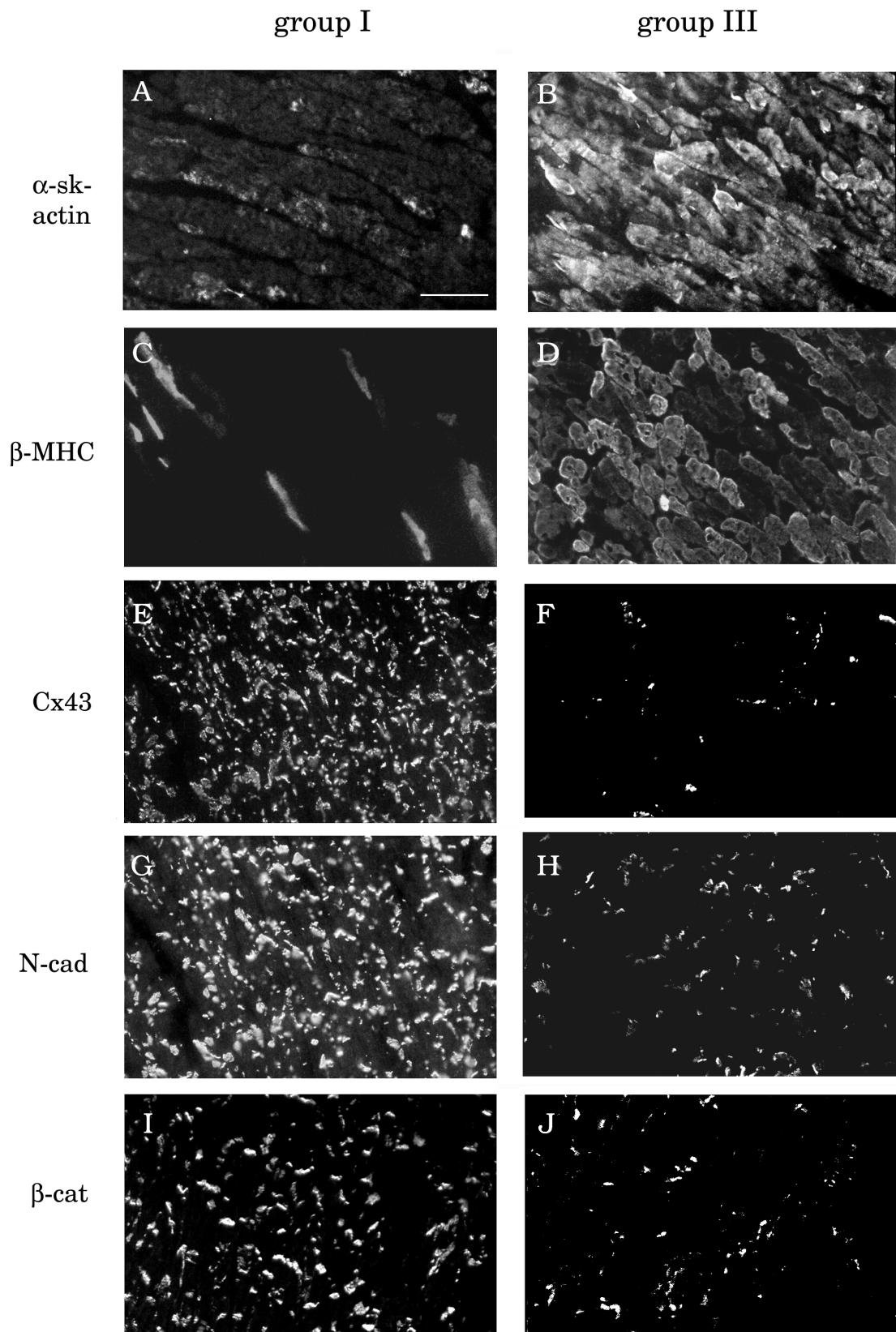


Figure 7.3 A: LVFW epicardial activation maps of a group I (upper three panels) and a group III (lower three panels) hearts. B: Example of a LVFW activation map of a group III heart with regional conduction block and ectopic activity. Numbers indicate activation time in ms. SR= sinus rhythm, BCL = basis cycle length.



*Figure 7.4 Immunohistochemical staining of the midsection of the LVFW in group I (left panel) and group III (right panel) hearts. Bar (shown in A) for A-J is 100  $\mu$ m.*

maps (sinus rhythm) of group I, II and III were comparable but showed propagation of the electric impulse with earliest activation found at variable sites (data not shown).

After epicardial mapping, the left atrium was removed and the 8-point electrode grid was inserted through the mitral-valves and placed against the endocardial surface of the LVFW. As with the epicardial recordings, no ventricular arrhythmias were detected and significant ( $p=0.042$ ) conduction slowing of an extra stimulus was found in group III hearts compared to group I. When paced from the apical electrodes in the linear grid, conduction velocity in group I was  $43.0\pm4.2$  and  $36.8\pm3.5$  cm/s during basic and premature stimulation, respectively, and  $34.3\pm3.7$  and  $24.4\pm3.4$  cm/s in group III.

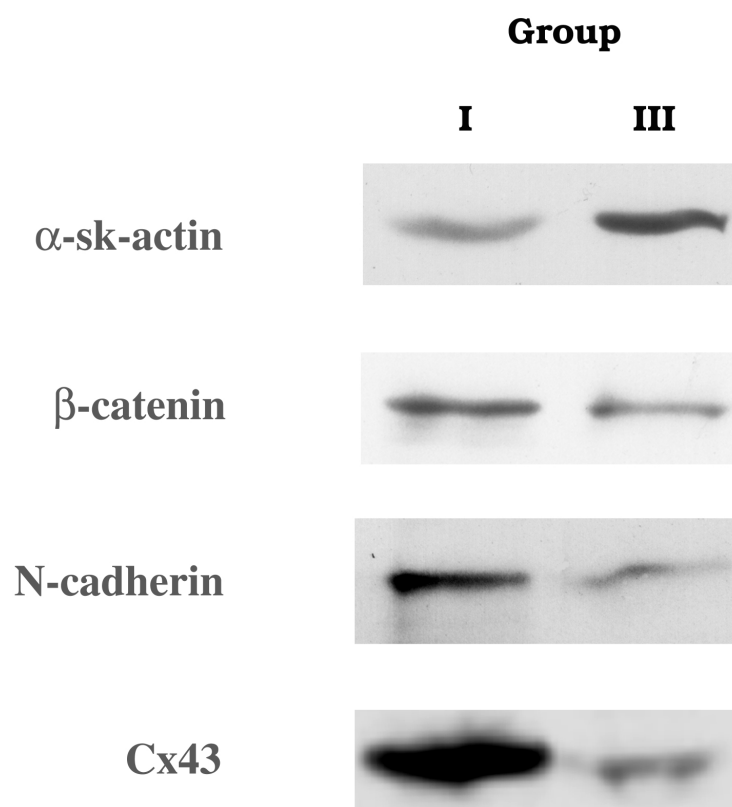


*Figure 7.5 Representative Western blots of LVFW samples derived from group I and group III hearts. In group III tissue, hypertrophic status is shown by a strong elevation of the  $\alpha$ -skeletal-actin signal while ID associated proteins as Cx43, N-cadherin and  $\beta$ -catenin are down-regulated.*

### **Expression of hypertrophic markers and down regulation of ID associated proteins.**

To characterize the degree of hypertrophy in the transgenic hearts, cryo-sections consecutive to those stained with LacZ, were incubated with antibodies raised against the hypertrophic markers Atrial Natriuretic Peptide (ANP), b-MHC and  $\alpha$ -skeletal-actin. In group I, II and III, ANP was found in the atria as small punctate labeling while no ventricular labeling could be detected (not shown). Both in the

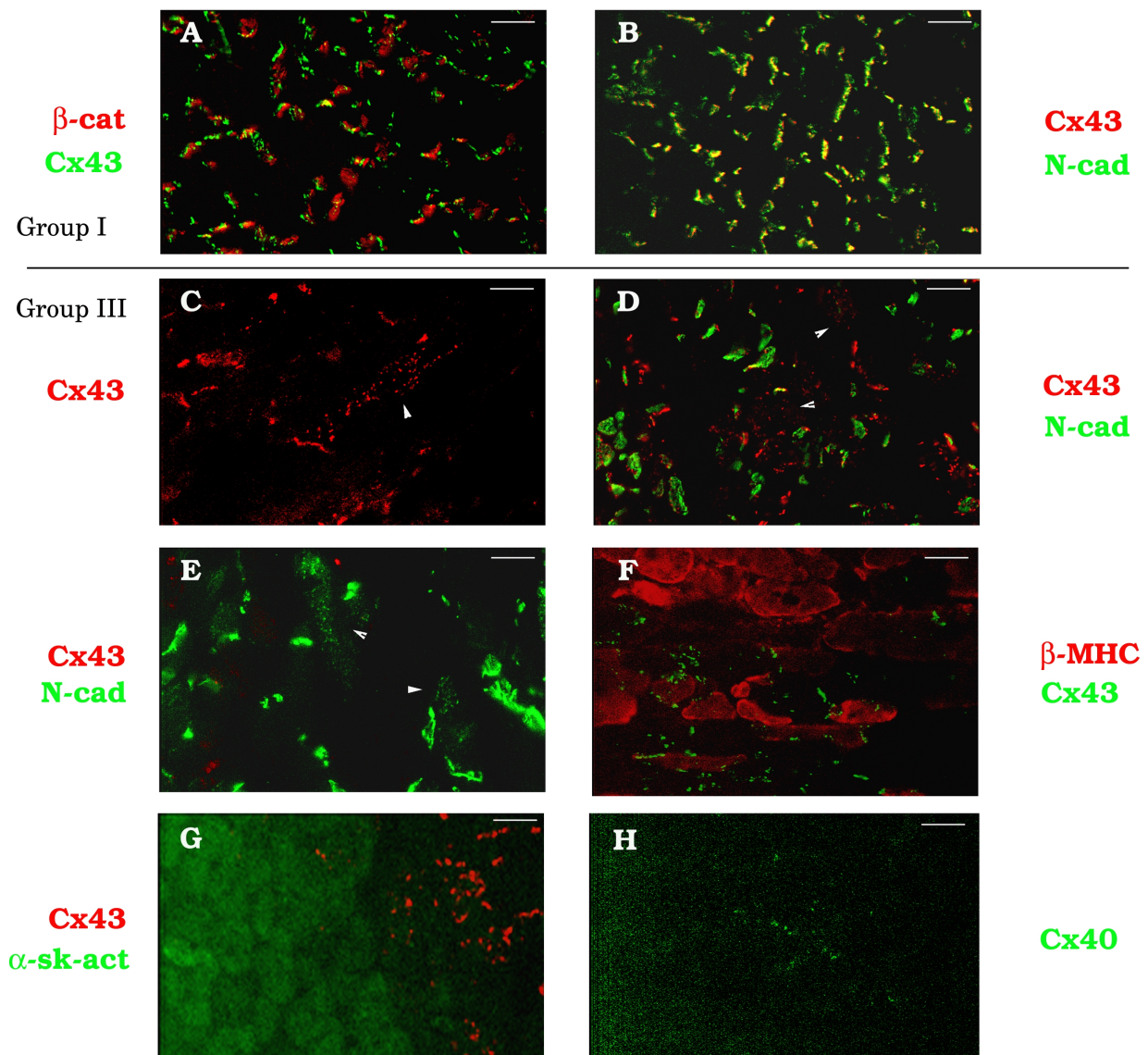


Figure 7.6 Immunohistochemical staining of the midsection of the LVFW of group I (A and B), and group III hearts (C-H). Bars represent 20  $\mu$ m in C,E and H, 40  $\mu$ m in A,B,D,F,G,.

RVFW and LVFW of group I, a small number of myocytes, primarily located near the apex and near the outflow tract, labeled positive for b-MHC and  $\alpha$ -skeletal-actin. In group III, no aberrant labeling was found in the RVFW and the IVS but abundant labeling for b-MHC (Fig.7.4B) and  $\alpha$ -skeletal-actin (Fig.7.4D) was detected intramurally in the LVFW. Here, nearly all cells were positive while at comparable location in group I (Fig. 7.4A and 7.4C, respectively) this was below 10%. The intensely b-MHC and  $\alpha$ -skeletal-actin positive regions coincided with the intense LacZ staining in consecutive sections.

In group I hearts, labeling with a monoclonal antibody raised against the gap junction protein Cx43 revealed a homogeneous characteristic pattern in the LVFW, the IVS and the RVFW. Labeling is primarily situated on the IDs at the longitudinal cell-cell contacts (Fig.7.4E). A similar labeling pattern was obtained using

antibodies against N-cadherin (Fig. 7.4G) and  $\beta$ -catenin (Fig. 7.4I). N-cadherin, a transmembrane protein in the adherens junction mechanically connects adjacent cells by anchoring the cytoskeleton via  $\beta$ -catenin to the sarcolemma. In group III LVFW, the intramural region with the highest intensity of LacZ staining and marked up-regulation of  $\beta$ -MHC and  $\alpha$ -skeletal-actin, many cells were almost completely devoid of Cx43 labeling (Fig. 7.4F). Depending on the transgene copynumber and the degree of LacZ staining, the size of this area ranges from small clusters of 5-10 cells to ~40% of the LVFW. Down-regulation of N-cadherin (Fig. 7.4H) and  $\beta$ -catenin (Fig. 7.4J) was also found in the LVFW of group III. In those sections, immunonegative area's could be observed which varied in size but were smaller compared to Cx43 negative area's.

Western blotting experiments supported the results obtained with immunohistochemical analysis. As compared to group I, no differences in expression levels of Cx43, N-cadherin,  $\beta$ -catenin and  $\alpha$ -skeletal actin were found in the pooled atria, the RVFW and the IVS of group III (data not shown). However, figure 7.5 shows that in samples from the LVFW of group III mice, Cx43, N-cadherin and  $\beta$ -catenin are strongly reduced compared to LVFW samples of group I hearts. In contrast,  $\alpha$ -skeletal actin is upregulated in the group III mice compared to group I. Antibodies against  $\beta$ -MHC were inappropriate to use for Western blotting.

### **Heterogeneity in remodeling.**

In group I LVFW (and group I, III RVFW and IVS), the IDs are marked by a strong co-localization of Cx43 and  $\beta$ -catenin (Fig. 7.6A) and Cx43 and N-cadherin (Fig. 7.6B). Down-regulation of Cx43 in group III hearts appeared very heterogeneous since cells in the very apical, basal and epicardial layers of the LVFW are less affected or even show a fairly normal expression pattern. Labeling with a second, but polyclonal, anti-Cx43 antibody confirmed the prior observations although the level of diffuse residual Cx43 labeling in the severely affected regions was slightly higher compared to labeling with the monoclonal anti-Cx43 antibody (data not shown). Next to down-regulation, cells were found which showed a redistribution of Cx43 both in group II hearts (small affected area's) and at the borders of the large Cx43 negative area's in group III hearts. In those cells, diffuse labeling marked the complete sarcolemma (Fig. 7.6C, arrowhead). Furthermore, co-expression of Cx43 with both  $\beta$ -catenin and N-cadherin (Fig. 7.6D) appeared to be lost. In transitional cells between the Cx43 positive and Cx43 negative area,  $\beta$ -catenin and N-cadherin expression and distribution seemed fairly unaffected while a substantial amount of Cx43 is found as lateral labeling (Fig. 7.6D, arrowhead). Changes in expression and distribution of N-cadherin and  $\beta$ -catenin seem to lag behind remodeling of Cx43 expression since in Cx43 negative area's, remnant labeling of  $\beta$ -catenin and N-cadherin was observed which mainly localized at lateral cell-cell contacts (Fig. 7.6E, arrowheads). Double-labeling for Cx43 and  $\beta$ -MHC (Fig. 7.6F) or for Cx43 and  $\alpha$ -skeletal-actin (Fig. 7.6G) revealed that cells which labeled positive for  $\beta$ -MHC or  $\alpha$ -skeletal-actin are marked by the absence of Cx43 while surrounding  $\beta$ -MHC and  $\alpha$ -skeletal-actin negative cells still express Cx43. In 3 out of 10 group III animals, a small amount of Cx40 re-expression was found as lateral labeling between myocytes of the LVFW (Fig. 7.6H), while no Cx40 could be detected both in group I hearts and group III working ventricular myocytes of the IVS and RVFW. Finally, no specific labeling of Cx45 gap junctions in the LVFW was found (data not shown).

## **Discussion**

This study shows that: 1) In  $\beta$ -MHC-hRAR $\alpha$  transgenic mice, functional expression of the transgenic construct results in an increase in heart weight as reflected by elevated HW/BW and HW/TL ratio's. The degree of phenotypical changes depends on the number of inserted copies. 2) In affected animals, ECG analysis shows a prolongation of P-Q and Q-j interval-length while R-R interval-length remains unchanged. Epicardial mapping shows a delayed ventricular activation with regional conduction block and ectopic activity but no severe spontaneous or pacing-induced ventricular arrhythmia's. 3) In the LVFW, functional expression of the transgene is marked and coincides with re-expression of the (early) sarcomeric proteins  $\beta$ -MHC and  $\alpha$ -skeletal-actin while ID-associated proteins like Cx43, N-cadherin and  $\beta$ -catenin are subcellularly redistributed prior to heterogeneous down-regulation.

### ***Development of dilated cardiomyopathy.***

Transgenic mice overexpressing a constitutively active form of the human retinoic acid receptor develop a classical form of dilated cardiomyopathy. The severity of pathophysiological and structural alterations depends on the number of copies inserted that give rise to functional expression level of the transgenic construct<sup>5</sup>. The mice used in this study contained 0-12 inserted copies and were divided in three groups based on copy number and degree of LacZ expression. Compared to group I, the control group with no inserted copies, only animals with 7-12 inserted copies (group III) are marked by an increased HW/BW ratio and HW/TL ratio. 3-5 inserted copies (group II) did not change both ratio's compared to control mice. To exclude false positive/negative results caused by fluctuating bodyweight, heart weight was also related to tibia length to assess severity of the myopathy<sup>24</sup>. The  $\beta$ -MHC promotor, which was used to drive hRAR $\alpha$  expression, causes expression primarily in the left ventricle (this study). As the pathophysiological process proceeds, or when a large number of copies are functionally inserted, expression of the transgene is found also in the right ventricles, though at a significantly lower level. Consequently, primarily left ventricular myocytes exhibit increased expression of hypertrophic markers like  $\beta$ -MHC and  $\alpha$ -skeletal actin. Integration of these proteins in the contractile architecture of the myocytes will likely affect the contractile properties of the cells adversely as shown in<sup>5,11</sup>.

### ***Mechanical and electrical dysfunction.***

In the LVFW, where the expression of the transgene evokes expression of above mentioned hypertrophic markers, structural remodeling of the ID has also been identified. At the level of the IDs, which mediate the electrical and mechanical coupling of myocytes, a severe and heterogeneous downregulation of Cx43, and to a lower degree of N-cadherin and  $\beta$ -catenin have been found. This implies that both electrical (Cx43) and mechanical coupling (N-cadherin and  $\beta$ -catenin) are affected. Mechanical dysfunction of these hearts has been reported before and shows a marked reduction in shortening fraction, velocity of circumferential fiber shortening and systolic performance<sup>5</sup>. At the subcellular level, impairment of the intracellular connection of the contractile fibers to adherens junctions (caused by  $\beta$ -catenin depletion) and impairment of the intercellular mechanical coupling (caused by N-cadherin depletion) both contribute to the development of mechanical dysfunction of affected hearts. In this context, it was recently shown that a dystrophin missense mutation<sup>25</sup>, or deletion of muscle LIM protein<sup>26</sup>, triggers development of DCM accompanied with structural reorganization of the intercalated disks.

Next to mechanical dysfunction, electrical function is also impaired. ECG analysis revealed a prolongation of the P-Q interval in group III but not in group II when compared to control (group I). This prolongation is mainly caused by increased P-wave duration (~10 ms in group I and II, ~15 ms in group III) which suggests a conduction delay in the atria resulting from slowed conduction or atrial enlargement<sup>27-29</sup>. The QRS complex (measured as Q-j interval) was considerably prolonged in affected animals with in 3 mice (out of 10) a split QRS morphology suggesting an asynchronous activation of the left and right ventricle or impairment of propagation through the conduction system. However, immunohistochemical analysis revealed normal connexin expression in the conduction system. Consequently, to explain the prolonged QRS duration, a delay in ventricular conduction was expected. Both epicardial mapping and mapping of the left ventricular endocardial free wall confirmed this hypothesis as in group III hearts a conduction delay of the electrical impulse was shown. In nearly all affected hearts, regional conduction block was found and occasionally, ectopic activity was recorded. However, neither during *in vivo* measurements nor in Langendorff perfusion, ventricular arrhythmias occurred. Programmed stimulation did not induce arrhythmias either. Since ventricular arrhythmias can be life threatening, the fact that we did not observe any copy-number related spontaneous death of mice in our breeding colony indicates that probably *in vivo* ventricular arrhythmias were absent too.

#### **Redistribution and down-regulation of Cx43, N-cadherin and $\beta$ -catenin.**

Immunohistochemical analysis of the LVFW of group III hearts showed a profound and heterogeneous decrease in expression of Cx43, the main connexin isoform expressed between ventricular working cardiomyocytes. Similar to N-cadherin and  $\beta$ -catenin, the alterations were found at spots where the transgene was functionally expressed. In all hearts expression of Cx43, N-cadherin and  $\beta$ -catenin was unaffected in the working myocardium of the IVS and the RVFW which confirms dependence of alterations on expression of the transgene. Depletion of Cx43 in the LVFW seems to precede that of N-cadherin and  $\beta$ -catenin since expression of N-cadherin and  $\beta$ -catenin at the borderzone of an affected area generally is still present while Cx43 is already lost. More to the center of an affected area all markers are lost. A second characteristic of the structural changes is re-distribution of Cx43 and to a minor extent of N-cadherin and  $\beta$ -catenin from the IDs to lateral cell borders. This phenomenon is mainly observed in the borderzone between normal and affected tissue and thus seems to precede total loss.

#### **Consequences of gap junction remodeling for electrical activation.**

Alterations in expression level and/or redistribution of Cx43 are consistently described observations in various models of ventricular hypertrophy and is proposed to increase the propensity to induce arrhythmia's<sup>14-17</sup>. In this respect, heterogeneity in expression might be as potent<sup>30</sup>. In  $\beta$ -MHC-hRAR $\alpha$  transgenic mice, hearts are marked both by a redistribution and a strong heterogeneous reduction in Cx43 expression. Remarkably, these profound changes (assumed to affect electrical coupling) did not result in spontaneous or inducible ventricular arrhythmia's. Several possible explanations for this phenomenon may be suggested:

- 1) Re-expression of other connexin isoforms might compensate for the loss of Cx43. Of the other two tested isoform known to be expressed in heart (Cx40 and Cx45), Cx45 was not detected in the LVFW and even though in 3 out of 10 severely affected hearts re-expression of Cx40 was detected, the low level excludes

compensation by this connexin isoform.

2) Immuno-staining with the polyclonal anti Cx43 antibody revealed a higher degree of residual diffuse staining as compared to the monoclonal anti Cx43 antibody. This residual diffuse expression of gap junctions in the affected area might cause a delay in propagation without inducing reentry. If changes in phosphorylation were involved and the Cx43 antibodies used had different preferences to bind phosphorylated and unphosphorylated forms of Cx43, this would result in inappropriate detection. However, specificity of both antibodies was confirmed on Western blots from mouse Cx43 transfected Hela cells which in addition showed that both antibodies possessed equal preferences for the (un)phosphorylated states of Cx43 (data not shown).

3) In cardiac-restricted conditional Cx43 knock-out mice, ventricular arrhythmia's and sudden death were observed<sup>31</sup>. However in this model, average reduction of Cx43 expression in the ventricles was 90%. This decrease in Cx43 expression is substantially larger and more uniform as compared to our model. In  $\beta$ -MHC-hRAR $\alpha$  transgenic mice, size of Cx43 depleted area ranged from small clusters of about 5-10 cells in mildly affected hearts to about 40% of total LVFW area in severely affected hearts. In this respect, the small size of mouse ventricles and the even smaller size of normal area in the affected hearts could be the limiting factor excluding the occurrence of reentry circuits while heterogeneity in Cx43 depletion might contribute to the regional character of conduction block.

### **Acknowledgements**

A.A.B. Van Veen and H.V.M. Van Rijen were financially supported by a project grant no.97.184 from the Netherlands Heart Foundation (to H.J.J.). The authors wish to thank Dr.AFM Moorman for providing the  $\beta$ -MHC antibody.

### **References**

1. Konstam MA, Remme WJ. Treatment guidelines in heart failure. *Prog Cardiovasc Dis.* 1998;41:65-72.
2. Morgan HE, Baker KM. Cardiac hypertrophy. Mechanical, neural, and endocrine dependence. *Circulation.* 1991;83:13-25.
3. Hein S, Kostin S, Heling A, Maeno Y, Schaper J. The role of the cytoskeleton in heart failure. *Cardiovasc Res.* 2000;45:273-278.
4. Jongsma HJ, Wilders R. Gap junctions in cardiovascular disease. *Circ.Res.* 2000;86:1193-1197.
5. Colbert MC, Hall DG, Kimball TR, Witt SA, Lorenz JN, Kirby ML, Hewett TE, Klevitsky R, Robbins J. Cardiac compartment-specific overexpression of a modified retinoic acid receptor produces dilated cardiomyopathy and congestive heart failure in transgenic mice. *Journal of Clinical Investigation.* 1997;100:1958-1968.
6. Mangelsdorf DJ, Evans RM. The RXR heterodimers and orphan receptors. *Cell.* 1995;83:841-850.
7. Kastner P, Messaddeq N, Mark M, Wendling O, Grondona JM, Ward S, Ghyselinck N, Chambon P. Vitamin A deficiency and mutations of RXR $\alpha$ , RXR $\beta$  and RAR $\alpha$  lead to early differentiation of embryonic ventricular cardiomyocytes. *Development.* 1997;124:4749-4758.
8. Subbarayan V, Mark M, Messaddeq N, Rustin P, Chambon P, Kastner P. RXR $\alpha$  overexpression in cardiomyocytes causes dilated cardiomyopathy but fails to rescue myocardial hypoplasia in RXR $\alpha$ -null fetuses. *J Clin Invest.* 2000;105:387-394.
9. Lammer EJ, Chen DT, Hoar RM, Agnish ND, Benke PJ, Braun JT, Curry CJ, Fernhoff PM,

- Grix AW, Jr., Lott IT, et al. Retinoic acid embryopathy. *N Engl J Med.* 1985;313:837-841.
10. Zhou MD, Sucov HM, Evans RM, Chien KR. Retinoid-dependent pathways suppress myocardial cell hypertrophy. *Proc Natl Acad Sci U S A.* 1995;92:7391-7395.
  11. Hall DG, Morley GE, Vaidya D, Ard M, Kimball TR, Witt SA, Colbert MC. Early onset heart failure in transgenic mice with dilated cardiomyopathy [In Process Citation]. *Pediatr Res.* 2000;48:36-42.
  12. Bruzzone R, White TW, Paul DL. Connections with connexins: The molecular basis of direct intercellular signaling. *European Journal of Biochemistry.* 1996;238:1-27.
  13. Gros D, Jongsma HJ. Connexins in mammalian heart function. *BioEssays.* 1996;18:719-730.
  14. Sepp R, Severs NJ, Gourdie RG. Altered patterns of intercellular junction distribution in human patients with hypertrophic cardiomyopathy. *Heart.* 1996;76:412-417.
  15. Severs NJ. The cardiac muscle cell. *Bioessays.* 2000;22:188-199.
  16. Uzzaman M, Honjo H, Takagishi Y, Emdad L, Magee AI, Severs NJ, Kodama I. Remodeling of gap junctional coupling in hypertrophied right ventricles of rats with monocrotaline-induced pulmonary hypertension. *Circ Res.* 2000;86:871-878.
  17. Tomaselli GF, Marbán E. Electrophysiological remodeling in hypertrophy and heart failure. *Cardiovascular Research.* 1999;42:270-283.
  18. Laird PW, Zijderfeld A, Linders K, Rudnicki MA, Jaenisch R, Berns A. Simplified mammalian DNA isolation procedure. *Nucleic Acids Res.* 1991;19:4293.
  19. van Rijen HV, van Veen TA, van Kempen MJ, Wilms-Schopman FJ, Potse M, Krueger O, Willecke K, Opthof T, Jongsma HJ, de Bakker JM. Impaired conduction in the bundle branches of mouse hearts lacking the gap junction protein connexin40. *Circulation.* 2001;103:1591-1598.
  20. Lowry OH, Rosebrough NJ, Farr AL, Randall RJ. Protein measurement with the folin phenol reagent. *Journal of Biological Chemistry.* 1951;193:265-275.
  21. Clement S, Chaponnier C, Gabbiani G. A subpopulation of cardiomyocytes expressing alpha-skeletal actin is identified by a specific polyclonal antibody. *Circ Res.* 1999;85:e51-58.
  22. Cash DE, Bock CB, Schughart K, Linney E, Underhill TM. Retinoic acid receptor alpha function in vertebrate limb skeletogenesis: a modulator of chondrogenesis. *J Cell Biol.* 1997;136:445-457.
  23. Kass DA, Hare JM, Georgakopoulos D. Murine cardiac function: a cautionary tail. *Circ Res.* 1998;82:519-522.
  24. Vincent M, Boussairi EH, Cartier R, Lo M, Sassolas A, Cerutti C, Barres C, Gustin MP, Cuisinaud G, Samani NJ, et al. High blood pressure and metabolic disorders are associated in the Lyon hypertensive rat. *J Hypertens.* 1993;11:1179-1185.
  25. Ortiz-Lopez R, Li H, Su J, Goytia V, Towbin JA. Evidence for a dystrophin missense mutation as a cause of X-linked dilated cardiomyopathy. *Circulation.* 1997;95:2434-2440.
  26. Ehler E, Horowitz R, Zuppinger C, Price RL, Perriard E, Leu M, Caroni P, Sussman M, Eppenberger HM, Perriard JC. Alterations at the intercalated disk associated with the absence of muscle lim protein. *J Cell Biol.* 2001;153:763-772.
  27. Chen YJ, Chen SA, Tai CT, Yu WC, Feng AN, Ding YA, Chang MS. Electrophysiologic characteristics of a dilated atrium in patients with paroxysmal atrial fibrillation and atrial flutter. *J Interv Card Electrophysiol.* 1998;2:181-186.
  28. Verheule S, van Batenburg CA, Coenjaerts FE, Kirchhoff S, Willecke K, Jongsma HJ. Cardiac conduction abnormalities in mice lacking the gap junction protein connexin40. *J Cardiovasc Electrophysiol.* 1999;10:1380-1389.
  29. Hagedorff A, Schumacher B, Kirchhoff S, Lüderitz B, Willecke K. Conduction disturbances and increased atrial vulnerability in Connexin40 deficient mice analyzed by transesophageal stimulation. *Circulation.* 1999;99:1508-1515.
  30. Fast VG, Darrow BJ, Saffitz JE, Kleber AG. Anisotropic activation spread in heart cell monolayers assessed by high-resolution optical mapping. Role of tissue discontinuities. *Circ Res.* 1996;79:115-127.
  31. Gutstein DE, Morley GE, Tamaddon H, Vaidya D, Schneider MD, Chen J, Chien KR,

Stuhlmann H, Fishman GI. Conduction slowing and sudden arrhythmic death in mice with cardiac-restricted inactivation of connexin43. *Circ Res*. 2001;88:333-339.

# Chapter 8

---

## Summarizing discussion

Toon A.B. van Veen

**Background of the thesis.**

To guarantee an adequate cardiac performance, contraction is orchestrated in a highly coordinated fashion. From the onset of a heartbeat in the SAN to synchronous contraction of both ventricles, the electrical impulse is propagated from myocyte to myocyte by depolarizing current flow through gap junction channels. Cardiac gap junction channels may be composed of three different connexin isoforms; Cx40, Cx43 and Cx45, which possess different properties and are not uniformly expressed throughout the various cardiac compartments (see chapter 2.2). As indicated by the differences in properties, gap junctions are not simple passive holes in the intercellular membrane but intricate protein channels subject to various levels of regulation. The extent of intercellular coupling depends on the number of channels, the open probability of a channel and the conductance of each contributing single channel. Impulse propagation in cardiac tissue is additionally dependent on the subcellular distribution of gap junctions, cytoplasmic resistivity (i.e. tissue geometry) and composition of the extracellular matrix. Furthermore, but beyond the scope of this thesis, conduction velocity is affected by the expression level of ion channels which determine the rate of rise of the action potential. The aim of our project was to determine how modulation of single channel conductance, gap junction expression and (subcellular) distribution contribute to changes in electrical coupling between cells and what the consequences are for propagation of the electrical impulse in the rodent heart. We structured the project in three levels of increasing complexity; 1) experiments on communication incompatible cells transfected with a single connexin isoform, 2) experiments on isolated cardiomyocytes cultured in a defined pattern, 3) experiments on intact rat and mouse heart.

**Modulation of single channel characteristics by phosphorylation.**

Phosphorylation is one of the post-translational modulatory modes which affects the properties of all three cardiac isoforms. Especially in their cytoplasmic carboxy-terminus, multiple amino acid residues are located which are susceptible to phosphorylation by different classes of protein kinases. Sequence analysis learned that for different protein kinases, the three isoforms possess variable numbers of potentially phosphorylatable residues (chapter 2, table I). For each isoform, this number of residues differs between human, mouse and rat. Up to now, a limited number of them have been identified as actual targets for different protein kinases. To study the effects of phosphorylation on intercellular communication, communication deficient cells transfected with a single connexin isoform have proven their applicability. However, since expression of the transfected isoforms in these cells is controlled by an unnatural promoter, they are not useful to gather information about changes in number of channels as induced by prolonged stimulation of protein kinases. Although in these cells direct (instead of receptor mediated) stimulation of the various kinases with agents relatively insensitive to cellular clearance exaggerates the natural situation and excludes a controlled feed back response, it provides information about the possible effects a certain kinase can evoke without being suppressed by pre-kinase cross-talk of signal transduction pathways.

If we compare (chapter 2.3) the actual knowledge about phosphorylation of Cx40, Cx43 and Cx45 channels as derived from experiments on transfected cells, it is obvious that information on Cx40 and especially Cx45 is scant compared to that

on Cx43. In addition, information about phosphorylation of Cx40 and Cx45 is incomplete between species and the role of some kinases has only summarily been evaluated. We studied phosphorylation of mouse Cx45 (mCx45) channels transfected into communication deficient HeLa cells. On Western blot, unlike human Cx45<sup>1</sup>, mCx45 separates in two bands of 46 kD and 48 kD. Treatment with calf intestinal phosphatase revealed that the 46 kD band represented an unphosphorylated state and the 48 kD band a phosphorylated state. Short term stimulation of the cells with agents that directly activate protein kinases/phosphatases induced an increase in phosphorylation upon stimulation of PKA and inhibition of tyrosine-phosphatase. The increased phosphorylation of Cx45 did not affect single channel conductance but reduced total junctional conductance. Since no change in the number of channels was expected, this shift most likely reflected changes in the open probability of the channels. Even though mCx45 and hCx45 each bear one consensus site potentially sensitive to phosphorylation by PKA (see table I, chapter 2), hCx45 channel properties were not affected upon activation of PKA<sup>2</sup>.

Phosphorylation of Cx40 and the consequences for electrical conductance have thus far only been described in one report showing that PKA mediated phosphorylation of hCx40 channels increased total conductance because single channel conductance increased. Phosphorylation of Cx43 has been studied by many authors. These studies showed that phosphorylation by different kinases shifts single channel conductance to low values while dephosphorylation favors higher conductance states. Changes in total junctional conductance seem unrelated to the direction of changes in single channel conductance and differ depending on the kinase activated which points in our opinion to an important role for the open probability of the channels. Data explaining how phosphorylation affects the open probability of gap junction channels are as yet lacking but would be very welcome to clarify its influence on junctional conductance. In general, phosphorylation induced by stimulation of PKC and PKA seems potent to modulate all three cardiac connexin isoforms while PKG and MAPK are only effective regulators of Cx43 channels.

### **Expression and phosphorylation of gap junctions in cardiomyocytes.**

An important validation of the results obtained from experiments on transfected cells is provided by the similarity with results obtained from experiments on isolated, cultured cardiomyocytes (Chapter 2.3 and 2.4). This means that studying phosphorylation of gap junction channels in a reduced cell system is physiologically meaningful. Furthermore, studies on cardiomyocytes show that short term receptor mediated stimulation and direct stimulation with synthetic agents produce similar effects. Most of the studies on cardiomyocytes are performed on easily accessible neonatal or adult ventricular myocytes expressing predominantly Cx43 gap junctions. Since the expression level of Cx40 and Cx45 in most cardiomyocytes is low and restricted to fetal or early postnatal myocytes (which downregulate Cx40 in prolonged culture, chapter 4) and cells of the conduction system which are difficult to isolate in sufficient amounts, no data are available on regulation by phosphorylation of Cx40 and Cx45 in myocytes. To fill this lack of information, extension of experiments on cells transfected with Cx40 or Cx45 could be a useful approach. An interesting utilization for this approach is found with respect to Cx40 and Cx45 expressing myocytes of the ventricular conduction system (see chapter 5) where under pathophysiological conditions, elevated levels of cAMP have been measured<sup>3</sup>. We showed that phosphorylation of mCx45 by PKA decreases

total conductance (chapter 3) while phosphorylation by PKA of hCx40 on the other hand increases total conductance<sup>1</sup>. If the effect of PKA on mCx40 would be comparable to that on hCx40, than Cx40 and Cx45 gap junction channels between myocytes of the mouse conduction system could act contradictory.

Phosphorylation of Cx43 gap junction channels through stimulation of PKG, PKC and MAPK generally reduces junctional conductance while it is increased upon stimulation of PKA (chapter 2.4). Long-term stimulation of PKA and PKC, increases expression of Cx43<sup>4,5</sup>, and Cx45<sup>5</sup>. In strands of cultured myocytes, the increase in connexin expression was associated with an increase in conduction velocity of the action potential<sup>5</sup>. In still ongoing research, described in chapter 4, we wished to investigate the dependence of conduction velocity on expression and phosphorylation of Cx43. Therefore, we used isolated neonatal rat cardiomyocytes and cultured them in a defined pattern to study the effects of  $\alpha$ -adrenergic stimulation which acts through activation of PKC and  $\beta$ -adrenergic stimulation which acts through activation of PKA. Although conduction velocity increased upon  $\beta$ -adrenergic stimulation, we were unable to detect changes in phosphorylation or expression of Cx43. Probably this can be explained by the suppressive effect of serum in our culture medium, because in the studies referred to, serum-free culture medium was used<sup>4,5</sup>. Because action potential duration (in  $\alpha$ -adrenergic stimulated cells) and rate of rise of the upstroke (in  $\beta$ -adrenergic treated cells) were changed, we additionally investigated the expression level of ion channels which contribute to generation of the action potential. We did find changes in expression level which were, however, insufficiently clarifying. Therefore, additional experiments will be performed on cultures in serum free medium. Also the (protein) expression level of all ion channels contributing to the shape of the action potential will be investigated.

### **Expression and distribution of gap junctions in the intact heart; consequences for propagation of the action potential.**

Reports on a modulatory role for gap junction (de)phosphorylation in the intact heart are very scarce, although dephosphorylation has been shown to be involved in a model of acute ischemia<sup>6</sup> and increased phosphorylation decreases junctional conductance in hypertrophic cardiomyopathy<sup>7</sup>. We focussed our attention on expression and distribution of gap junctions in the ventricular conduction system (chapter 5 and 6) and the ventricles (chapter 7).

A comparison of the mouse and rat interventricular septum regarding expression and distribution of gap junctions, morphology of involved tissue and the local electrical activation pattern revealed several differences (chapter 5). In both species, working myocardial cells of the septum are predominantly coupled by large Cx43 gap junctions which are found in intercalated disks on the longitudinal cell borders. This polarized distribution over the cell favors longitudinal over transverse coupling and thus gives rise to anisotropic conduction.

The proximal ventricular conduction system in mice and rats is characterized by a differential expression level of contractile proteins and a perpendicular fiber orientation as compared to that in the working myocardium of the septum. Throughout the ventricular conduction system of both mice and rats, myocytes are coupled by gap junctions composed of Cx40 and Cx45. In mice, Cx43 is only found in the distal parts of the bundle branches while in rat Cx43 is already expressed just below the bifurcation of the common bundle into the bundle branches. The subcellular distribution of gap junctions in rat bundle branches shows that some labeling for all three connexins is found in the longitudinal

intercalated disks but the majority as diffuse labeling covering the entire cell surface. In contrast, in mouse proximal bundle branches, intense labeling is observed in a pattern of multiple step-like regions over the entire cell while in the distal branches labeling is rather diffuse. Interestingly, both in mice and rat proximal bundle branches, conduction velocity is similar despite the differences both in nature of expressed connexins and distribution over the cell. As compared to the proximal parts, conduction velocity in the distal parts of mouse bundle branches is reduced by half. We suggest that this reduction is caused by load mismatch induced by electrical interaction of the small distal bundle branches with the surrounding septal working myocardium (mediated by Cx43). As far as we could measure, conduction velocity in the rat bundle branches remained constant because at this level the bundle branches are electrically separated from the septum by a sheath of connective tissue.

Connective tissue does also explain the difference between rats and mice in electrical activation of the septal working myocardium. In rats, an isolating sheet of connective tissue separates the common bundle from the top of the septal myocardium and thus the electrical impulse is propagated from the common bundle through the bundle branches resulting in earliest activation of the mid-septum (chapter 5). In mice, the sheet of connective tissue is penetrated by physically connected myocytes which co-express Cx43 and Cx45. Therefore in mice the septal myocardium is activated from base to apex (chapter 5 and 6). In conclusion, the morphology and electrical activation pattern in rats conforms to that of larger mammals<sup>8</sup>, rather than to its closest family member the mouse.

The electrical connection between the common bundle and the septal working myocardium as found in mice, triggered the question to what extent impulse propagation through the bundle branches in mice contribute to activation of the ventricles. In Cx40 KO mice conduction through the bundle branches was impaired on the left side and blocked on the right side. This difference can be explained by the difference in thickness of the branches (chapter 6). Cx40 depletion however did not induce ventricular arrhythmias or abnormal electrical activation patterns of the interventricular septum and the ventricular epicardia. Targeted deletion of Cx45 induced more dramatic effects as it caused these mice to die on day 9.5 pc probably resulting from conduction block<sup>9,10</sup>. Since we observed that the interaction of the common bundle and the septal myocardium likely is mediated by Cx43/Cx45 gap junctions (chapter 5), deletion of Cx45 would prevent this connection. In this situation, additional impairment or block of impulse propagation through the bundle branches to a comparable degree as found in Cx40 KO mice would completely prevent ventricular activation, resulting in the observed lethality.

In chapter 7, we described the consequences of changes in Cx43 expression and distribution for the electrical activation pattern of the left ventricular free wall. Transgenic mice overexpressing a constitutively active form of the human retinoic acid receptor (hRAR) develop a dilated cardiomyopathy characterized by an increased heart/weight body weight ratio and heart weight/tibia length ratio. ECG analysis of affected mice revealed a prolongation of the Q-j interval from which a delay in ventricular activation was expected. Epicardial mapping of the left ventricular free wall indeed showed activation delay and occurrence of regional conduction block. Endocardial mapping confirmed this and showed that conduction velocity was reduced. In the left ventricular free wall, forced activity of the hRARs induced re-expression of early sarcomeric proteins characteristic for hypertrophic myocardium. In this region both Cx43 and other intercalated disk proteins were redistributed prior to severe and heterogeneous down regulation.

In severely affected animals, areas up to 40% of the total ventricular free wall were depleted from Cx43 while no re-expression of other connexins was observed. Strikingly, no severe and lethal arrhythmias were observed *in vivo* or *in vitro* nor could be induced through pacing with premature stimuli. This phenomenon seems to contradict the common idea that this degree of Cx43 down-regulation and the heterogeneous character of it, would strongly increase the propensity to develop ventricular arrhythmias. We postulate that the absence of such disorders in mouse heart depend on the small size of the ventricles and the even smaller size of normal area in the affected hearts which prevents the occurrence of reentry circuits.

In summary, we have described in this thesis the results obtained from experiments on transfected cells to those on intact heart and provided new data on connexin phosphorylation, expression and distribution. Transfected cells, regarded as the lowest level of complexity are a very useful and reliable tool to study the effects of gap junction phosphorylation. To relate changes in gap junctional conductance to propagation of the action potential, isolated cardiomyocytes cultured in defined patterns are a promising model though experimental conditions have to be optimized. Finally, the mouse as a model to study impulse propagation in the intact heart has proven its applicability to unravel the physiological connection between connexin expression/distribution and impulse propagation. On the other hand, the mouse heart is in several respects substantially different from hearts of larger mammals which hampers extrapolation of the acquired data.

## **References:**

1. Van Rijen HVM, van Veen AAB, Hermans MMP, Jongsma HJ. Human connexin40 gap junction channels are modulated by cAMP. *Cardiovascular Research*. 2000;45:941-951.
2. Kwak BR, Hermans MMP, De Jonge HR, Lohmann SM, Jongsma HJ, Chanson M. Differential regulation of distinct types of gap junction channels by similar phosphorylating conditions. *Molecular Biology of the Cell*. 1995;6:1707-1719.
3. Sugiyama A, McKnite S, Wiegand P, Lurie KG. Measurement of cAMP in the cardiac conduction system of rats. *Journal of Histochemistry and Cytochemistry*. 1995;43:601-605.
4. Dodge SM, Beardslee MA, Darrow BJ, Green KG, Beyer EC, Saffitz JE. Effects of angiotensin II on expression of the gap junction channel protein connexin43 in neonatal rat ventricular myocytes. *J Am Coll Cardiol*. 1998;32:800-807.
5. Darrow BJ, Fast VG, Kléber AG, Beyer EC, Saffitz JE. Functional and structural assessment of intercellular communication: Increased conduction velocity and enhanced connexin expression in dibutyryl cAMP-treated cultured cardiac myocytes. *Circulation Research*. 1996;79:174-183.
6. Beardslee MA, Lerner DL, Tadros PN, Laing JG, Beyer EC, Yamada KA, Kleber AG, Schuessler RB, Saffitz JE. Dephosphorylation and Intracellular Redistribution of Ventricular Connexin43 During Electrical Uncoupling Induced by Ischemia. *Circ Res*. 2000;87:656-662.
7. Toyofuku T, Yabuki M, Otsu K, Kuzuya T, Tada M, Hori M. Functional role of c-Src in gap junctions of the cardiomyopathic heart [see comments]. *Circ Res*. 1999;85:672-681.
8. Oosthoek PW, Viragh S, Lamers WH, Moorman AF. Immunohistochemical delineation of the conduction system. II: The atrioventricular node and Purkinje fibers. *Circ Res*. 1993;73:482-491.
9. Kumai M, Nishii K, Nakamura K, Takeda N, Suzuki M, Shibata Y. Loss of connexin45 causes a cushion defect in early cardiogenesis. *Development*. 2000;127:3501-3512.
10. Krüger O, Plum A, Kim J, Winterhager E, Maxeiner S, Hallas G, Kirchhoff S, Traub O, Lamers WH, Willecke K. Defective vascular development in connexin 45-deficient mice. *Development*. 2000;127:4179-4193.

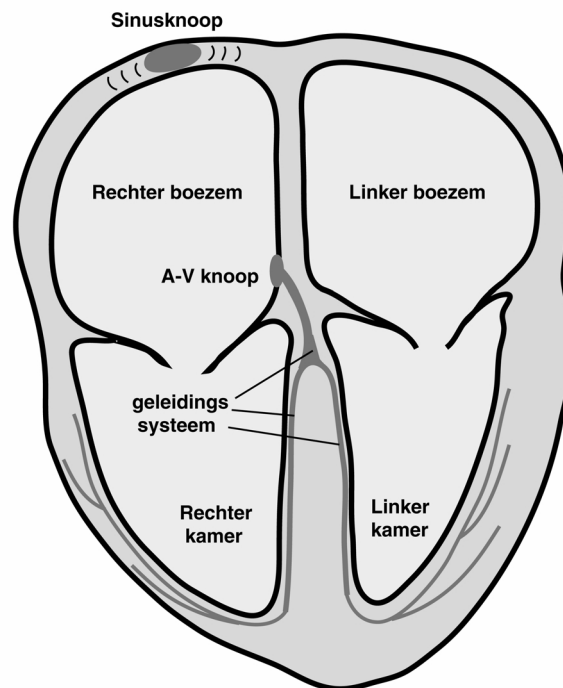
# Varia

---

Het hart is te beschouwen als een complexe (holle) spier bestaande uit vier compartimenten welke zijn opgebouwd door een aanéenschakeling van miljoenen afzonderlijke spiercellen (zie figuur). Het orgaan is vergelijkbaar met een pomp welke als belangrijkste functie het rondpompen van bloed door het lichaam heeft. Zuurstofarm bloed wordt vanuit de aders verzameld in de rechterboezem om vandaar via de rechterkamer naar de longen te worden gepompt om van nieuw zuurstof te worden voorzien. Vanuit de longen komt het bloed in de linkerboezem en wordt vandaar via de linkerkamer in de lichaamsslagader gepompt zodat alle perifere delen van het lichaam van 'vers bloed' worden voorzien. De pompfunctie van het hart is een ingewikkeld fenomeen en is derhalve onderhevig aan een strakke regulatie.

Het samentrekken (contraheren) van het hart wordt elektrisch aangestuurd en begint in de sinusknop, een interne pacemaker, welke zich boven in de rechterboezem bevindt. Vanuit dit gebiedje wordt een elektrische prikkel (actiepotentiaal) overgedragen van cel naar cel en deze prikkel zorgt er voor dat de cel zich samentrekt. Agglomeraten van kanaaltjes (gap junctions) in de celwanden tussen aanéengrenzende cellen verbinden de interne mileus van de cellen en maken zo de prikkel verspreiding mogelijk. Doordat deze prikkel overdracht heel snel verloopt trekken nagenoeg al die afzonderlijke cellen gelijktijdig samen en wordt voldoende kracht ontwikkeld voor het hart om te kunnen pompen. Om adequaat te kunnen pompen moeten eerst de beide boezems en vervolgens de beide kamers samentrekken. Een specifiek geleidingssysteem in de relatief grote kamers (ten opzichte van de boezems) draagt zorg voor een extra snelle prikkel geleiding in dit gebied.

## het hart



De elektrische activiteit in de verschillende delen van het hart tijdens een hartslag kunnen we aflezen in een elektrocardiogram (ECG). Het hartritme wordt bepaald door de vraag van het lichaam om zuurstofvoorziening. Het ECG laat een snel ritme zien onder inspanning en een langzaam ritme in rust. In beide gevallen echter is het ritme regelmatig van aard; dat wil zeggen dat de periode tussen de contracties constant is. Het moge een ieder bekend zijn dat heel veel voornamelijk oudere, maar ook jongere mensen jaarlijks overlijden als gevolg van een niet goed functionerend hart. Eén van de grote oorzakelijke boosdoeners is het optreden van hartritmestoornissen. De grondslag van hartritmestoornissen is nog niet geheel begrepen maar zeker is dat velerlei factoren een rol spelen. Eén van de factoren is waarschijnlijk het niet goed functioneren of verminderd aanwezig zijn (tot expressie

komen) van de gap junction kanaaltjes tussen de cellen. Hierdoor wordt de zo strikt gereguleerde elektrische impuls overdracht binnen het hart verstoord wat de kans op ritmestoornissen vergroot. In dit proefschrift wordt een beschouwing gegeven over de eigenschappen van deze kanaaltjes en de factoren waardoor deze eigenschappen worden beïnvloed. Daarnaast hebben we het functioneren bekeken van kanalen onder condities die voorkomen in zieke harten en de gevolgen van veranderingen in functioneren en expressie voor de hart functie.

De gap junction kanalen bestaan uit 2 halve kanalen die door de betrokken aaneengrenzende cellen worden geleverd en elkaar op het grensvlak van de twee cellen 'vinden'. Elk halfkanaal bestaat op zijn beurt uit 6 hexagonaal gerangschikte eiwitten, connexines (Cxs) genaamd. Deze connexines zijn onderdeel van een grote familie van membraaneiwitten en zijn structureel vrijwel identiek doch functioneel verschillend. Van de verschillende connexine isovormen komen 3 leden, te weten connexine40 (Cx40), connexine43 (Cx43) en connexine45 (Cx45), tot expressie tussen hartspiercellen. Het blijkt dat er opmerkelijke verschillen bestaan tussen de diverse regio's van het hart ten aanzien van de expressie patronen van de 3 connexines. Grofweg kun je stellen dat Cx40 te vinden is in de boezems en in het geleidingssysteem, Cx43 in zowel de boezems als de kamers en Cx45 alleen in het geleidingssysteem. Tevens is gebleken dat de specifieke eigenschappen van de verschillende kanalen sterk bepaald worden door de connexines waaruit ze zijn opgebouwd wat suggereert dat de verschillen in expressie een functionele achtergrond hebben.

Een belangrijk biologisch mechanisme om het functioneren van eiwitten te reguleren is fosforylering van bepaalde bouwstenen (aminozuren) in het eiwit. Deze fosforylering wordt uitgevoerd door een specifieke groep eiwitten, kinases genaamd. Ook connexines, en de door hen gevormde kanalen blijken te worden gereguleerd door fosforylering. Hoofdstuk 2 laat zien wat gap junctions nu precies zijn en waar de verschillende isovormen in het hart tot expressie komen. Tevens wordt er een overzicht gegeven van de huidige kennis betreffende fosforylering van en veranderingen in expressie van de isovormen, en dit alles wordt gerelateerd aan de effecten op prikkeloverdracht cq hartfunctie. Connexine45 is de isovorm die in het hart het meest spaarzaam tot expressie komt en waarover relatief nog weinig bekend is. Op welke wijze deze kanalen gereguleerd worden door middel van fosforylering wordt beschreven in hoofdstuk 3. Om dit te kunnen onderzoeken, hebben we het eiwit geforceerd tot hoge expressie gebracht in cellen die normaal geen connexines hebben. Uit de studie blijkt dat slechts bepaalde kinases Cx45 fosforyleren en dat met name protein kinase A een interessante rol speelt.

Vervolgens hebben we gekeken hoe deze vorm van regulatie zich nu in echte hartspiercellen manifesteert en wat de gevolgen hiervan zijn voor de voortgeleidingssnelheid van de actiepotentiaal. Daartoe hebben we hartspiercellen geïsoleerd uit hartjes van pasgeboren ratten en deze gekweekt op glaasjes in een stervormig patroon. Wanneer we deze cellen nu stimuleren met factoren als isoproterenol en phenylephrine, die onder meer respectievelijk PKA dan wel PKC (verschillende proteïne kinases) kunnen activeren, dan blijkt dit eigenlijk weinig effect te hebben op zowel de fosforylering als de expressie van Cx43 kanalen. Daarentegen blijkt isoproterenol maar niet phenylephrine de snelheid van voortgeleiding met 25% te doen toenemen. Waarschijnlijk komt dit dus niet door veranderingen op gap junction nivo maar meer waarschijnlijk door een veranderd expressie patroon van allerlei ionkanalen welke verantwoordelijk zijn voor de 'opbouw' van de actiepotentiaal.

In de laatste 3 hoofdstukken wordt de stap van studies op celniveau naar intacte

harten gemaakt. In hoofdstuk 5 hebben we het ratten- en muizenhart aan een kritische beschouwing onderworpen. Het blijkt dat er aanzienlijke verschillen bestaan met betrekking tot de plaats in deze harten waar de verschillende isovormen tot expressie komen. Daarnaast is tevens de organisatie (verdeling) van expressie verschillend, niet alleen tussen de rat en de muis maar tevens tussen 'normale hartspiercellen' en die in het geleidingssysteem. Ook blijkt de weefselmorfologie van het interventriculaire septum afwijkend in het muizenhart ten opzichte van die in het rattenhart. We laten zien dat deze verschillen zich reflecteren in functionele verschillen met betrekking tot de elektrische activatie van beide harten.

Wanneer we nu met een genetisch trucje muizen fokken waarin connexine40 (bevindt zich ondermeer in het geleidingssysteem) niet meer tot expressie komt (Cx40 knock-out muizen), dan blijkt dit een blokkade te induceren van de prikkel overdracht in het geleidingssysteem van de rechterkamer terwijl de voortgeleiding aan de linkerzijde vertraagd wordt (hoofdstuk 6). In een tweede maar anders genetisch gemodificeerde muis, komt er een bepaald gen (de retinoïc-acid receptor) continu tot expressie met als gevolg dat er een ongewilde vergroting (hypertrofie) van het hart ontstaat. Een vergelijkbare hypertrofie vinden we terug in een grote groep patiënten die bijvoorbeeld lijden aan jarenlange hoge bloeddruk of lekkende hartkleppen wat uiteindelijk kan leiden tot hartfalen. In dit muis model laten we zien dat veel klassieke kenmerken van hypertrofie terug te vinden zijn, dat Cx43 verdwijnt uit forse delen van de linkerkamer en dat de karakteristieke celopbouw veranderd is. Hierdoor is de activatie van de kamers niet alleen vertraagd maar ook blokkeert de elektrische voortgeleiding op sommige plaatsen. Desondanks vinden we in deze muizen geen dodelijke ritmestoornissen, terwijl in mensen door vergelijkbare veranderingen, veel ernstigere gevolgen te verwachten zijn. De kleinschaligheid van het muizenhart beschermt het beestje waarschijnlijk tegen dit soort dodelijke ritmestoornissen.

Met het in dit proefschrift beschreven onderzoek is fundamentele kennis vergaard ten aanzien van de structuur en elektrische activatie van kleine harten zoals in muis en rat, hoe de verschillende soorten gap junctions tot expressie komen in het hart, hoe ze gereguleerd worden en welke rol ze spelen in het doorgeven van de actiepotentiaal van de ene cel naar de andere.

## **Dankwoord**

Het dankwoord is traditioneel het meest gelezen onderdeel van het proefschrift. Dit waarborgt voor de schrijver de aandacht van de mensen die hij in nadrukkelijke zin wil danken voor de geleverde inspanningen, maar maakt het tevens tot een gevaarlijk stukje daar er altijd mensen zich vergeten voelen (echter niet vergeten, maar niet bij naam genoemd). Met nadruk wil ik dan ook iedereen die de afgelopen vier jaar zijn input heeft gehad in mijn werk, functioneren en plezier, hartelijk dank zeggen voor zijn of haar bijdrage. Onderzoek doe je niet alleen maar het succes en de lol ervan staat of valt bij de specifieke kennis en vaardigheid van velen. Hierbij kan ook de kleinste bijdrage een belangrijke bouwsteen vormen!

Toch wil en zal ik mij niet onttrekken aan wat persoonlijke dankzegging.

Ten eerste, Habo, promotor en meedenker, ik wil je danken voor de vrijheid, het vertrouwen en de steun die je me gegeven hebt om zelf mijn onderzoek in te kunnen richten en me zo te kunnen vormen als onderzoeker. Zelf vallen en leren opstaan is me meer waard dan aan het handje naar de finish geleid te worden. Die ruimte heb ik zeer gewaardeerd en ik hoop dan ook nog een poosje te kunnen blijven. Daarnaast was je er wanneer nodig ook voor discussie van mijn wetenschappelijke hersenspinsels en om mijn schrijfselen uitvoerig rood te maken. Harold, paranimf en 'roommie', we kennen elkaar al heel lang en ik ben erg blij dat we samen dit project hebben kunnen uitvoeren. Ik wil je niet alleen danken voor de enorme elektrofysiologische output (blijft soms hocus-pocus voor mij) en mijn computer 'onderwijs' (denk aan je voorhoofd), maar zeker ook voor je vriendschap en voor van alles en nog niks.

Daarnaast waren de volgende mensen onlosmakelijk verbonden met mijn onderzoek in de achterliggende periode: Marjan, voor de introductie van het mooie terrein der (immuno)histologie en voor je persoonlijke vrolijke noot binnen ons collega-schap. Marti, busmaatje en fan van de verkeerde club, en Marcel voor de moleculair biologische rituelen en de vaak niet gestructureerde gesprekken (wel belangrijk trouwens), Jacques (soms onnavolgbaar elektrofysiologisch professorandus) en Tobias (miskent voetbal-analyticus en karaoke zanger), voor jullie goede ideeën en het kritisch lezen van mijn schrijfselen, Tonny voor alle gezelligheid en jouw vrolijke lach en Rob, student in twee projecten met een enorme bijdrage in de hele-hart-muizelogie (trouwens ik hoorde dat de trein....).

Mijn verdere, maar zoals gezegd anonieme dank gaat uit naar alle andere (ex)-medewerkers van de Medische Fysiologie en (toen nog) Sportgeneeskunde voor hun persoonlijke noot, gezelligheid en input en naar de mensen van de proefdiervoorziening voor de fok van mijn muizen en hun flexibiliteit als ik weer eens een spontaan opborrelend experiment had.

Tenslotte, in mijn niet wetenschappelijke omgeving wil ik Eikie (paranimf en vismaatje), Kas, Mark en Frits voor de Utrechtse festiviteiten, en de hele club uit Boskoop, bedanken voor de broodnodige ontspanning buiten het werk.

Tenslotte mijn direkte (schoon)familie voor de liefde, steun en de dingen die mij duidelijk maken dat er veel meer van belang is in dit leven dan alleen werk en natuurlijk El en Luna: jullie zijn het belangrijkste, en te vaak onuitgesproken fundament in mijn leventje.

## **Curriculum Vitae**

Antonius Adrianus Bartholomeus van Veen, roepnaam Toon, werd op 3 juni 1970 geboren te Leiden. De middelbare schoolopleiding genoot hij aan de Samenwerkingsschool te Waddinxveen alwaar in 1988 het VWO diploma werd behaald. In hetzelfde jaar startte hij een studie Biologie aan de Universiteit Utrecht volgens een medisch biologisch profiel. Tijdens de specialisatiefase werd een tweetal stages gelopen waarin zijn cardiovasculaire interesse zich uitkristalliseerde: de eerste bij de vakgroep EMSA, Faculteit Biologie, Universiteit Utrecht onder begeleiding van Dr. Rene Musters en Prof. Arie Verkleij, de tweede bij de vakgroep Medische Fysiologie, Universiteit Utrecht, onder begeleiding van Dr. Brenda Kwak. De studie werd in 1994 afgerond met het doctoraal examen. Vervolgens was hij werkzaam bij: het Max Planck Instituut für Experimentele Kardiologie, Bad Nauheim, Duitsland onder begeleiding van Prof. Wolfgang Schaper, wederom bij de eerder genoemde vakgroep Medische Fysiologie onder begeleiding van Dr. Antoinette Groenewegen en als AIO bij de vakgroep Farmacologie, Erasmus Universiteit Rotterdam, onder begeleiding van Dr. Regien Schoemaker. Uiteindelijk werd in oktober 1997 een start gemaakt met het in dit proefschrift beschreven promotie onderzoek wat is uitgevoerd binnen de inmiddels bekende vakgroep Medische Fysiologie, onder supervisie van Prof. Habo Jongsma.

**List of publications.**

Kwak BR, **van Veen AAB**, Analbers LJS, Jongsma HJ. TPA increases conductance but decreases permeability in neonatal rat cardiomyocyte gap junction channels. *Exp Cell Res* 220 (1995) 456-463.

Musters RJP, Probstl-Biegelmann E, **van Veen AAB**, Hoebe KHN, Op den Kamp JAF, Verkleij AJ, Post JA. Sarcolemmal phospholipid reorganization during simulated ischemia and reperfusion: reversibility and ATP dependency. *Mol Membr Biol* 13 (1996) 159-164.

Groenewegen WA, **van Veen AAB**, van der velden HMW, Jongsma HJ. Genomic organization of the rat connexin40 gene: identical transcription start sites in heart and lung. *Cardiovas Res* 38 (1998) 463-471.

Kubin T, Ando H, Scholz D, Bramlage P, **van Veen AAB**, Heling A, Hein S, Fischer S, Breier A, Schaper J, Schaper W. Microvascular endothelial cells remodel cultured adult cardiomyocytes and increase their survival. 1999 *Am J Phys* 276 (6Pt2) H2179-H2187.

Van Rijen HVM, **van Veen AAB**, Hermans MP, Jongsma HJ. Human connexin40 gap junction channels are modulated by cAMP. *Cardiovas Res*.45 (2000) 941-951.

**Van Veen AAB**, van Rijen HVM, Jongsma HJ. Electrical conductance of mouse connexin45 gap junction channels is modulated by phosphorylation. *Cardiovas Res*.46 (2000) 496-510.

Van der Velden HMW, Ausma J, Rook MB, Hellemons AJCGM, **van Veen AAB**, Allessie MA, Jongsma HJ. Gap junction remodeling in relation to stabilization of atrial fibrillation in the goat. *Cardiovas Res*. 46 (2000) 476 486.

Van Kerckhoven R, **van Veen AAB**, Saxena PR, Schoemaker R. Chronic administration of moxonidine surpresses symphatic activation in a rat heart failure model. *Eur J Pharm*. 397 (2000) 113-120.

Van Rijen HVM, **van Veen AAB**, van Kempen MJA, Wilms-Schopman FJG, Potse M, Kreuger O, Willecke K, Opthof T, Jongsma HJ, de Bakker JMT. Impaired conduction in the bundle branches of mouse hearts lacking the gap junction protein connexin40. *Circulation* 103 (2001) 1591-1598.

**van Veen AAB**, van Rijen HVM, Opthof T. Cardiac gap junction channels: modulation of expression and channel properties. *Cardiovas Res* 51 (2001) 217-229.

Malfait M, Gomez P, **van Veen AAB**, Parys JB, De Smedt H, Vereecke J, Himpens B. Effects of hyperglycemia and protein kinase C on connexin43 expression in

cultured rat retinal pigment epithelial cells. *J Membr Biol* 181 (2001) 31-40.

**van Veen AAB**,. van Rijen HVM, Wiegerinck RF, de Bakker JMT, Colbert MC, Clement S, Opthof T, Jongsma HJ. Remodeling of gap junctions in mouse hearts hypertrophied by forced retinoic acid signaling. *Submitted*

**van Veen AAB**, van Rijen HVM, van Kempen MJA, de Bakker JMT, Opthof T, Jongsma HJ. Electrical activation of rodent ventricular conduction systems: correlation with expression of cardiac connexins and tissue morphology. *To be submitted.*